OFDM-PAPR Reduction using Statistical Clipping and Window based Noise Filtering

Thesis submitted in partial fulfillment of the requirement for the award of the degree of

MASTER OF ENGINEERING

In

ELECTRONICS & COMMUNICATION ENGINEERING

Submitted by

Aman Sehgal

Roll no. 801161003

Under the Guidance of

Dr. Amit Kumar Kohli

Assistant Professor, ECED, TU

Electronics and Communication Engineering Department

Thapar University, Patiala, Punjab-147004 (PUNJAB)

June - 2013

CERTIFICATE

I, **Aman Sehgal** hereby certify that the work, which is being presented in this thesis entitled "**OFDM-PAPR Reduction using Statistical Clipping and Window based Noise Filtering**" by me in partial fulfillment of the requirements for the award of degree of Master of Engineering in Electronics and Communication Engineering at Thapar University, Patiala, is an authentic record of my own work carried out under the guidance of **Dr. Amit Kumar Kohli**, Assistant Professor, **Electronics and Communication Engineering Department**, Thapar University, Patiala.

The matter presented in this thesis has not been submitted in any other university or institute for the award of the degree of Master of Engineering.

Asehgal

Aman Sehgal

Date 28/06/2013

This is certified that the above statement made by the candidate is correct to the best of my knowledge.

Amit Kohli

Dr. Amit Kumar Kohli
Assistant Professor, ECED
Thapar University, Patiala
Date 28/06/2013

Countersigned by:

Dr. R. Khanna
Professor & Head, ECED,
Thapar University, Patiala
Date 2/7/13

Dr. S.K. Mohapatra
Dean of Academic Affairs
Thapar University, Patiala
Date _____

ACKNOWLEDGEMENT

No volume of words is enough to express my gratitude towards my guide, **Dr. Amit Kumar Kohli**, Assistant Professor, Electronics and Communication Engineering Department, Thapar University, who has been very concerned and has aided for all the material essential for the preparation of this thesis report. He has helped me to explore this vast topic in an organized manner and provided me with all the ideas on how to work towards a research-oriented venture.

I am also thankful to **Dr. Rajesh Khanna**, Head of Department, ECED, **Dr. Kulbir Singh** P.G. Coordinator, ECED and **Dr. Sanjay Sharma,** Professor, ECED for the motivation and inspiration that triggered me for the thesis work.

I would also like to thank the staff members and my colleagues who were always there in the need of the hour and provided with all the help and facilities, which I required, for the completion of my thesis.

Most importantly, I would like to thank my parents and the almighty for showing me the right direction out of the blue, to help me stay calm in the oddest of the times and keep moving even at times when there was no hope.

Aman Sehgal

Roll No.- **801161003**

ABSTRACT

Orthogonal Frequency Division Multiplexing (OFDM) is an attractive modulation and multiple access technique for the channels with a non-flat frequency response, as it alleviates the need for complex equalizers. It can offer high quality performance in terms of bandwidth efficiency, robustness against the multipath fading and cost-effective implementation.

It has been currently under intense research for the broadband wireless transmission due to its many advantages. The large peak to average-power-ratio (PAPR) of multiplexing OFDM transmission is one of the major drawbacks for mobile communication that requires severe power saving. A large PAPR increases the complexity of the analog to digital and digital to analog converter and it also reduces the efficiency of the radio frequency (RF) power amplifier.

This thesis work presents an alternate approach for the iterative clipping and filtering (ICF) method used for the PAPR reduction in OFDM systems. As the resultant in-band noise due to clipping after z consecutive iterations is approximately proportional to the clipping noise generated in the single iteration, therefore this in-band noise obtained after first iteration is statistically scaled to measure the in-band clipping noise for z iterations. This approximated in-band clipping noise may be further used for refining the OFDM signal by using statistical clipping (SC) approach [1]. However, the out of band clipping noise is also a significant drawback for OFDM systems, which restricts the efficiency of transmitter.

Therefore, the main focus of presented thesis work is on the out of band clipping noise suppression using the window based filtering, in addition to the in-band clipping noise excision using SC method, which may be termed as statistical clipping and window based filtering approach (SC-W). The simulation results are presented to compare the bit error rate (BER) performance of the underlying wireless OFDM systems using the ICF, SC, SC-W techniques for PAPR reduction. The complementary cumulative density function (CCDF) and power spectral density (PSD) characteristics are also investigated to infer the results, which depict that the proposed SC-W PAPR reduction technique meets the

requirements of transmit mask specified in IEEE 802.11a. The exclusive advantage of SC-W method over ICF approach is the low computational complexity.

Keywords*: orthogonal frequency division multiplexing; peak to average power reduction; statistical clipping; clipping and filtering; window method*

TABLE OF CONTENTS

LIST OF FIGURES

LIST OF TABLES

LIST OF ACRONYMS

3GPP	3rd generation partnership project
ADSL	asynchronous digital subscriber line
AM	amplitude modulation
BER	bit error rate
CCDF	complementary cumulative density function
CDMA	code division multiple access
CIR	carrier to interference ratio
CP	cyclic prefix
C-PTS	conventional partial transmit sequence
CR	clipping ratio
D/A	digital to analog conversion
DFT	discrete fourier transform
DMT	discrete multi tone
DVB	digital video broadcasting

BPSK	bipolar phase shift keying
EC	exponential companding
FEC	forward error correction
FEQ	frequency domain equalizer
FFT	fast frequency transform
FIR	finite impulse response
HPA	high power amplifier
IBO	input back off
ICF	iterative clipping and filtering
ISI	inter symbol interference
ICI	inter carrier interference
IDFT	inverse discrete fourier transform
IEEE	institute of electrical and electronics engineers
IFFT	inverse fast fourier transform
i.i.d.	independent identically distributed

LCT	linear companding transform
LST	linear symmetrical transform
LTE	long term evolution
MIMO	multiple input and multiple output
MPSM	multi point square mapping
NLNST	non linear non symmetrical transform
NLST	non linear symmetrical transform
OFDM	orthogonal frequency division multiplexing
OOB	out of band
PAPR	peak to average power ratio
PM	phase modulation
PSK	phase shift keying
PTS	partial transmit sequence
QAM	quadrature amplitude modulation
QPSK	quadrature phase shift keying

RF	radio frequency
RMS	root mean square
SC	statistical clipping
SC-W	statistical clipping with window based noise filtering
SI	side information
SL	soft limiter
SLM	selected level mapping
SNDR	signal to noise plus distortion ratio
SNR	signal to noise ratio
S/P	serial to parallel
SSPA	solid state power amplifier
TC	trapezoidal companding
TDBC	trapezium distribution based companding
TDMA	time division multiple access
TWT	travelling wave tube

WLAN	wireless land area network
WMAN	wireless metropolitan area network

CHAPTER 1

INTRODUCTION

1.1 Motivation

Orthogonal frequency division multiplexing (OFDM) is a multicarrier modulation technique that divides the available spectrum into subcarriers, with each subcarrier containing a low rate data stream. The subcarriers have proper spacing to satisfy orthogonality as shown in Figure 1.1. OFDM play an important role in realizing cognitive radio concept by providing a proven, scalable, adaptive technology for wireless communications. Inter symbol interference (ISI) is reduced completely by using a guard band in every OFDM symbol. In OFDM, using guard band is cyclically extended in order to avoid inter-carrier interference (ICI). The advantage of OFDM system is robustness to channel fading in wireless communication environment. Frequency selective fading is reduced by increasing the number of subcarriers. By choosing the coherence bandwidth is greater than the subcarrier spacing of the channel, each subcarrier is going to be affected by a flat channel and thus no or simple channel equalizer is needed.

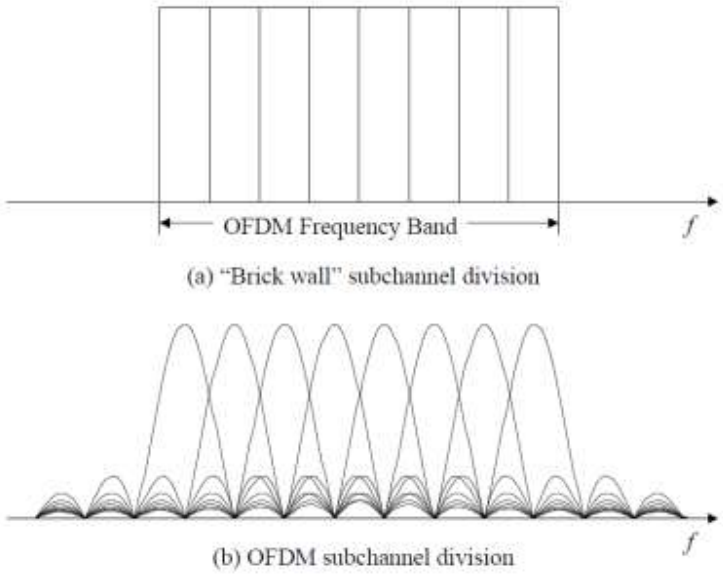

Figure 1.1. *Brick wall sub-channel division in OFDM system*

OFDM is used in many wireless applications today. Already it is used in different WLAN standards (e.g. HIPERLAN-2, IEEE 802.11a), wireless metropolitan area networks (WMAN), digital video broadcasting (DVB), 3GPP-LTE, asymmetric digital subscriber Line (ADSL) and power line communications.

Despite of OFDM advantages, it has a major potential drawback in the form of high peak to average power ratio (PAPR). The high PAPR has nonlinear nature in the transmitter and it degrades the power efficiency of the system.

1.2 OFDM System Model

A Basic OFDM system is described in Figure 1.2. Here an input data symbols are supplied into a FEC encoder and are mapped onto BPSK/QPSK/QAM constellation. Then the coded serial bit-streams is parsed into *N* parallel bit-streams by using S/P converter.

The data symbols are converted from S/P are inverse discrete fourier transformed (IDFT) to achieve the time domain OFDM symbols. Time domain symbols can be represented as:

$$x_n = IDFT\{X_k\}$$

$$x_n = \frac{1}{N}\sum_{k=0}^{N-1} X_k e^{\frac{j2\pi kn}{N}} \qquad 0 \le n \le N-1 \tag{1}$$

Where, X_k is the transmitted symbol on the k^{th} subcarriers and *N* is the number of subcarriers.

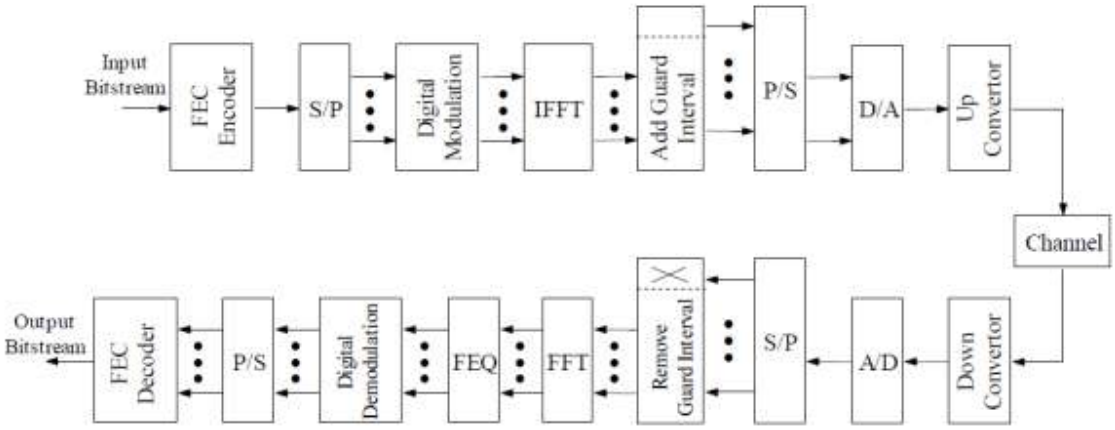

Figure 1.2. *Block diagram of OFDM system*

The data symbols in each OFDM block are therefore modulated into different sub-carriers. Time domain signal x_n is cyclically extended to prevent ISI from the former OFDM symbol using cyclic prefix (CP). After adding the cyclic prefix, the discrete time OFDM signal is converted to a serial signal by using the P/S. The obtained discrete time signal is then transferred into the continuous time domain by using a digital to analog (D/A) converter. Finally, this signal is amplified by using a high power amplifier (HPA) and is up converted to the carrier frequency to facilitate its transfer in the actual wireless channel.

1.3 Mathematical Definition of OFDM Signal

OFDM consists of multiple carriers. Each carrier can be presented as a complex waveform like:

$$S_c(t) = A_c(t)e^{j(\omega_c t+\emptyset_c(t))} \tag{2}$$

Where, A_c(t) is the amplitude and $\emptyset_c t$ is the phase of the signal $S_c(t)$.

The complex signal can be described as

$$S_S(t) = \frac{1}{N}\sum_{n=0}^{N-1} A_n(t)e^{j[\omega_n t+\emptyset_n(t)]} \tag{3}$$

This is a continuous signal. Each component of the signal over one symbol period can take fixed values of the variable like:

$$\emptyset_n(t) \rightarrow \emptyset_n$$

$$A_n(t) \rightarrow A_n$$

Where *n* is the number of OFDM blocks.

T is a time interval and the signal is sampled by *1/T* then it can be represented by:

$$S_S(kT) = \frac{1}{N}\sum_{n=0}^{N-1} A_n e^{j[(\omega_0+\omega\Delta n)kT+\emptyset_n]} \tag{4}$$

Let ω_0 be 0 then the signal becomes

$$S_S(kT) = \frac{1}{N}\sum_{n=0}^{N-1} A_n e^{j[(\omega\Delta n)kT+\emptyset_n]} \tag{5}$$

The signal is compared with general inverse discrete fourier transform (IDFT):

$$g(kT) = \frac{1}{N}\sum_{n=0}^{N-1} G(\frac{n}{NT})e^{[2\pi nk/N]} \quad (6)$$

Here, $S(kT)$ is in time domain.

Both are equivalent if

$$\Delta f = \frac{\Delta\omega}{2\pi} = \frac{1}{NT} = \frac{1}{\tau} \quad (7)$$

Where, τ is symbol duration period.

The OFDM signal can be defined by fourier fransform. The discrete fourier transform (DFT) can obtain frequency domain OFDM symbols and inverse discrete fourier transform (IDFT) can obtain time domain symbols. They can be written as:
discrete fourier transform

$$X(k) = \sum_{n=0}^{N-1} x(n)e^{-j[2\pi nk/N]} \quad (8)$$

inverse discrete fourier transform

$$x(n) = \sum_{n=0}^{N-1} x(n)e^{j[2\pi nk/N]} \quad (9)$$

where $0 \leq n \leq N-1$.

At the transmitter, data symbols on each subcarrier are chosen from a given M_k point signal constellation (k = 0, ...,N − 1), each of time duration T_s. M_k may be different for different subcarriers if bit loading algorithms are used (e.g., in DMT systems). On the other hand, usually $M_k \equiv M$ in wireless communication systems.
Each N data symbols form an OFDM block X_k = [X_0, ...X_{N-1}], which are modulated to N subcarriers and then added together and up converted to the carrier frequency for transmission. From (1) baseband equivalent time domain signal after D/A conversion is

$$x_l(t) = \frac{1}{\sqrt{N}}\sum_{k=0}^{N-1} X_{l,(k+N)}\, e^{j2\pi k\Delta f t}\ ,\ 0 \leq t \leq T \quad (10)$$

with (k + N) denoting (K + N) modulo N, $\Delta f = 1/T$ representing the frequency spacing, and $T = NT_s$ being the time duration of the OFDM symbol. Because different OFDM symbols do not overlap, only one OFDM symbol needs to be considered, and the subscript "l" can be dropped.
Equation (10) can be calculated more conveniently in the discrete time domain. By sampling $x(t)$ at frequency $f_s = JN/T$, where J is the oversampling factor, the discrete time OFDM symbol x_n can be written as

$$x_n = \frac{1}{\sqrt{N}} \sum_{k=0}^{N-1} X_{(k+N)}\, e^{j2\pi nk/JN} \;,\; n=0,\ldots\ldots,\, JN\text{-}1 \qquad (11)$$

When $J = 1$, the above equation (11) reduces to the nyquist rate sampling case. (10) can be implemented by using a length (JN) IDFT operation with the input vector

$$X_{\text{ext}}=[X_0,\ldots\ldots\ldots\ldots, X_{N/2-1}, 0,\ldots\ldots,0 \;, X_{N/2},\ldots\ldots, X_{N-1}]. \qquad (12)$$

Thus, X_{ext} is extended from X_k by using the so called zero-insertion scheme, i.e., by inserting $J(N-1)$ zeros in the middle of X_k.
In this literature, the zero-padding scheme, which appends $J(N-1)$ zeros at the end of X, is used. By using the zero-padding scheme, (10) and (11) may be written as

$$x(t) = \frac{1}{\sqrt{N}} \sum_{k=0}^{N-1} X_k\, e^{j2\pi k\Delta f t} \;,\; 0 \le t \le T \qquad (13)$$

$$x_n = \frac{1}{\sqrt{N}} \sum_{k=0}^{N-1} X_{(k+N)}\, e^{j2\pi nk/JN} \;,\quad n=0,\ldots\ldots,\, JN\text{-}1 \qquad (14)$$

and the implementation of (14) is a length (JN) IDFT with the input vector

$$X_{\text{ext}}=[X_0, X_1,\ldots\ldots\ldots\ldots X_{N-1}, 0,\ldots\ldots,0\,] \qquad (15)$$

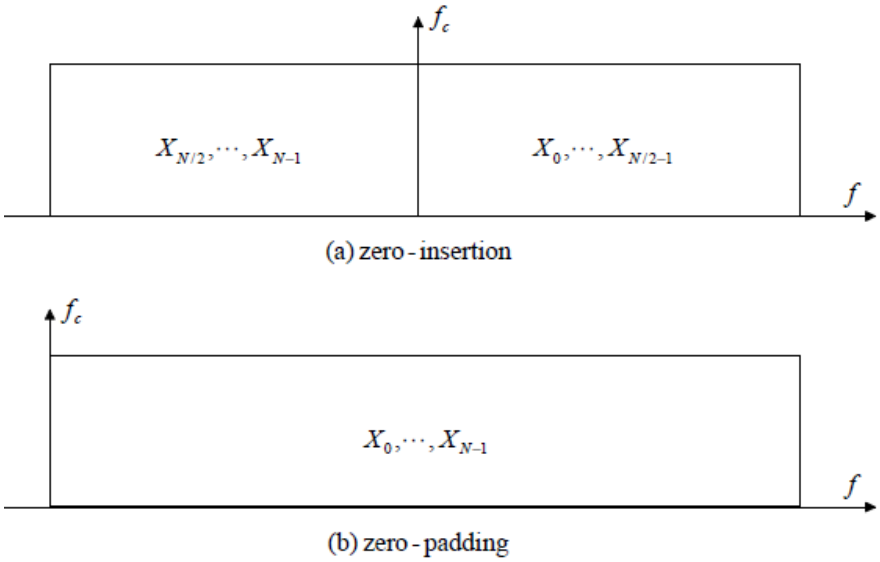

Figure 1.3. *OFDM spectrum of zero padding and insertion system*

The difference between the zero-insertion and zero-padding schemes is the position of the carrier frequency f_c. Figure 1.3 illustrates the frequency spectrum of both schemes. If zero-insertion is used, f_c is in the middle of the OFDM spectrum, $X_{N/2}$, ...,X_{N-1} are modulated to the lower side-band (i.e., to the negative frequencies in the baseband equivalent model), and the $(N/2-1)^{th}$ and $(N/2)^{th}$ subcarriers are of the highest and lowest frequencies, respectively. On the other hand, if zero-padding is used, f_c is on the left end of the OFDM spectrum, no lower side-band exists, and the 0^{th} and $(N-1)^{th}$ subcarriers are of the highest and lowest frequencies, respectively. Both schemes matches practical situations and is easy to use for clipping analysis by using the level crossing theory.

At the receiver, the received signal is first down converted to baseband and is partitioned into signal blocks $y_l(t)$, each with time duration T. Then the l^{th} OFDM block can be extracted from the $y_l(t)$ by using a set of orthogonal signal basis $e^{-j2\pi k\Delta ft}$, k = -N/2,….., N/2-1. Also, because any pair of $y_l(t)$ will not overlap, the subscript "l" can be dropped in our analysis.

In practice, the received signal $y(t)$ is first sampled at the nyquist frequency to obtain the discrete-time signal y_n. Then, the OFDM block is demodulated by using a length-N DFT operation in accordance with

$$Y_k = \frac{1}{\sqrt{N}}\sum_{n=0}^{N-1} y_n\, e^{-j2\pi nk/N}\ ,\quad k=0,\ldots\ldots N\text{-}1. \tag{16}$$

1.4 Cyclic Prefix and FEQ

The cyclic prefix (CP) of a discrete-time signal x_n is the last v samples of x_n. It is inserted at the beginning of x_n to combat the ISI without using complicated equalization techniques. Because of the multipath delay spread, signal dispersion and overlapping will occur, leading to ISI. In other words, if the channel impulse response is h_n, $n = 0, ..., L_h - 1$, with L_h representing the length of h_n, the received signal y_n (without considering the channel noise) is the linear convolution of x_n and h_n.

However, with the use of a cyclic prefix, y_n can be written as the circular convolution of x_n and h_n, provided that $v \geq L_h - 1$; i.e.,

$$y_n = x_n \otimes h_n \tag{17}$$

where $\otimes$ denotes circular convolution. In this case, after the DFT operation and dropping the cyclic prefix, we have

$$Y_k = X_k H_k \, , \, k = 0, ..., N - 1 \tag{18}$$

where H_k's are the N-point DFT of h_n. Therefore, if H_k's are known, X_k can be recovered at the receiver by using a set of FEQ $W_k = 1/H_k$ in accordance with

$$X_k = Y_k W_k = Y_k / H_k \tag{19}$$

The cyclic prefix is only a replica of x_n and will not affect our PAPR analysis and simulation results. Hence, this prefix will not be considered in the following analysis.

1.5 Advantages and Disadvantages of OFDM System

There are some advantages and disadvantages of OFDM are summarized below:

1.5.1 Advantages of OFDM

Some of the advantages of an OFDM system are as follows:-

1. OFDM is computationally efficient to employ the modulation and demodulation techniques by using fast fourier transform FFT.

2. The OFDM signal is robustness in multipath propagation environment and more tolerant of delay spread.

3. OFDM is more resistant to frequency selective fading than single carrier transmission systems.

4. OFDM system gives good protection against co-channel interference and impulsive parasitic noise.

5. Pilot subcarriers are used in OFDM system to prevent frequency and phase shift errors.

6. It is possible to use maximum likelihood detection with reasonable complexity.

7. OFDM is a good candidate for cognitive radio because of its flexibility and adaptability.

8. The orthogonality preservation procedures in OFDM are much simpler compared to CDMA/TDMA technique in multipath conditions.

1.5.2 Disadvantages of OFDM

Some of the disadvantages of an OFDM system are as follows:-

1. The OFDM signal suffers high PAPR of transmitted signal.

2. OFDM is very sensitive to carrier frequency offset.

3. It is difficult to synchronize when subcarriers are shared among different transmitters.

1.6 Problem statement

This thesis report presents the following work

1. Firstly, the conventional ICF method explained by Jean Armstrong is analyzed.
2. Then the present ICF method is modified by frequency domain filtering using Kaiser window, as it produces less peak re-growth.
3. Next, we have scaled the in-band noise due to clipping after z consecutive iterations approximately to the clipping noise generated in first iteration.
4. The OOB power due to clipping is attenuated by modified frequency domain filtering using Kaiser window, to minimize the interference between OFDM symbols.

1.7 Organization of thesis

This thesis is organized as follows:

CHAPTER 1: Presents an introduction of OFDM and describe its principles, advantages, disadvantages and the basic OFDM transceiver model.

CHAPTER 2: Explains the literature survey for the different PAPR reduction methods.

CHAPTER 3: Explains the one of the major problem associated with OFDM system i.e. PAPR.

CHAPTER 4: Explains some of the widely accepted PAPR reduction techniques.

CHAPTER 5: Explains the iterative clipping and filtering (ICF) method for PAPR reduction.

CHAPTER 6: Explains Proposed method: Statistical clipping with window based noise filtering (SC-W).

CHAPTER 7: Explains the simulation results of the new proposed method SC-W in comparison with ICF.

CHAPTER 8: Concluding remarks and future work

REFERENCES.

CHAPTER 2

LITERATURE SURVEY

Many PAPR reduction techniques are proposed in the literature [1-17] to reduce the PAPR of the OFDM signal. The PAPR reduction schemes are majorly divided into two categories
a) Distortion based Techniques [1-9] b) Non-distortion Techniques [10-17]
The schemes that introduce spectral re-growth belong to distortion based category. These techniques are the most straight forward PAPR reduction methods. The clipping [1, 2] is one of the simplest distortion based technique to reduce the PAPR of OFDM signal. It reduces the peak of the OFDM signal by clipping the signal to the desired level but it introduces both in-band distortion and out of band radiation. To limit out of band radiation and PAPR, Jean Armstrong proposed iterative clipping and filtering scheme [3].

Companding is another popular distortion based scheme for PAPR reduction in OFDM system. In [4], Wang *et al.* proposed a scheme based on μ-law companding to reduce the PAPR of OFDM signal. In μ-law companding scheme the peak value of the OFDM signal before and after companding remains same, which keeps peak power of the OFDM signal unchanged but the average power of the OFDM signal after companding increases and therefore the PAPR of the OFDM signal gets decreased. But due to increase in the average power of the OFDM signal the error performance of μ-law companding scheme degrades.

Jiang *et al.* proposed exponential companding (EC) function [5] to transform Rayleigh distributed magnitude of OFDM signal to a uniformly distributed OFDM signal using an exponential function and this scheme is known as "Exponential Companding" scheme. Exponential companding scheme can effectively reduce the PAPR of the OFDM signal but its BER performance also degrades with PAPR reduction.

Huang *et al.* proposed four companding transformation functions [6] to reduce the PAPR of the OFDM signal, which includes: linear symmetrical transform (LST), linear non symmetrical transform (LNST), non linear symmetrical transform (NLST) and non linear non-symmetrical transform (NLNST). It has been shown that LNST performs the best among four companding

function [6]. In LNST an inflexion point is introduced to treat large and small signals on different scale to achieve better BER and PAPR performance.

Linear companding transform (LCT) [7] has been proposed by Sulaiman *et al.* to reduce the PAPR of the OFDM signal. LCT also treats large and small signals on different scale but has two inflexion points to achieve more flexibility in designing the companding function. The abrupt change in the transformed signal at inflexion point degrades the power spectral density (PSD).

Trapezoidal companding (TC) [8] proposed by Hou *et al.* is an efficient method to reduce the PAPR of OFDM signal with low BER. TC [8] transforms the Rayleigh distributed magnitude of original OFDM signal to a trapezoidal distribution and called "Trapezoidal Companding". Trapezoidal companding utilizes a piecewise function defined in three intervals of OFDM signal magnitude.

Jeng *et al.* proposed [9] trapezium distribution based companding (TDBC) to transform the Rayleigh distribution of original OFDM signal to biased linear distribution called "Trapezium distribution".
All the companding schemes [4-9] distort the shape of the original OFDM signal and PAPR reduction capability is achieved at the cost of BER performance degradation.

Non-distortion PAPR reduction schemes do not distort the shape of the OFDM signal and therefore no spectral re-growth takes place. Coding technique [2] is one of the simplest non distortion PAPR reduction schemes, which can be applied for reducing the PAPR of OFDM signal. But these type of schemes result in significant loss of data rate in OFDM system.
Two more distortionless PAPR reduction techniques namely partial transmit sequence (PTS) [10] and selective mapping (SLM) [11] are also proposed in the literature. In PTS scheme all the subcarriers are partitioned into multiple disjoint sub blocks and then each of the sub blocks is multiplied by a set of rotating phase factors and combined to achieve a signal with lowest PAPR. In SLM, parallel data signal of length N is multiplied by a predetermined set of U phase vectors of length N and generates U alternative signals. Out of U alternative signals, one of them with the least PAPR is selected for transmission. In both of the schemes the information about the

phase factors by which these sub blocks/data symbols are multiplied, needs to be conveyed to the receiver and it is known as side information (SI). The SI has the highest importance because it is used to recover the original data signal. If SI gets corrupted then entire OFDM symbol block can be damaged and error performance of SLM and PTS-OFDM system degrades severely. In PTS technique, if the number of sub blocks increases then it not only increases computational complexity for selecting the optimum set (provide least possible PAPR) of phase sequence but also increases the amount of SI to be conveyed to the receiver. The SI results loss of data rate in OFDM system. Similarly in SLM-OFDM systems as the number of alternative OFDM signal increases, the number of bits required to encode the side information also gets increased, which results in data rate loss. The SI bits are extremely important for data recovery and it may be necessary to allocate few redundant bits to ensure accurate recovery of SI, but this operation will further increases the loss of data rate in OFDM system.

Many schemes for embedding the SI have been proposed in [12-13] for PTS-OFDM systems. In [14-16] many SI embedding schemes have been proposed for SLM-OFDM system. These schemes [12-16] embed SI in the OFDM signal without using any extra bit. At the receiver, SI is extracted from the received OFDM signal, and decoded to obtain the information about the phase factor used at the transmitter to minimize PAPR. The demodulated signal is multiplied by the reciprocal of recovered phase factors, due to which the computational complexity at the receiving end gets increased. In many of the SI embedding schemes, the SI detection at lower values of SNR is very poor, due to which error performance of the OFDM system degrades severely.

Existing SI embedding schemes [12-16] eliminates the requirement of SI transmission but these suffer from one drawback or the other, whether in terms of computational complexity, poor PAPR reduction capability or incorrect SI detection.

In [17], Zhou *et al.* proposed MPSM-PTS scheme which extends the QPSK constellation points to disjoint points of 16-QAM constellation and eliminates the requirement of side information. The MPSM-PTS scheme [17] is completely free from SI, i.e. extraction of SI from the received signal is not required. Hence the receiver structure of the scheme proposed in [17] is computationally less complex.

In wireless standards like long term evolution (LTE), OFDM is used in downlink, where mobile station acts as receiver. The mobile stations have limited computational resources, therefore a PAPR reduction scheme with less computational complexity at receiving end will be more beneficial. As discussed above, the schemes proposed in [12-16] have computationally complex receiver in comparison to the schemes proposed in [12, 13]. Hence, MPSM-PTS scheme is a viable choice for PTS-OFDM system.

Based on our review of the existing literature, the MPSM-PTS method of [17] is a suitable scheme to eliminate the requirement of SI in PTS-OFDM system, in terms of complexity and performance.

As discussed earlier, OFDM system is very sensitive to small carrier frequency offset; a small carrier frequency offset in between transmitter and receiver carrier frequencies can disturb the orthogonality of the subcarriers and causes ICI. The ICI interference degrades the overall performance of the OFDM system. It is generally characterized by carrier to interference ratio (CIR).

Various ICI cancellation techniques have been proposed in the literature to eliminate the effect of ICI, these include ICI self-cancellation[18], new ICI self-cancellation[19], general ICI self-cancellation scheme[20], ICI conjugate cancellation scheme[21], general phase rotated conjugate transmission ICI cancellation scheme[22] etc.

In [18] Zhao and Haggman proposed an ICI cancellation scheme called “ICI self cancellation” to combat the effect of ICI. In this scheme the data symbols are repeated on multiple adjacent subcarriers using polynomial coding but it results in PAPR performance degradation. The CIR performance of ICI self cancellation can be further improved by the scheme [19] proposed by Santhananthan *et al.* and called “New ICI self-cancellation scheme”. In this scheme [19] data symbols are repeated symmetrically using polynomial coding, which achieves frequency diversity effect of multipath fading channel. The CIR and the BER performance of ICI cancellation schemes [18], [19] are claimed to be further improved by General ICI cancellation scheme[20], proposed by Seyedi *et al.*, which is based on windowing technique used at the transmitter and receiver of OFDM system.

In [21] ICI cancellation schemes called “ICI conjugate cancellation” have been proposed. In these schemes time domain OFDM signal and its conjugate signal are transmitted over two parallel paths. It has been shown that ICI conjugate cancellation scheme[13] in presence of small frequency offset provides better CIR performance and BER performance in fading channels as compared to ICI self -cancellation schemes [18-19].

The CIR and BER performance of [18-21] are further improved by the scheme proposed by Wang *et al.* [22] called “General phase rotated conjugate transmission ICI cancellation scheme”. It [22] is a combination of carrier frequency estimation technique and ICI conjugate cancellation scheme [22]. It has been shown that ICI conjugate cancellation scheme [21] is a special case general phase rotated conjugate cancellation [22].

CHAPTER 3

THE PROBLEM OF PAPR

In OFDM systems, because the transmitted signal is the sum of a set of modulated signals, the peak power of the transmitted signal can be very high compared to its average power. Although occurring only with low probability, such large peaks have negative ramifications for the overall system. For instance, the HPA for radio frequency (RF) transmission has to have a large linear range, which, however, is inefficiently used.

Moreover, the distortion incurred by the nonlinearity of the HPA leads to in-band distortion and out of band radiation. The in-band distortion leads to increased BER. On the other hand, the out of band distortion may severely interfere with the signal transmitted in the adjacent frequency bands.

The PAPR of the transmitted signal can be defined as the ratio of the instantaneous power over the average power of the transmitted signal [23]:

$$\mathrm{PAPR}_{x_c(t)} \triangleq \frac{\max|x_c(t)|^2}{\mathrm{E}\{|x_c(t)|^2\}},\ 0 \le t \le T\,, \tag{20}$$

where $\mathrm{E}\{\cdot\}$ represents the mean value. On the other hand, the PAPR problem can also be measured by using the baseband equivalent signal $x(t)$. Because [24]

$$\max |x_c(t)| \approx \max |x(t)|, \tag{21}$$

and

$$\mathrm{E}\{|x_c(t)|^2\} \approx \frac{1}{2}\mathrm{E}\{|x(t)|^2\}, \tag{22}$$

We have

$$\mathrm{PAPR}_{x_c(t)} \approx 2\ \mathrm{PAPR}_{x(t)}. \tag{23}$$

The above definition of the PAPR can be called the continuous time PAPR. In practical situations, usually the PAPR is calculated based on the oversampled baseband equivalent signal x_n obtained from (11), in accordance with

$$\text{PAPR} \triangleq \frac{\max|x_n|^2}{\text{E}\{|x_n|^2\}} \tag{24}$$

This PAPR distribution is referred to as the discrete time PAPR in this thesis. It was shown in [25, 26] that nyquist sampling ($J = 1$) may not capture all peaks of $x(t)$. Therefore, oversampling is necessary to approximate the continuous time PAPR by using the discrete time PAPR. It has been shown [23] that for an acceptable approximation, the oversampling factor J is required to be $J \geq 4$. From (11) and (14),

$$\text{E}\{|x_n|^2\} = \frac{1}{N}\sum_k |X_k|^2, \tag{25}$$

If X_k are independent, identically distributed random variables, the PAPR of an OFDM system is N. Therefore, in practice, a statistical definition of PAPR is more frequently used. An OFDM signal is said to have a peak at ξ with probability P_c if $\Pr[\text{PAPR}(X) \leq \xi] = P_c$.

The PAPR complementary cumulative distribution function (CCDF), also called the clip probability, is defined as $P(\xi) = \Pr[\text{PAPR}(X) > \xi] = 1 - P_c$; i.e., the probability that PAPR exceeds ξ is $1 - P_c$. For example, the PAPR distribution for different oversampling factors and for different N's are shown in Figures 3.1 and 3.2, respectively, which show that $J = 4$ can provide an acceptable approximation to the continuous time PAPR distribution.

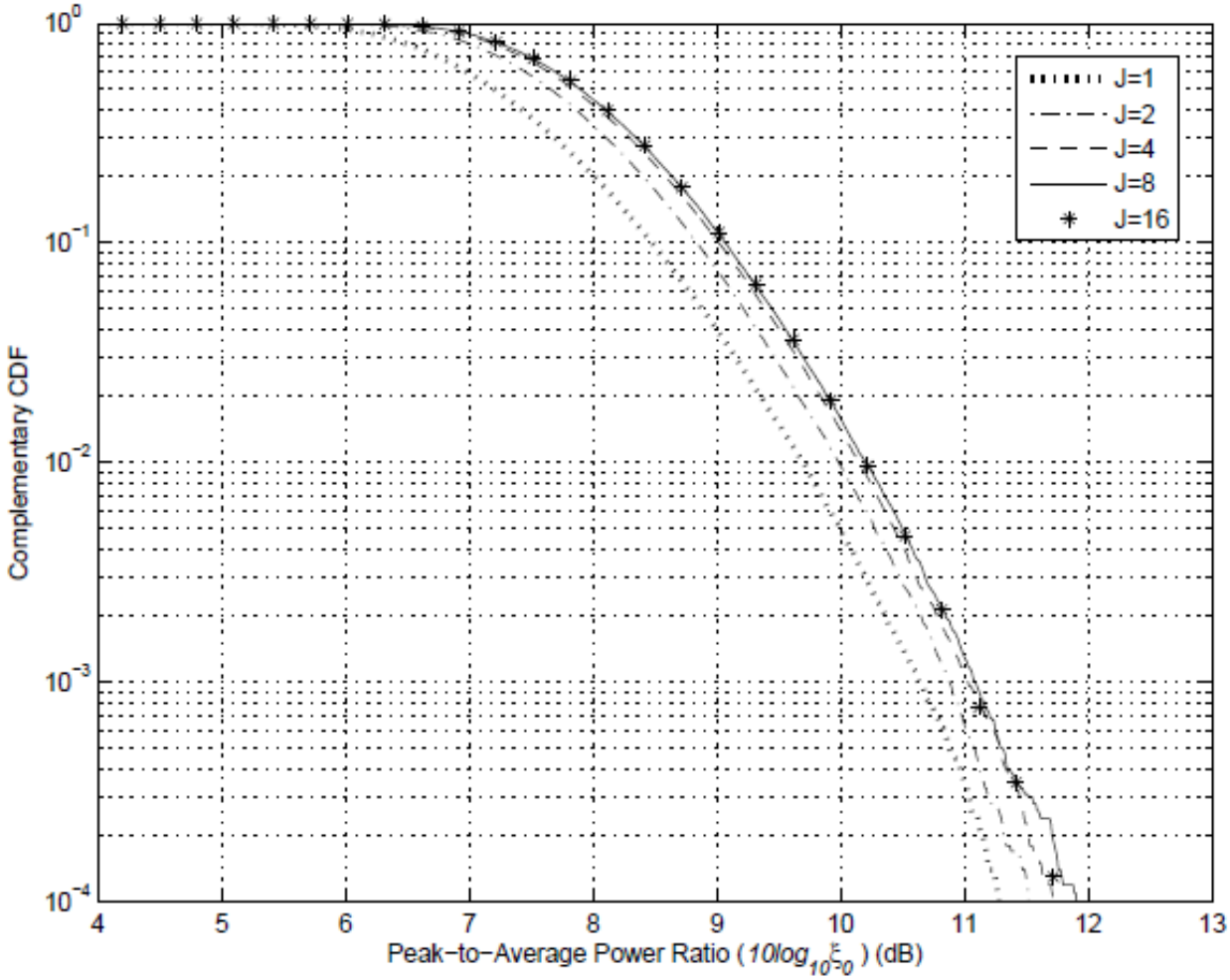

Figure 3.1. *PAPR distribution for different oversampling factors, N=128*

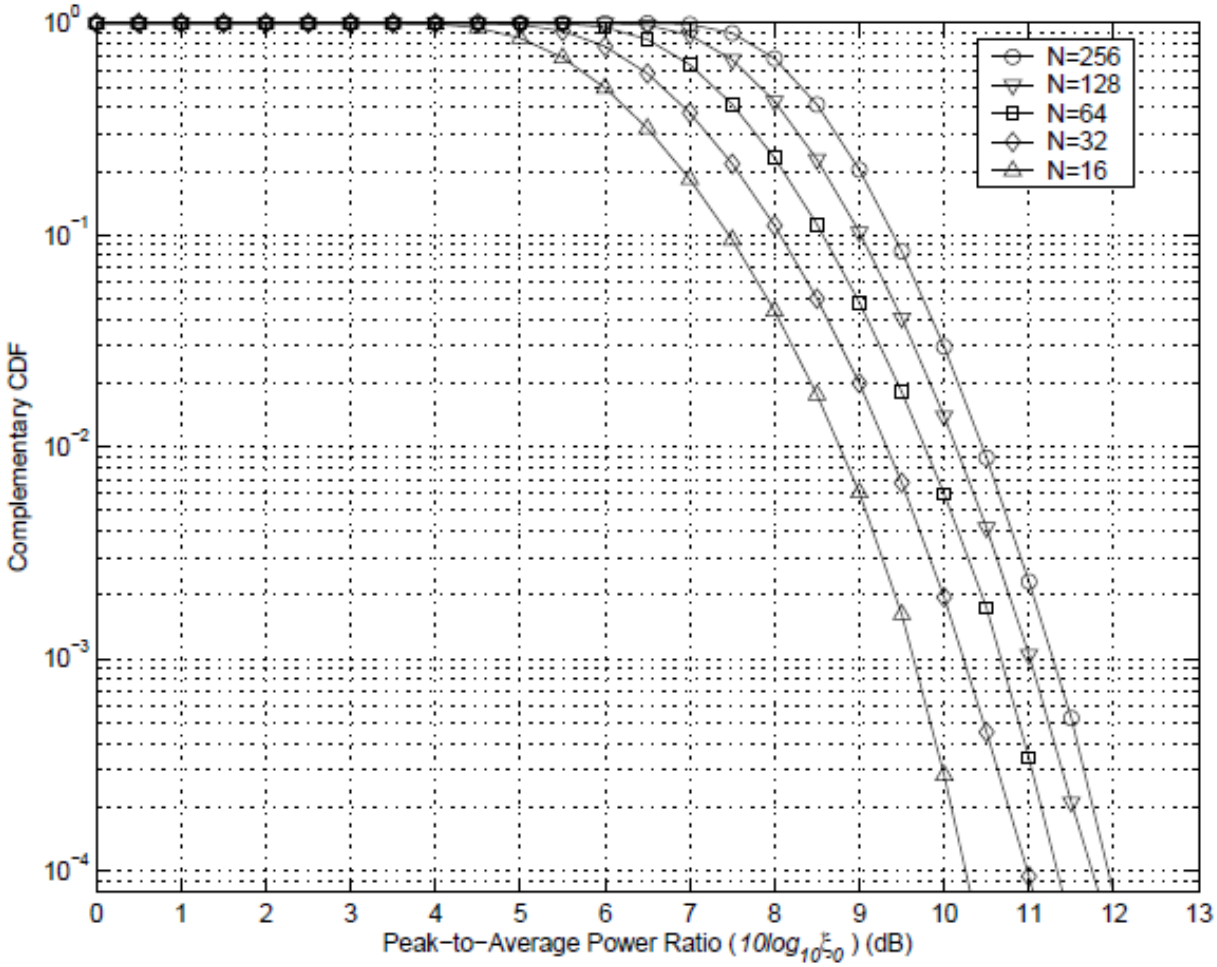

Figure 3.2. *PAPR distribution for different N, J=4*

CHAPTER 4

PAPR REDUCTION TECHNIQUES

4.1 High-Power Amplifiers

The purpose of PAPR reduction is to counteract the nonlinear effect of the HPA. Usually, HPAs are characterized as memoryless nonlinear amplifiers in accordance with

$$g(x(t)) = F(|x(t)|)e^{J(\phi(t)+|\Phi(t)|)} \tag{26.1}$$

where $g(x(t))$ is the output of the HPA, $x(t) = |x(t)|e^{j\phi(t)}$ is the time domain signal input to the HPA, $F(|x(t)|)$ and $\Phi(|x(t)|)$ are respectively the AM/AM and the AM/PM distortion functions, where AM denotes the amplitude modulation and PM denotes the phase modulation. Usually HPAs can be partitioned into three categories: the soft limiter (SL), the solid state power amplifier (SSPA) and the traveling wave tube (TWT). Their characteristics can be described as follows.

4.2 Soft Limiter

The soft limiter [27] is the simplest model of the HPA. It introduces no distortion in the phase of the input signal and simply clips the signal magnitude when it exceeds a threshold. Therefore, the output of the soft limiter can be written as

$$g(x(t)) = \begin{cases} Ae^{j\phi(t)}, & |x(t)|>A, \\ x(t), & otherwise, \end{cases} \tag{26.2}$$

where $A > 0$ represents the threshold of the SL.

4.3 Solid State Power Amplifier (SSPA)

The SSPA is the most commonly used amplifier in wireless communications. The output of SSPA can be written as [28]

$$g(x(t)) = \frac{|x(t)|}{\left(1+\left(\frac{|x(t)|}{A}\right)^{2p}\right)^{\frac{1}{2p}}} e^{j\emptyset_n} \tag{27}$$

i.e., it introduces no distortion in the signal phase. When $p \rightarrow \infty$, the SSPA becomes the SL. Usually p =2 or 3 is chosen for a practical SSPA.

4.4 Traveling-Wave Tube

TWTs are wideband amplifiers widely used in satellite communications [28]. The AM/AM and AM/PM functions of TWT can be written as

$$F(|x(t)|) = \frac{|x(t)|}{1+\left(\frac{|x(t)|}{2A}\right)^2} \tag{28}$$

$$\Phi(|x(t)|) = \frac{\pi}{3}\frac{|x(t)|^2}{|x(t)|^2+4A^2} \tag{29}$$

As a comparison, the AM/AM functions of SL, SSPA (for p = 3 and p = 10), and TWT are shown in Figure 4.1. The AM/PM function of TWT is shown in Figure 4.2.

4.5 PAPR Distribution and BER Performance

When X_k are PSK symbols, an upper bound of the PAPR can be easily obtained as [29]

$$\xi \leq 1 + \frac{2}{N}\sum_{n=1}^{N-1} |R_X(n)|\,, \tag{30}$$

where $R_x(n)$ is the aperiodic autocorrelation function of X_k defined as

$$R_X(n) = \sum_{k=0}^{N-n-1} X_{k+n} X_k^* , \tag{31}$$

with $(\cdot)^*$ representing the complex conjugate. With the assumption that X_k are independent identically distributed (i.i.d.) random variables and based on the central limit theory, x_n can be approximated as (complex) gaussian random variables when N is large. Then, $|x_n|$ is Rayleigh distributed. The PAPR distribution can be approximated as [30]

$$\Pr[\xi \le \xi_p] \approx (1 - e^{-\xi_p/2\sigma^2})^{\alpha N} , \tag{32}$$

Where σ^2 is the variance of the real or imaginary part of x_n, and α= 2.8 (obtained from empirical experiments). More accurate approximations are available in [31–50].

In [40], by using the theory of the level-crossing rate and normalizing $r(t) = |x(t)|$ such that $2\sigma^2 = 1$, the probability that all peaks are lower than r is

$$\Pr(\max[r(t)] < r) \approx \begin{cases} (1 - \frac{re^{-r^2}}{\bar{r}e^{-\bar{r}^2}})^{\sqrt{\frac{\pi}{3}}e^{-\bar{r}^2}N\bar{r}} & for\ r > \bar{r} \\ 0 , & for\ r \le \bar{r} \end{cases} \tag{33}$$

where $\bar{r}$ is empirically obtained as $\bar{r} = \sqrt{\pi}$ for quadrature phase shift keying (QPSK) and slightly lower for 16QAM. The PAPR distribution can then be found by replacing r and $\bar{r}$ with $\sqrt{\xi_p}$ and $\sqrt{\xi}$ respectively.

The effect of signal clipping on BER performance has been extensively studied.

Such analysis focuses mainly on the signal to noise plus distortion ratio (SNDR) and BER after the passage of $x(t)$ through an SL.

Clipping $x(t)$ by the SL introduces a clipping noise $f(t) = x(t) - g(x(t))$, which includes in-band distortion and out of band radiation. Fig. 4.3 illustrates the power spectral density (PSD) of unclipped and clipped OFDM signals. 9 dB clipping leads to relatively small (−51 dB) out of band radiation. However, deeper clipping, e.g., 6 dB and 3 dB clipping, significantly increases out of band radiation to −31 dB and −21 dB, which may be unacceptable in practical

communications. In [39], it is shown that by applying Bussgang's theorem [27], the clipped signal can be written as

$$\hat{x}_n = \alpha x_n + d_n \,, \quad n=0,\ldots\ldots,JN-1 \tag{34}$$

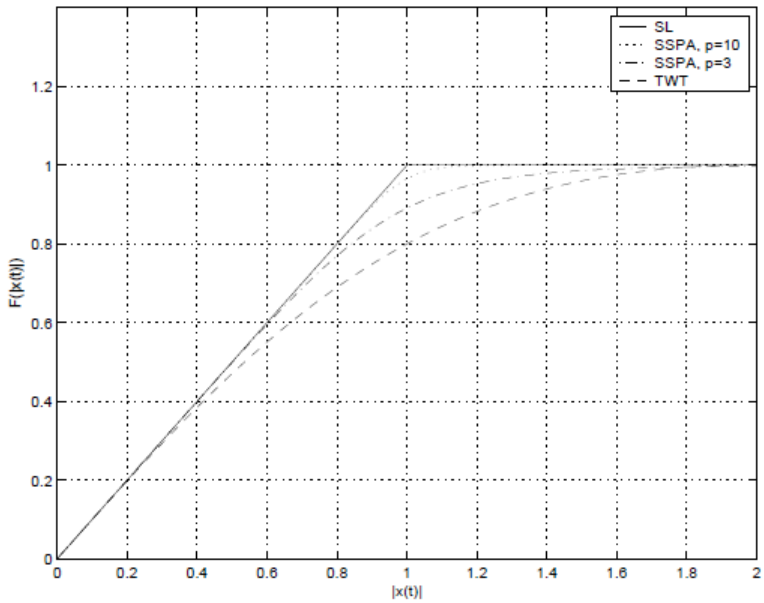

Figure 4.1. *AM/AM functions of SL, SSPA (for p = 3 and p = 10), and TWT*

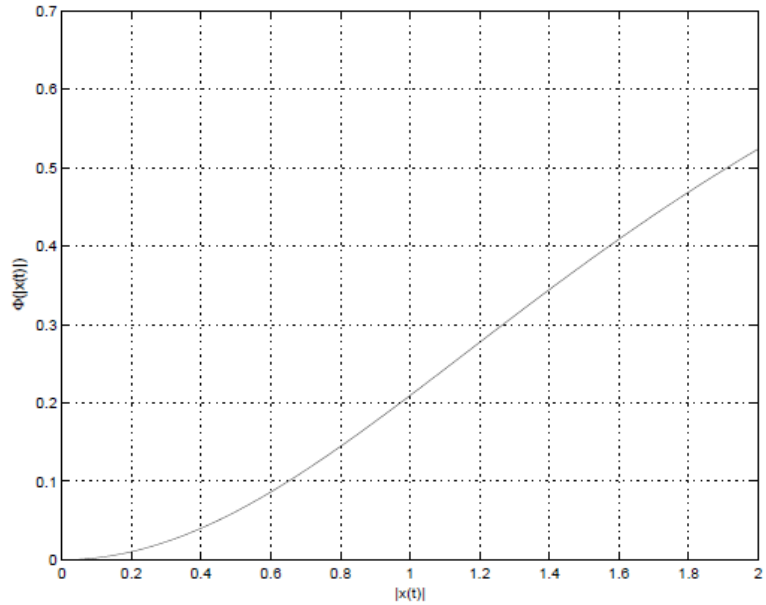

Figure 4.2. *AM/PM function of TWT*

where x_n and d_n are uncorrelated, and the attenuation factor α can be found as

$$\alpha=1-e^{-\gamma^2}+\frac{\sqrt{\pi}\gamma}{2}erfc(\gamma) \tag{35}$$

with $\gamma = A/\sqrt{P_i}$.

For large N and small A, the clipping noise can be approximated as a gaussian process. For nyquist-rate clipping (x_n is nyquist-rate sampled), no out of band radiation exists. In this case, the SNDR for additive white gaussian noise (AWGN) channel is given by [39]

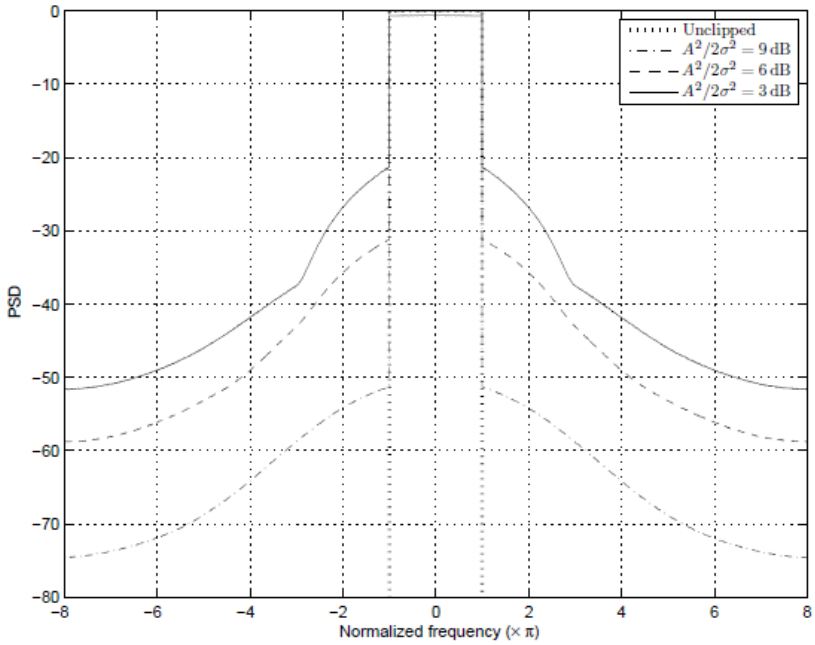

Figure 4.3. *Power spectral density of unclipped and time-domain-clipped OFDM signals*

$$\text{SNDR} = \frac{K_\gamma E_s/N_0}{\frac{(1-K_\gamma)E_s}{N_0}+1} \tag{36}$$

where E_s/N_0 is the ratio of the signal energy over the noise power spectral density (PSD) after clipping, and $K_\gamma = \alpha^2/(1-e^{-\gamma^2})$. The BER of QPSK is then given by

$$P_b = Q(\text{SNDR}), \tag{37}$$

Where $Q(x) = \frac{1}{2\pi}\int_x^\infty e^{-t^2/2}dt$.

The assumption of gaussian clipping noise holds only for small *A*. When *A* is large, the clipping noise is a series of pulses which can be approximated as parabolic arcs [51]. Based on this approximation, the BER of a real valued time domain OFDM signal (which is used for DMT applications) can be calculated as [52, 53]

$$P_b = \frac{8N(L-1)}{\sqrt{3}L} e^{\frac{\gamma^2}{2}} Q\left(\left[\frac{3\pi\gamma^2}{\sqrt{8(L^2-1)}}\right]^{\frac{1}{3}}\right), \quad (38)$$

where a square constellation of L^2 points with a minimum distance of *2d* is assumed. In [43], the performance of OFDM with a strictly limited peak power requirement is analyzed. The analytical results show that the clipping technique exhibits the lowest input back off (IBO) requirement compared to the probabilistic techniques, especially when *N* is large.

4.6 PAPR-Reduction Techniques

Various techniques have been proposed to reduce the PAPR, including clipping based techniques, probabilistic techniques and coding techniques.

4.6.1 Categorization of the PAPR Problem

PAPR research can be divided into two categories: 1.) PAPR distribution and BER evaluation and 2.) the development of efficient PAPR reduction techniques. Figure 4.4 illustrates this categorization. PAPR reduction techniques can be further divided into two categories: techniques with distortion and without distortion. Techniques with distortion are usually based on signal clipping and lead to continuous solutions where the OFDM signals are modified in a continuous manner. These techniques include iterative clipping and filtering [1, 3, 54, 55] and companding [56]. A detailed discussion of iterative clipping and filtering will be presented in the next subsection and chapter 5.

For techniques with distortion, distortion cancellation techniques are necessary in order to reduce a possible BER loss. A task common to both categories is the development of low complexity algorithms.

Distortionless PAPR reduction techniques are more attractive because they do not increase the BER. In fact, the BER can even be decreased by exploiting the inherent redundancy. These techniques can be divided into three categories: 1.) techniques having continuous solutions such as tone reservation and active constellation extension (ACE) 2.) techniques having discrete solutions such as SLM, PTS and tone injection and 3.) coding techniques. Distortionless techniques may need side information for correct detection. Developing efficient decoding techniques is also a related research area.

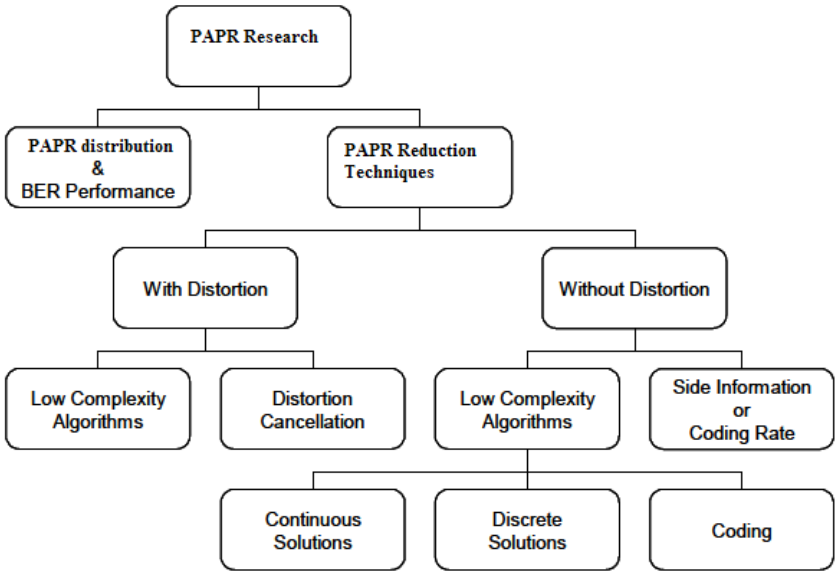

Figure 4.4. *Categorization of the PAPR problem*

While the PAPR problem has obvious practical value, it is also related to many theoretical research areas such as discrete optimization and coding theories.

4.6.2 PAPR Reduction Techniques with Distortion

The simplest PAPR reduction technique is clipping and filtering [1, 3, 54, 55]. This technique clips the OFDM signal to a predefined threshold and uses a filter to eliminate the out of band

radiation. The purpose of this technique is to satisfy the spectral constraints so that the OFDM signal will not interfere with communications in the neighboring frequency bands. The in-band distortion, however, cannot be eliminated, leading to increased BER. Because the probability of large peaks is small, the in-band distortion is also small when the clipping threshold is large. Consequently, the BER increase may be small when, e.g., 4QAM is used, and may be tolerable in some applications.

On the other hand, the in-band distortion may be limited to a predefined strength [57–60] to reduce the BER increase, with the cost of degraded PAPR reduction performance. In [30], each clipping noise sample is multiplied by a window function (e.g., gaussian, kaiser, or hamming) to suppress the out of band noise. Because the overall effect is the convolution of the clipping samples and the windowing function, this approach leads to a bandwidth increase. Alternatively, the in-band distortion can also be partly canceled at the receiver with additional computational cost. [61–64].

Filtering out of band radiation can be done in the time domain by using a low pass filter [54] or in the frequency domain by using a DFT/IDFT pair [1, 3, 65]. By using frequency domain filtering, which requires less execution time than using a time domain low pass filter, the clipping noise is converted to the frequency domain by using oversampled DFT and all out of band terms are set to zero. An IDFT is also required to convert the filtered clipping noise back to the time domain. Nevertheless, a side-effect of filtering is peak re-growth, shown in Figure 4.5.

After filtering, the signal peaks grows higher than the clipping threshold (but lower than the original peaks). Generally, peak re-growth can be combated by iterative clipping and filtering (ICF) [65]. However, the convergence is extremely slow after several iterations. To speed up the convergence, [65] proposes using a slightly lower clipping threshold, say, 95% of the desired PAPR level [55], to better suppress peak re-growth.

Clipping the OFDM signal is equivalent to passing the signal through a soft limiter. The clipped portion of the signal cannot be perfectly recovered. In contrast, the companding transform [56] passes the OFDM signal through a smooth nonlinear function.

$$y(t) = g(x(t)) \,, \tag{39}$$

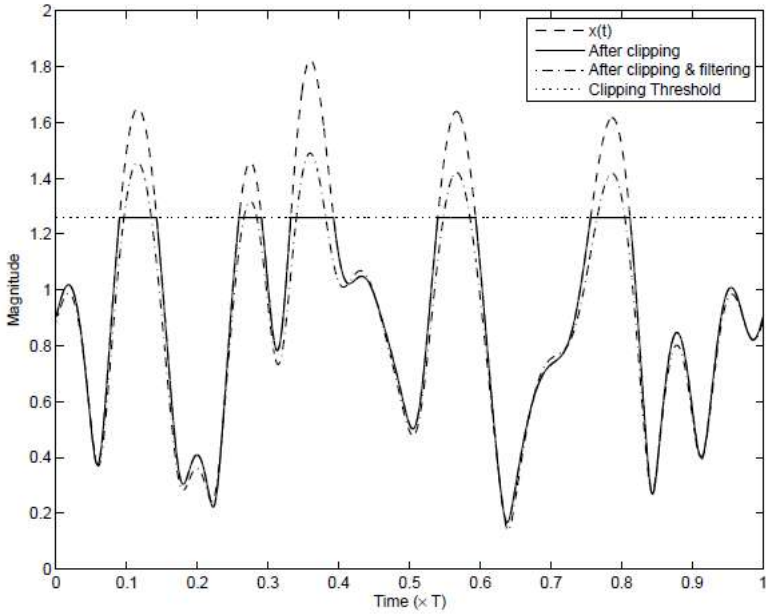

Figure 4.5 *Peak re-growth*

where $x(t)$ is the input OFDM signal, and $g(x)$ is the nonlinear companding transform, to compress the large peaks in $x(t)$. The probability that $y(t)$ has large peaks is then much smaller than before companding transforming.

At the receiver, $x(t)$ is recovered by using $g^{-1}(t)$, the inverse transform of $g\ (t)$.

The recovered OFDM signal can be written as

$$\hat{x}(t) = g^{-1}(g\big(x(t)\big) + z(t))\ , \tag{40}$$

where $z(t)$ is the channel noise. The companding transform has two drawbacks. First, the signal bandwidth is expanded after the transform (the bandwidth of the compressed signal is the same as the original signal only when the companding transform is applied to the nyquist-rate samples. However, the PAPR reduction performance is poor in this case). Second, the channel noise $z(t)$ is enhanced at the receiver when recovering the compressed samples. The bandwidth expansion and noise enhancement depend on the target PAPR level of the companding transform. If the target PAPR level is low, filtering is required at the transmitter to eliminate the out of band radiation, which introduces in-band distortion and peak re-growth. At the receiver, the BER may be unacceptable.

4.6.3 Clipping Noise Cancelation

Clipping noise can be partly cancelled at the receiver. In [66], the clipping noise is estimated and then cancelled by using oversampled signal reconstruction, which reconstructs the clipped samples by interpolating the oversampled signal. This method requires the transmission of a portion of the out of band radiation to the receiver.

Thus, the OFDM bandwidth must be expanded by 25% or more. [67] proposes a decision aided reconstruction method to mitigate the clipping noise. After channel equalization, this method first makes a hard decision (in the frequency domain) on the received signal samples $\hat{x}_n$ to estimate the data symbols, and then converts them back to the time domain to obtain $\bar{x}_n$. If the channel distortion and channel noise are omitted (the channel distortion and channel noise degrade the performance of clipping noise cancelation), $\hat{x}_n = x_n$ at the positions of $|x_n| \leq A$, where A is the clipping threshold. On the other hand, $\bar{x}_n$ contains samples larger than A at the positions of $|x_n| > A$, which may be a better estimation of x_n than $\hat{x}_n$ if the clipping is not severe. Therefore, x_n can be estimated more accurately by

$$\bar{x}_n = \begin{cases} \hat{x}_n, & x_n \leq A \\ \bar{x}_n, & \text{otherwise} \end{cases} \tag{41}$$

This method is further improved in [61–64] by reconstructing the clipping noise, and is later applied to coded OFDM [68, 69] and MIMO OFDM [70]. By using (34), the received samples after the DFT operation can be written as

$$Y_k = \alpha H_k X_k + H_k D_k + Z_k \,, \tag{42}$$

where Y_k, H_k, D_k and Z_k are the received signal, channel response, clipping noise, and AWGN on the k^{th} subcarrier, respectively. Assuming that H_k is known, a coarse estimation $\bar{X}_k$ can be obtained by making a hard decision on Y_k/H_k. By converting $\bar{X}_k$ to the time domain, clipping it

in the same fashion as at the transmitter, and converting the clipped signal back to the frequency domain, we have

$$\tilde{X}_k = \alpha \bar{X}_k + \bar{D}_k \ . \tag{43}$$

Assume that most $\hat{X}_k$ are correct. Then $\bar{D}_k \approx D_k$, and one can use $\bar{D}_k$ to obtain a better estimation of X_k i.e.,

$$\hat{Y}_k = Y_k - H_k \bar{D}_k = \alpha H_k X_k + H_k (D_k - \bar{D}_k) + Z_k \tag{44}$$

This procedure can be repeated to improve the estimation accuracy.

4.6.4 Tone-Reservation

The tone-reservation technique reserves N_r tones for PAPR reduction and uses the remaining ($N - N_r$) tones for data transmission [71, 72]. The reserved tones may be randomly selected, or be selected from the subcarriers that have low SNR and are not suitable for data transmission. The tone-reservation ratio $R = \frac{N_r}{N}$ is typically small. The peak-canceling signal $c(t)$ is generated based on the reserved tones, and the peak-reduced signal is given by

$$\hat{x}_t = x(t) + c(t) = \frac{1}{\sqrt{N}} \sum_{k=0}^{N-1} (X_k + C_k) e^{2\pi k t / T} \ , \ \ 0 \le t \le T, \tag{45}$$

where C=[C_0,.....,C_{N-1}] is the set of peak-canceling tones. $\hat{x}_t$ is amplified by the HPA and transmitted to the receiver. Let R = {i_0,….., i_{r-1} } be the locations of the reserved tones, where $-\frac{N}{2} \le i_0 < i_1 <\ldots\ldots < i_{r-1} \le \frac{N}{2} - 1$. Let the index set R^c be the complement of R in $N = \{0, \ldots . N-1\}$. The constraint on *c(t)* is that C must satisfy $C_k \equiv 0$ for $k \in R^c$. On the other hand, X must satisfy $X_k \equiv 0$ for $k \in R$. X and C are not allowed to be nonzero on the same subcarriers; i.e.,

$$X_k + C_k = \begin{cases} X_k & k \in R^c, \\ C_k & k \in R \end{cases} \tag{46}$$

Clearly, this technique reduces the normalized system throughput to (1−*R*). For a frequency selective fading channel (ignoring the nonlinear amplification), demodulation is done on a per-tone basis. Thus, (46) allows the reserved tones to be readily discarded. With this method, the BER of the data tones is the same as that of the original OFDM system. However, the BER of the whole system is slightly increased due to the slightly increased average transmit power. With the tone-reservation, the PAPR is redefined as

$$\xi = \frac{\max |x(t)+c(t)|^2}{\mathrm{E}\{|x(t)|^2\}} \tag{47}$$

that is, the peak-canceling signal *c*(*t*) is excluded from the calculation of the average power to prevent the solution of a *c*(*t*) having an averaged power much larger than that of *x*(*t*). The denominator in (47) is a constant. Thus, *C* must be chosen to minimize the maximum of the time-domain signal:

$$C^{opt} = \arg\min_{\mathrm{C}\in C} \max_{0\le t\le T} \left| \sum_{k=0}^{N-1} (X_k + C_k) e^{\frac{j2\pi kt}{T}} \right|^2 . \tag{48}$$

Equation (48) can be reformulated as a quadratically constrained quadratic program (QCQP) [71]:

$$\min_{\mathrm{C}\in C} \text{subject to } |x_n + q_n \mathrm{C}|^2 \le E \tag{49}$$

for $n = 0, 1, ..., JN - 1$, where q_n is n^{th} row of the IDFT matrix. Equation (49) is convex, and the global optimum exists. However, finding the optimal solution requires a high computational cost. Suboptimal solutions are typically employed.

The simplest optimization technique for tone-reservation is iterative clipping and filtering [65]. In each iteration, this technique clips the OFDM signal to a predefined threshold *A*. The clipped

signal is then filtered such that the clipping noise exists only on reserved tones. The convergence rate of this technique is extremely slow [71].

The controlled clipper algorithm [71] iteratively calculates the peak reduced time domain OFDM signal as follows:

$$\bar{\mathrm{x}}^{i+1} = \bar{\mathrm{x}}^{i} - \mu \sum_{|\bar{x}_n^i|>A} \alpha_n^i \mathrm{P}_n^{||2} \tag{50}$$

where $\bar{\mathrm{x}}^i$ is the peak-reduced signal at the i^{th} iteration, $\bar{\mathrm{x}}^0$ = x, x is the OFDM signal, A is the target magnitude upper bound of the peak-reduced signal, α_n^i are the clipping noise samples at the i^{th} iteration, $\mathrm{P}_n^{||2}$ is the prototype peak-canceling signal, and C is the sample vector of the peak-canceling signal $c(t)$. The convergence rate of this algorithm slows down after several iterations, and many iterations are usually required to obtain a reasonable PAPR reduction [71].

An active-set algorithm is proposed in [72] for tone-reservation. This algorithm first approximates the peak boundary (a circle centered at the origin of the complex plane) as a polygon. For example, Fig 4.6 shows an octagon of radius A. The magnitude of point X can be approximated by

$$|X| \approx |X|_{Approx} = \max\left[\mathcal{R}[X], j[X], \mathcal{R}[Xe^{\frac{j\pi}{4}}], j[Xe^{\frac{j\pi}{4}}]\right], \tag{51}$$

where $\mathcal{R}[X]$ and $j[X]$ represent the real and imaginary parts of x, respectively. On the other hand, all points that satisfy $|X|_{Approx} \leq A$ are within the octagon of radix A. In other words, if we reduce the approximated peak of an OFDM signal to A, its actual peak would be only slightly larger than A.

With this polygonal approximation, the complex OFDM vector x is written as a real vector $\hat{\mathrm{x}}$ consisting of the real and imaginary parts of x and its phase-shifted. The active-set algorithm uses the same prototype peak-canceling signal $\mathrm{P}_n^{||2}$ (but is rewritten to a real vector $\widehat{\mathrm{P}}$, as explained above) to reduce the PAPR. This algorithm maintains an active set containing the peaks of $\hat{\mathrm{x}}$, whose magnitudes are reduced to the same level as that in previous iterations. Each sample x_{ni} in the active set is associated with a peak-canceling kernel $\hat{\mathrm{p}}_i$ (a shifted version of $\widehat{\mathrm{P}}$ whose peak is at n_i). These $\hat{\mathrm{p}}_i$ are weighted and summed together to form the peak-canceling

signal $\bar{p}$. In each iteration, the weighting factors of $\hat{p}_i$ are calculated by solving a set of l linear equations, where l is the iteration number, to find a proper optimization direction.

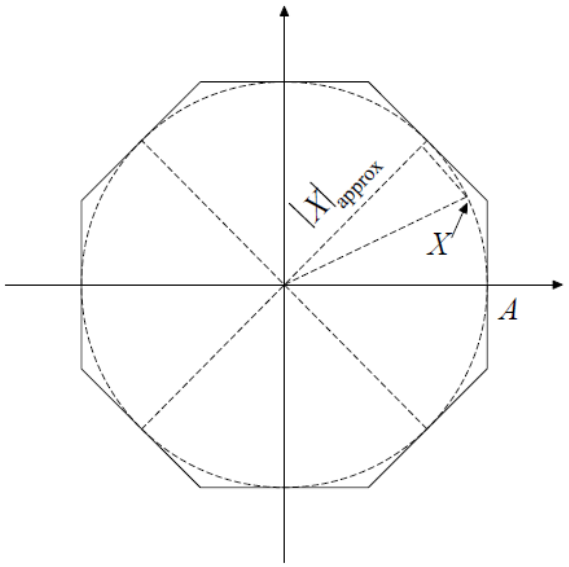

Figure 4.6 *Polygonal approximation of the peak boundary*

Then, at least all peaks of both $\hat{x}$ and $\bar{p}$ outside the active set (to ensure the active set criteria, generally all samples of $\hat{x}$ outside the active set must be tested are tested) to find a proper optimization step size μ. The peak-canceling signal $\bar{p}$ is weighted by μ and is subtracted from $\hat{x}$. Then, the magnitudes of all samples in the active set are equally reduced. The largest peak outside the active set is also reduced to the same magnitude of the samples in the active set, and is included in the active set. After several iterations, the PAPR is reduced to a moderate level.

4.6.5 Active Constellation Extension

The ACE technique allows the constellation be extended (by the clipping noise) so that the minimum Euclidian distance between any two constellation points does not increase. For example, the shaded areas in Figure 4.7 are the feasible extension regions for the 16QAM constellation.

Finding the optimal peak-canceling signal is similar to (49) but with the additional constraint that the peak-canceling signal in the frequency domain does not allow the use of any value beyond

the feasible region. The optimization methods discussed above can be applied to the ACE technique.

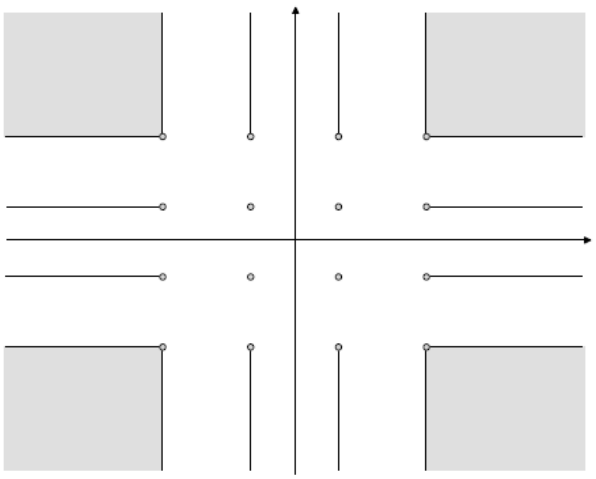

Figure 4.7. *Feasible extension region for 16-QAM constellation*

The ACE technique does not reduce the throughput. However, this technique slightly increases the average transmit power, leading to a slightly increased BER. Its PAPR-reduction capability depends on the signal constellation. Only the outer signal points in the constellation are allowed to move. If PSK or 4QAM constellations are used, all input data symbols are free to move in the feasible region, and a large PAPR reduction is obtained. On the other hand, when an M-ary QAM constellation, $M > 4$, is used, in average only $\frac{4\sqrt{M}-4}{M} N$ subcarriers in each OFDM block are available for PAPR reduction. Thus, the PAPR-reduction capability of ACE is small for large QAM constellations.

4.6.6 Probabilistic Techniques

By modifying the phase, amplitude and/or subcarrier position of input symbols, these techniques use several candidate OFDM signals to represent the same information, and select the one with the lowest PAPR. Side information may be required at the receiver for correct detection.

4.6.7 Phase-Adjustment Techniques

A widely used technique is the modification of the phase of the input modulation symbols to reduce the PAPR. Let X=[X_0,….., X_{N-1}] be an OFDM vector, and let $\mathrm{s} = [\mathrm{s}_0, \ldots\ldots, \mathrm{s}_{N-1}] = [e^{j\phi_0}, \ldots\ldots, e^{j\phi_{N-1}}]$ be a phase adjustment vector. Then the objective function is

$$\min_s(\text{PAPR of IDFT}(\mathrm{s} \odot \mathrm{x})) \tag{52}$$

Where $\odot$ represents the element wise multiplication. The optimal $\mathrm{s}^{(\mathrm{opt})}$ may be sent to the receiver as side information for the correct detection of the input modulation symbols. The distribution of s_k are i.i.d.'s, N is large, and $\mathrm{s}^{(\mathrm{opt})}$ is selected from K randomly generated phase adjustment vectors $\{\mathrm{s}^{(1)},\ldots.,\mathrm{s}^{(k)}\}$ according to a predefined distribution of s_k. If the PAPR is calculated on the nyquist-rate discrete time domain samples (i.e., J = 1 for calculating the IDFT), it has been proved that the PAPR of IDFT($\mathrm{s}^{\mathrm{opt}} \odot \mathrm{x}$) is minimized when E{$s_k$} = 0. Thus, we may choose s_k 1 or -1 with equal probability to minimize the resulting throughput loss. On the other hand, if the PAPR is calculated on the oversampled discrete time domain samples (i.e., J > 1) or on the continuous time domain signal, choosing s_k from a larger set (e.g., $s_k \in \{1, \mathrm{j}, -1, -\mathrm{j}\}$) leads to only minor improvement in the PAPR reduction.

Equation (52) describes a combinatorial optimization problem over the N dimensional binary space $\{1, -1\}^N$. Let $s_0 \equiv 1$ without loss of generality. The size of the search space is 2^{N-1}, which grows exponentially with N. Also, finding the PAPR of a phase sequence requires the evaluation of all the JN samples of the phase adjusted OFDM block. The execution time of finding the optimal phase sequence is thus prohibitively large when N is large. Many suboptimal techniques have been proposed to reduce the optimization complexity by reducing the search space and/or by efficiently computing the PAPR of each phase sequence.

[73] proposes an method to estimate the PAPR of a phase sequence without computing all the JN samples. If the estimated PAPR is large, the phase sequence is rejected. Otherwise, the exact PAPR is calculated as usual and compared with that of other sequences to find the optimum

sequence. In [74], the polygonal approximation of the peak boundary [72], (52) is used to reduce the number of multiplications in finding the PAPR of a sequence, at the cost of an increased number of additions.

However, because the total number of arithmetic operations (multiplications and additions) is still large, this method does not reduce the execution time when the multiplier-accumulator is used. In [75], a fast algorithm is proposed to compute the PAPR. The above methods can be combined with other methods that reduce the search space to further speed up the optimization.

To reduce the search space, [76] proposes two criteria for constructing a phase sequence set that may lead to a low PAPR. By studying the PAPR relationship between two sign sequences, [76] proves that the upper bound of the PAPR difference between two sign sequences is statistically maximized when the two sign sequences are orthogonal.

Moreover, the element wise product of any two sequences in the set should not be periodical or similar to periodical. However, a systematic construction method has not been found.

The SLM method [77] uses a set of K, $K >> 2^{N-1}$, randomly generated phase sequences $\{s^{(1)}, ..., s^{(K)}\}$. For each OFDM block, the phase sequence $s^{(i)}$ leading to the lowest PAPR is selected to adjust the phases of the OFDM block. Thus, the search space is reduced to a set of K phase sequences. SLM reduces the probability of large peaks. If the probability that s_i ($i = 1,...,K$) leads to a PAPR larger than ξ is P_ξ, then the probability that all s_i leading to a PAPR larger than ξ is $P_\xi^K < P_\xi$. SLM requires K IDFTs for each OFDM block, and the minimum side information is $\log_2 K$ bits.

The PTS technique [78] partitions each OFDM block X into K, $K << N$, disjoint sub-blocks $X = [X_1, ...,X_K]$. The sign sequence s is also partitioned into K corresponding sub-blocks $s = [s_1, ..., s_K]$, where the elements within each s_i are the same; i.e., $s_i = [s_i, s_i,, ..., s_i]$. The size of the search space is then reduced from 2^{N-1} to 2^{K-1}, making an exhaustive search possible. 2^{K-1} IDFTs are required for each OFDM block if the PAPR of each sign sequence is calculated by using an IDFT. However,

$$x = \mathrm{IDFT}(s \odot x) \tag{53}$$

Where $\odot$ denotes element wise multiplication.

A sign flipping method is proposed to reduce the execution time of PTS [79], where, in each iteration, the sign of a sub-block is flipped between +1 and −1, and the one leading to the lower PAPR is retained. The whole search space can be formulated as a binary tree. The sign flipping method searches only one branch of the tree.

By searching more branches, a larger PAPR reduction can be obtained with increased execution time; for example, we may search only the all -1 phase sequence and its neighbors having a Hamming distance less than or equal to r . In addition to the 2^{K-1} phase sequences (i.e., K sub-blocks) that modify the OFDM block to reduce the PAPR, extra modifications of the OFDM block can be obtained by complex conjugating, frequency reversing or circular shifting a sub-block, or multiplying a sub-block by a predefined phase sequence. A dual layer search scheme is proposed in [80], where an OFDM block is divided into D subgroups, called divisions, and each division is further divided into M sub-blocks. A suboptimal sign sequence can be found by, e.g., first optimizing the signs of each sub-block and then optimizing the signs of each division.

In [81, 82], the IDFT algorithm (used for converting the OFDM block to the time domain) is modified such that the original OFDM block is first processed by the IDFT algorithm for k stages (the complete N-point IDFT algorithm has $\log_2 N$ stages) to obtain a intermediate sequence.

Different phase sequences are applied to the intermediate sequence and then converted to the time domain by completing the last $n - k$ stages. Because the last $n - k$ stages involve only small sized IDFTs, the total execution time is then reduced. By exploiting the structure of IFFT, a set of specially designed phase sequences can be constructed such that, after calculating the PAPR of a “base” phase sequence, the PAPR of the other phase sequences can be calculated from this base sequence by using additions only.

A threshold may be used to reduce the execution time. That is, we search the whole solution space until a phase sequence leading to a PAPR lower than a threshold is found. The average execution time is low. However, the latency varies because, with a small occurrence probability, some OFDM blocks may need to test a large number of phase sequences to reach the threshold. Such a latency problem can be alleviated by using an input buffer and an output buffer [83].

4.6.8 Amplitude/Phase-Adjustment Techniques

The PAPR of OFDM signals can be reduced by modifying the amplitude and phase of the data symbols. The tone injection technique [71] expands the constellation. For example, (4.9) shows the extension of 16QAM, where a point A_1 of the original 16QAM (the shaded area) can be mapped to A_1, A_2 A_3 or A_4. A search in a discrete solution space is then required to find the optimum mapping. To simplify the search, usually only the points within the dashed square are used, and each 16QAM symbol has two mapping choices. No side information is required at the receiver. However, the average power is slightly increased.

Trellis shaping, which is ordinarily used for reducing the average power at the same bit rate [84], can also be used to reduce the PAPR. This technique uses the same constellation expansion as tone injection. However, by using a convolutional code, this technique gives rise to higher throughput than tone injection. For example, trellis shaping encodes each five bits to a point in (4.9). Similar to tone injection, the trellis shaping technique first maps four bits to a point, say A_1, in the shaded area.

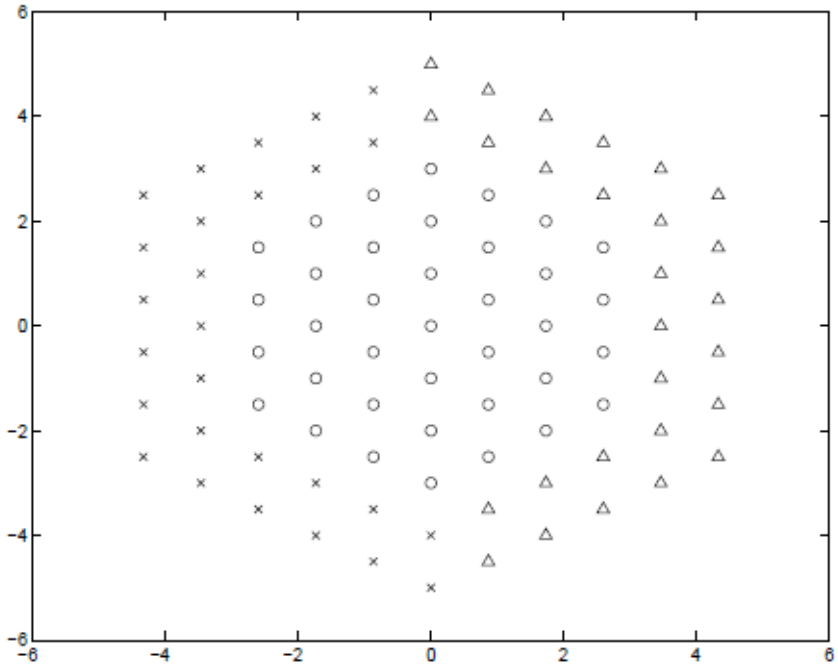

Figure 4.8. *The 91-point hexagonal constellation*

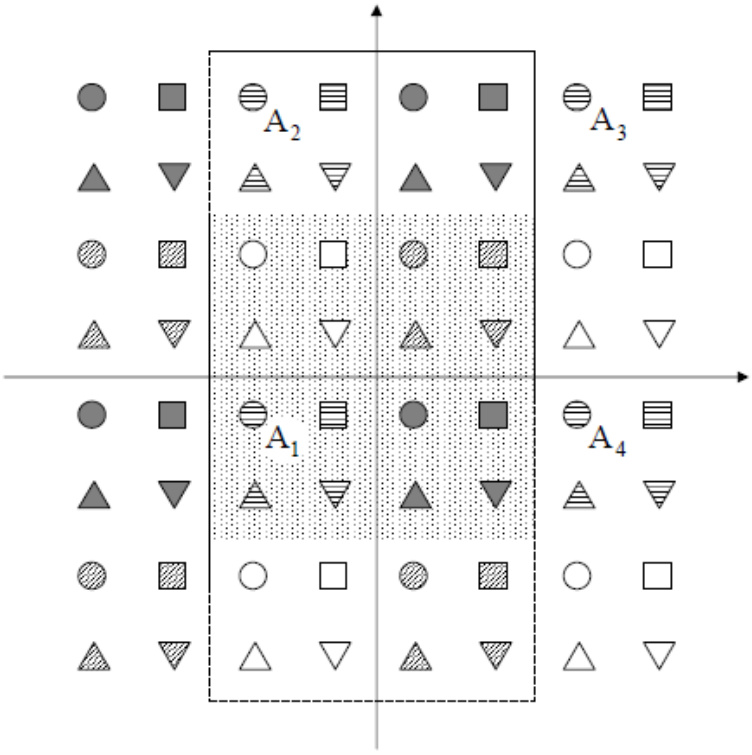

Figure 4.9. *Tone Injection*

The other bit s is extended to a 2-bit inverse syndrome of a rate-1/2 convolutional codeword $z = s(H^{-1})^T$, where H is the generator matrix of the convolutional code, and $(\cdot)^T$ represents the matrix transpose. By using the Viterbi decoder, a codeword y is generated such that y + z selects the one among A_1, ...,A_4 that leads to the lowest PAPR.

4.6.10 Coding Techniques

Coding techniques transmit only the low PAPR codewords [25]. Golay complementary sets may be used to generate polyphase sequences with a low PAPR [85].

K sequences X_1, ...,X_K are said to be complementary if the sum of their aperiodic autocorrelation functions satisfies

$$\sum_{k=1}^{K} Rx_k(n) = \delta(n) \sum_{k=1}^{K} Rx_k(0) , \quad (54)$$

where $\delta(n)$ is the kronecker delta function, and $Rx_k(n)$ is defined in (31). Golay complementary sets become golay complementary pairs when $K = 2$. We can show that

$$\text{PAPR}_{x_k} \leq K, \quad k = 1, \ldots\ldots K \ . \tag{55}$$

Golay complementary sequences can also be generated by concatenating or interleaving two short complementary sequences. [85] shows that most golay complementary sets are related to first-order reed-muller codes. Therefore, a golay complementary sequence can be generated by

$$\text{X}=[u_0, u_1, \ldots\ldots, u_\text{m}, c_1, c_2, \ldots\ldots, c_\text{K}]\text{G} \ , \tag{56}$$

where $u_i \epsilon \{0, \ldots\ldots, M-1\}$ (i = 0, ...,m, and M is an even number) are phase indices of M-ary PSK symbols, $c_k \in \{0, \frac{M}{2}\}$ (k = 1, ...,K, and $K = \binom{m}{2}$)defines the second-order coset, G is the generator matrix of the second-order reed-muller code with elements of 0 or 1 and the dimension of $(m + K + 1) \times 2^m$, and the addition and multiplication operations in the matrix multiplication are defined over the modulo-M. The corresponding M-PSK OFDM block is $e^{j\text{x}/M}$.

For a given c_k, the minimum Hamming distance is $d_\text{min} = 2^{m-1}$, and the coding rate is

$$R = \frac{m+1}{2^m} = \frac{log_2 N + 1}{N} \ , \tag{57}$$

where N is the length of the coded codewords. With N increasing, R goes to zero. Many choices of c_k lead to codewords with a PAPR of less than 2. If all these codewords are used, the minimum hamming distance is $d_\text{min} = 2^{m-2}$, and the increased coding rate is bounded as

$$R \leq \frac{m+1+\binom{m}{2}}{2^m} \tag{58}$$

However, R is close to zero when N is very large.

Reed-Muller codes can be written as a boolean function f($x_1, \ldots x_m$), where $[x_m, \ldots, x_1]^T$ forms a m by 2^m matrix with columns, from left to right, being the binary representation of 1, 2, ..., 2^m, respectively. The second-order reed-muller code contains only the terms of x_i and $x_i x_j$. [85]

shows that, for any permutation π of the symbols {1, 2, ...,*m*} and for any u, $u_k \in \mathrm{Z}_{2^h}$, where h is an integer,

$$a(x_1, \ldots . x_m) = \sum_{k=1}^{m} u_k x_k + 2^{h-1} \sum_{k=1}^{m-1} x_{\pi(k)}\, x_{\pi(k+1)} + u \,, \tag{59}$$

is a golay complementary sequence over Z_{2^h} of length 2^m. The second term determines the value of c_k in (56). This equation gives $m!/2$ cosets of first-order reed-muller codes. Therefore, the coding rate is

$$R = \frac{m+1+[\log_2\left(\frac{m!}{2}\right)]}{2^m} \tag{60}$$

[86] proves that (59) forms a path on a graph *G(Q)* with vertices of $x_1, x_2, \ldots x_m$.
If deleting k vertices of the graph results in a path, then all codewords of the coset $Q+ R\mathrm{M}_q(1,m)$ (q is an even number) have a PAPR no larger than 2^{k+1}. Therefore, a tradeoff is allowed between the coding rate and the PAPR. Similarly, [87, 88] proposed multiple shift codes, which also make a tradeoff between the coding rate and the PAPR. The main property of multiple shift codes is

$$R_{\mathrm{x}}(n) + R_{\mathrm{y}}(n) = 0, \text{for } 1 \le n \le N-1 \text{ and } n \bmod L = 0 \,, \tag{61}$$

where $L \in \{1, 2, \ldots, N-1\}$ The PAPR of X or Y is then no larger than L.

CHAPTER 5

ITERATIVE CLIPPING AND FILTERING PAPR REDUCTION METHOD

In this chapter, we analyze the clipping noise under the iterative clipping and filtering method [3] for peak reduction and out of band attenuation in OFDM systems [75]. To facilitate our analysis, we use the zero-padding OFDM system described in chapter 1, where the carrier frequency is in the left of the OFDM frequency band. The time domain OFDM symbol $x(t)$ and its discrete time samples x_n may be written as

$$x(t) = \frac{1}{\sqrt{N}} \sum_{k=0}^{N-1} X_k \, e^{j2\pi k \Delta f t} \, , \; 0 \le t \le T \, , \tag{62}$$

Where N data symbols (X_k)form an OFDM block X=[X_0,……..X_{N-1}], and T is the OFDM symbol period, and

$$x_n = \frac{1}{\sqrt{N}} \sum_{k=0}^{N-1} X_k \, e^{j2\pi nk/JN} \, , \; n=0,\ldots\ldots JN-1 \, , \tag{63}$$

Where J is the oversampling factor.

Clipping can be performed in two ways, one is to clip the complex envelope of OFDM signals and other is to clip the in-phase and quadrature phase signal separately. Clipping the complex envelope method is more effective in reducing PAPR [62]. In this thesis clipping of complex envelope is chosen. The peak envelope of the input signal (1) is clipped to a predetermined threshold A, or otherwise passed unperturbed, that is

$$\bar{x}_n = \begin{cases} A e^{j\theta(t)} \, , |x_n| > A \\ x(t) \, , \; |x_n| \le A \end{cases} \tag{64}$$

Where $\bar{x}_n$ is the clipped signal and $\theta(t)$ represents the phase of x_n.

In clipping algorithm clipping ratio (CR) is an important parameter also referred as normalized clipping level, defined as

$$CR = A/\sigma \tag{65}$$

Or in decibels as

$$CR(dB) = 20log_{10}\frac{A}{\sigma} \tag{66}$$

Where σ is the root mean square (RMS) value of signal x_n.

Therefore CR=1 means that signal is clipped at RMS power level. A CR of 1.4 means that the clipping level is about 3dB higher than the RMS level and CR of 1.995 means that the clipping level is 6dB higher than the RMS level. In this paper 3dB and 6dB clipping is chosen assuming that the maximum limit of linear range of HPA is 7dB higher than the RMS level. Clipping is done digitally on the OFDM signal (1) at the transmitter as described in [42]. If the digitally clipped samples are trigonometric interpolated the peak power will re-grow over clipping threshold, also all clipping noise will fall in-band which will increase the BER [89].

5.1 Time Domain Analysis of Clipping Noise

In the analysis, we have assume that the real and imaginary parts of input data symbol X_k are independent identically distributed random variables with zero mean and variance σ^2. We also assume that A and N are large, T is small, and the OFDM bandwidth $W = N/T$ is a constant. In DMT systems, $x(t)$ is real. Based on the central limit theory, $x(t)$ is a gaussian random process when N is large. The clipping noise $f(t)$ is then the consequence of the upward level crossing of $x(t)$ at level A and the down level crossing of $x(t)$ at level $-A$ [90]. The level crossing of a gaussian process has been extensively studied [51, 27]. The spectrum of the clipped gaussian process is given in [91] and the BER of the clipped DMT signal is given in [52].

In OFDM systems, $x(t)$ is a complex signal. Let $x(t) = x_r(t)+jx_i(t) = r(t)e^{j\theta(t)}$, where $x_r(t)$, $x_i(t)$, $r(t) \geq 0$ and $\theta(t)$ are the real and imaginary parts, the magnitude and the phase of $x(t)$, respectively. Based on the central limit theory, $x_r(t)$ and $x_i(t)$ are i.i.d. gaussian random processes with zero mean and variance σ^2 , $r(t)$ is a Rayleigh process, $\theta(t)$ is uniformly distributed between

[0, 2π), and $r(t)$ is independent to $\theta(t)$. The power of $x(t)$ (i.e., $r^2(t)$), is a χ^2 process with two degrees of freedom.

The clipping noise $f(t)$ is the consequence of the upward level crossing of $r(t)$ at level A, or equivalently, of $r^2(t)$ at level A^2. We will use the results from these studies to analyze the time and frequency domain characteristics of the clipping noise $f(t)$.

The level crossing rate (the expected number of crossings of level A per second) can be found as [64]

$$\lambda_A = \frac{\dot{\sigma}}{\sqrt{2\pi}} \frac{A}{\sigma^2} e^{-A^2/2\sigma^2} , \tag{67}$$

where,

$$\dot{\sigma}^2 = E\{\dot{x}_I^2(t)\} = \frac{1}{2\pi} \int \omega^2 S(\omega) d\omega , \tag{68}$$

and $S(\omega)$ is the PSD of $x_r(t)$ or $x_i(t)$. When N is large, $S(\omega)$ is (approximately) constant over a frequency band [0, W], then we have

$$\dot{\sigma}^2 = \frac{(\pi N)^2 \sigma^2}{3T^2} = \frac{\pi^2}{3} W^2 \sigma^2 . \tag{69}$$

By substituting (69) into (67), the level crossing rate is

$$\lambda_A = \sqrt{\frac{\pi}{6}} \frac{A}{\sigma} \frac{N}{T} e^{-A^2/2\sigma^2} \tag{70}$$

With our assumption of a large A, each up-crossing of level A leads to a clipping pulse. Therefore, the average number of clipping pulses in one OFDM signal duration can be calculated as

$$\overline{N}_p = E\{N_p\} = \lambda_A T = N \sqrt{\frac{\pi}{6}} \frac{A}{\sigma} e^{-A^2/2\sigma^2} \tag{71}$$

The clipping pulse duration τ is a Rayleigh random variable with a probability density function [92]

$$p(\tau) = \frac{\pi\tau}{2\bar{\tau}^2}\exp\left(-\frac{\pi\tau^2}{4\bar{\tau}^2}\right), \tag{72}$$

Where $\bar{\tau}$ is the mean of τ. Because $\lambda_A\bar{\tau} = \Pr[r(t) > A]$, $\bar{\tau}$ can be calculated as

$$\bar{\tau} = \frac{\Pr[r(t)>A]}{\lambda_A} = \frac{\sigma^2\sqrt{2\pi}}{A\dot{\sigma}} = \sqrt{\frac{6}{\pi}}\frac{\sigma}{AW} \ . \tag{73}$$

Let us consider a clipping pulse $f_i(t)$ that reaches its maximum magnitude at t_i and has a time duration τ_i. That is, $f_i(t) = (r(t) - A)e^{j\theta(t)}$ within its pulse duration and is zero elsewhere. Equations (72) and (73) imply that, most probably, τ is very small in practical OFDM systems. Then, $r(t)$ can be approximated as a parabolic function by using its taylor's series expansion at $t = t_i$. Let $\Delta t_i = t - t_i$. Because $r(t_i) > A, \dot{r}(t_i) = 0$ and $\ddot{r}(t_i) < 0$, we have

$$\begin{aligned} r(t) = r(t_i + \Delta t_i) &\approx r(t_i) + \dot{r}(t_i)\Delta t_i + \frac{1}{2}\ddot{r}(t_i)\Delta t_i^2 \\ &= r(t_i) + \frac{1}{2}\ddot{r}(t_i)\Delta t_i^2 \ . \end{aligned} \tag{74}$$

With this approximation, $r(t_i + \Delta t_i)$ is symmetric to t_i. Then, $r(t_i + \Delta t_i)$ is symmetric to t_i. Then, $r(t_i - \frac{t_i}{2}) \approx A$, and $\tau_i \approx \sqrt{-\frac{8(r(t_i)-A)}{\ddot{r}(t_i)}}$.

Let $b_i = -\ddot{r}(t_i)$. We have

$$r(t_i + \Delta t) - A \approx \frac{1}{2}b_i\Delta t_i^2 + \frac{1}{8}b_i\tau_i^2, \ -\frac{\tau_i}{2} \le \Delta t_i < \frac{\tau_i}{2} \ . \tag{75}$$

Now let us look at the phase $\theta(t) = \theta(t_i + \Delta t)$. The phase change within $-\frac{\tau_i}{2} \le \Delta t_i < \frac{\tau_i}{2}$ is generally small. The phase of $f_i(t_i + \Delta t)$ is determined by all the constituent frequency

components of $x(t)$, where $x(t)$ is a band limited signal. The phase change of the k^{th} frequency component, from $t = t_i$ to $t = t_i + \frac{\tau_i}{2}$, is

$$\Delta\theta_k = 2\pi k \frac{\tau_i}{2T},\ k = 0\ to\ N-1 \tag{76}$$

Substituting τ_i by $\bar{\tau}$, we find

$$\Delta\theta_k = \frac{\sqrt{6\pi}k\sigma}{NA},\ k = 0\ to\ N-1 \tag{77}$$

The largest phase change happens on $k = 0$, and its values does not depend on N. By letting $\theta_k = \theta_0$ for all k, the phase variation of $f_i(t)$ from $t = t_i$ to $t = t_i + \frac{\tau_i}{2}$ is upper bounded by $\frac{\sqrt{6\pi}\sigma}{2A}$. Clearly, the upper bound is quite loose, and the actual phase variation $f_i(t)$ is much smaller than this bound because some negative and positive phase changes may cancel each other. Nevertheless, because this upper bound is small when A is large, we can approximate $\theta(t_i + \Delta t_i) = \arcsin\left(\frac{x_I(t_i+\Delta t_i)}{r(t_i+\Delta t_i)}\right)$ by its taylor's series expansion at $t=t_i$:

$$\theta(t_i + \Delta t_i) \approx \theta_i + \gamma_i \Delta t_i \tag{78}$$

Where $\theta_i = \theta(t_i)$ and

$$\gamma_i = \frac{\dot{x}_I(t_i)}{|x_R(t_i)|} \tag{79}$$

Then,

$$f_i(t) = f_i(t_i + \Delta t_i) = (r(t_i + \Delta t_i) - A)e^{j\theta(t_i+\Delta t_i)}$$

$$\approx \left(-\frac{1}{2}b_i\Delta t_i^2 + \frac{1}{8}b_i\tau_i^2\right)e^{j(\theta_i+\gamma_i\Delta t_i)} \quad -\frac{\tau_i}{2} \le \Delta t_i < \frac{\tau_i}{2} \tag{80}$$

The absolute value of the phase term $\gamma_i \Delta t_i$ is most probably small and can be omitted. Therefore we can approximate the clipping pulse as a constant phase parabolic function:

$$f_i(t) = f_i(t_i + \Delta t_i) \approx \left(-\frac{1}{2} b_i \Delta t_i^2 + \frac{1}{8} b_i \tau_i^2\right) e^{j(\theta_i)} \qquad -\frac{\tau_i}{2} \le \Delta t_i < \frac{\tau_i}{2}. \tag{81}$$

5.2 Frequency Domain Analysis of Clipping Noise

The frequency spectrum of the nyquist rate sampled discrete time real clipping noise is given in [53]. For the continuous time complex clipping noise, the frequency spectrum of $f_i(t)$ is the fourier transform of (80); i.e.,

$$F_i(\omega) = e^{j(\theta_i - \omega t_i)} \frac{b_i t_i}{\omega^2} \left(sinc \frac{\omega t_i}{2} - cos \frac{\omega t_i}{2}\right) \tag{82}$$

Where $sinc\ x = \frac{\sin x}{x}$. $F_i(\omega)$ is distributed over the whole frequency band from $\omega = -\infty$ to ∞. Figure 5.1 shows an example of $F_i(\omega)$, which is the Fourier transform of a clipping pulse we arbitrarily selected from the simulation. The solid curve represents $|F_i(\omega)|$, and the dashed line illustrates the OFDM frequency band. We observe that $F_i(\omega)$ contributes a large portion of the out of band radiation. The in-band clipping noise is only a small portion of $F_i(\omega)$.
By the definition

$$\begin{aligned} \frac{1}{T} E\left\{\sum_{i=1}^{N_p} |F_i(\omega)|^2\right\} &= \frac{1}{T} \lim_{n\to\infty} \frac{1}{n} \sum_{l=1}^{n} \sum_{i=1}^{N_c,l} |F_{i.l}(\omega)|^2 \\ &= \frac{N_p}{T} E\{|F_i(\omega)|^2\} = \lambda_A E\{|F_i(\omega)|^2\} \end{aligned} \tag{83}$$

Where subscript l represents the l^{th} trial. Therefore,

$$S_f(\omega) = \lambda_A E\{|F_i(\omega)|^2\} + \frac{1}{T} E\left\{\binom{N_p}{2}\right\} E\{F_i(\omega) F_k^*(\omega)\} \tag{84}$$

Where $i \neq k$. Note that

$$F_i(\omega) F_k^*(\omega) = \int_{-\infty}^{\infty} \int_{-\infty}^{\infty} f_i(\hat{t}) f_k^*(\bar{t}) e^{-j\omega(\hat{t}-\bar{t})} d\bar{t} d\,\hat{t} \tag{85}$$

Where $E\{F_i(\omega) F_k^*(\omega)\}$ is determined by

$$E\{f_i(\hat{t}) f_k^*(\bar{t})\} = E\{(r(t_i + \Delta t_i) - A)(r(t_k + \Delta t_k) - A)\} E\{e^{j\theta(t_i+\Delta t_i)} e^{j\theta(t_k+\Delta t_k)}\} \tag{86}$$

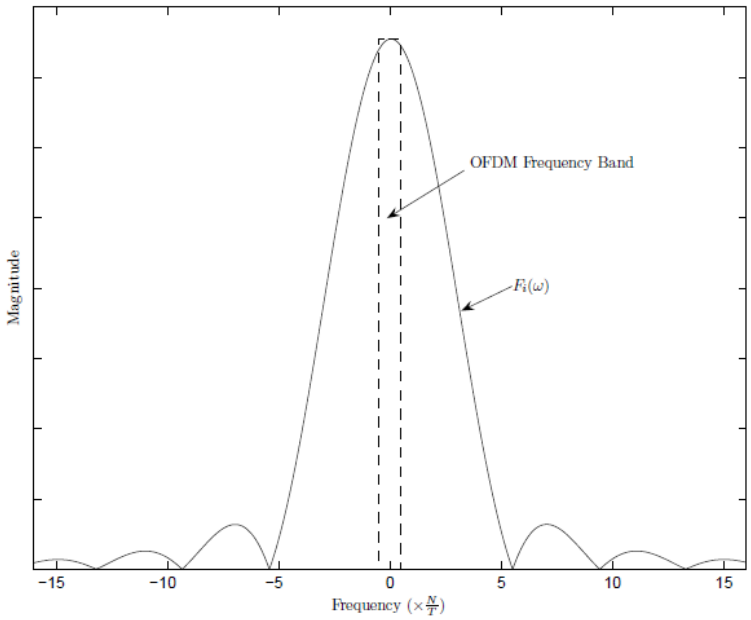

Figure 5.1. *Frequency spectrum of $f_i(t)$*

When $(t_i + \Delta t_i)$ and $(t_k + \Delta t_k)$ belong to different clipping pulses, $x(t_i + \Delta t_i)$ and $x(t_k + \Delta t_k)$ are approximately independent, and thus $\theta(t_i + \Delta t_i)$ and $\theta(t_k + \Delta t_k)$ are uncorrelated. Then, $E\{F_i(\omega) F_k^*(\omega)\} = 0$ and $S_f(\omega) = \lambda_A E\{|F_i(\omega)|^2\}$.

Then out of band radiation will be eliminated by filtering. Therefore we are interested in the in band clipping noise. When A is large, generally $\frac{\omega \tau_i}{2}$ is small for $|\omega| \leq \frac{\pi N}{T}$. Thus we may approximate $F_i(\omega)$ as

$$F_i(\omega) \approx e^{j(\theta_i \omega \tau_i)} \frac{b_i \tau_i^3}{12} \tag{87}$$

By using [17] $sinc\ x - \cos x \approx \frac{x^2}{3}$. Because $F_i(\omega)$ does not depend on the frequency ω. $S_f(\omega)$ is approximately constant over the frequency band.

5.3 Clipping Noise Power Spectral Density

In this subsection, we calculate the in-band clipping noise PSD by using a result in [53]. Define $y(t) = \frac{r^2(t)}{\sigma^2}, \lambda = \frac{\dot{\sigma}^2}{\sigma^2}\ and\ u = \frac{A^2}{\sigma^2}$. If *y(t)* crosses the level *u* at *t* = 0 with probability 1, *y(t)* around *t* = 0 can be written as

$$y(t) = -\lambda u t^2 + 2z\sqrt{\lambda u}t + u,\ when\ u\ \to \infty \tag{88}$$

Where z is a Rayleigh random variable, also the time duration τ between this crossing and successive down-crossing is

$$\tau = \frac{2z}{\sqrt{\lambda u}} \tag{89}$$

with probability 1 when $u \to \infty$. Because, most probably, τ is very small for large A/σ in practical OFDM systems, we may use (88) to approximate the whole clipping pulse. Expanding $r(t) = \sigma\sqrt{y(t)}$ by using its taylor's series at *t* = 0, we have

$$r(t) \approx -\frac{\dot{\sigma}^2 A}{2\sigma^2}(t - \frac{\tau}{2})^2 + \frac{\dot{\sigma}^2 A \tau^2}{8\sigma^2} + A, \quad 0 \le t \le \tau \tag{90}$$

Now we can approximate the $f_k(t)$ that occurs in $t_k \le t \le t_k + \tau_k$ as

$$f_k(t) \approx \left(-\frac{\dot{\sigma}^2 A}{2\sigma^2}\left(\Delta t_k - \frac{\tau}{2}\right)^2 + \frac{\dot{\sigma}^2 A \tau^2}{8\sigma^2}\right) e^{j(\theta_k + \eta_k \Delta t_k}, \ \ 0 \le \Delta t_k \le \tau \tag{91}$$

Since $\eta_k \Delta t_k$ is very small and can be ignored, then

$$F_k(\omega) \approx \frac{A\dot{\sigma}^2 \tau_k^3}{12\sigma^2} e^{\frac{j(\theta_k - \omega(t_{k+\tau_k}))}{2}} \tag{92}$$

The in-band clipping noise PSD is

$$\begin{aligned} S_f(\omega) &= \lambda_A E\{|F_i(\omega)|^2\} \\ &= \frac{16\sqrt{2}}{\pi\sqrt{3\pi}(\frac{A}{\sigma})^3} e^{-A^2/2\sigma^2} S_x \ , \end{aligned} \tag{93}$$

Where $S_x = \frac{2\sigma^2}{W}$ is the PSD of the OFDM signal $x(t)$.

5.4 Filtered Clipping Noise

The clipping process described above is a non-linear process. Since clipping is done on an oversampled signal, most of the clipping noise falls in OOB which reduces the spectral efficiency. Filtering after clipping is necessary and required to reduce the OOB noise and spectral splatter. The FIR filters used in many papers are very complicated like in [54], makes spectral side-lobes 50dB lower than the signal side-lobes and introduces in-band ripple of 1dB which may boost the power of some sub-channels while suppressing others. Such filters are complicated and expensive, in addition they cause peak re-growth and significant distortion in in-band.

For efficient filtering i.e. adding minimum noise in in-band, peak re-growth and maximally attenuate the OOB power, there is a technique called "frequency domain filtering" of the clipped signal. In the conventional ICF method explained in [44] the filtering consist of two DFT operations. The forward DFT transforms the clipped signal back into discrete frequency domain $\overline{\mathrm{X_n}}$. The in-band discrete frequency components of $\overline{\mathrm{X_n}}$ are passed unchanged to the inputs of the second IDFT while the OOB components are nulled. The process is same as multiplying $\overline{\mathrm{X_n}}$ by rectangular window function, (94).

$$R_N(m)=\begin{cases}1 & 0 \le m \le N-1 \\ 0 & otherwise\end{cases} \quad (94)$$

Let the pass band of the filter be $[-\omega_c, \omega_c]$, where $\omega_c = 2\pi\frac{JN}{T}$

The filtered clipping noise is then given by

$$\hat{f}(t) = \frac{1}{2\pi}\int_{-\omega_c}^{\omega_c}\sum_{i=1}^{N} F_i(\omega)\, e^{j\omega t} d\omega \quad (95)$$

$$\hat{f}(t) = \hat{f}(t+\Delta t_i) = \sum_{i=1}^{N}\hat{f}_i(t) = \sum_{i=1}^{N} e^{j\theta_i}\frac{b_i t_i^3 f_c}{6} sinc 2\pi f_c \Delta t_i \quad (96)$$

Without loss of generality, we consider the clipping pulse $f_i(t)$ and assume it occurs at $t_i = 0$ and has the phase $\theta_i = 0$. Its filtered version is

$$\hat{f}_i(t) = \frac{b_i t_i^3 f_c}{6} sinc 2\pi f_c t \quad (97)$$

Figure 5.2 shows $f_i(t)$ and $\hat{f}_i(t)$. Several observations can be made by comparing $f_i(t)$ with $\hat{f}_i(t)$:

1. $f_i(t)$ and $\hat{f}_i(t)$ reach their peaks at the same time instant $t = 0$.
2. $f_i(t)$ and $\hat{f}_i(t)$ have the same direction within the pulse duration of $f_i(t)$.
3. The mainlobe duration of $\hat{f}_i(t)$ is much wider than that of $f_i(t)$. The mainlobe duration of $\hat{f}_i(t)$ can be calculated as

$$\hat{\tau} = \frac{2T}{JN}$$

By using (72), the ratio of average clipping pulse duration $\bar{\tau}$ over $\hat{\tau}$ is

$$\frac{\bar{\tau}}{\hat{\tau}} = \sqrt{\frac{3}{2\pi}}\frac{J\sigma}{A} \ll 1$$

When A/σ is large.

4. The sidelobe peaks of $|\hat{f}_i(t)|$ decay with the rate of $1/t$. Specifically, the sidelobes peaks of $|\hat{f}_i(t)|$ are

$$\left|\hat{f}_i(t)\right| \approx \frac{b_i t_i^3 f_c}{3(2k+1)\pi} = \frac{2}{(2k+1)\pi}\left|\hat{f}_i(t)\right|_{\max}, \quad k = 1, 2, 3, \ldots., \tag{98}$$

With T_k representing the sidelobe peak occurrence time

$$T_k \approx \frac{(2k+1)T}{2JN} \tag{99}$$

5. The maximum of $\hat{f}_i(t)$ is much less than that of $f_i(t)$. In fact,

$$\left|\hat{f}_i(t)\right|_{\max} = \alpha\tau_i |f_i(t)|_{max},$$

Where α is defined as

$$\alpha = \frac{4}{3} f_c \tag{100}$$

and the expectation of is $\alpha\tau_i$ is

$$E\{\alpha\tau_i\} = \alpha\bar{\tau} = R\frac{2\sqrt{2}\sigma}{\sqrt{3\pi}A} \ll 1 \tag{101}$$

Point 5 explains why peak re-grows after filtering. Recall that the clipped signal is $\bar{x}(t) = x(t) - f(t)$, and that after filtering it becomes $\hat{x}(t) = x(t) - \hat{f}(t)$.

In this paper we have modified the filter action by replacing rectangular window function by kaiser window function (102). Only OOB components are attenuated using kaiser window function and in-band components are passed unperturbed. In systems where some band-edge subcarriers are unused, the components corresponding to these are nulled. The probability of peak re-growth reduces as the side-lobes of the clipped peaks in $\bar{x}_n$ offset each other.

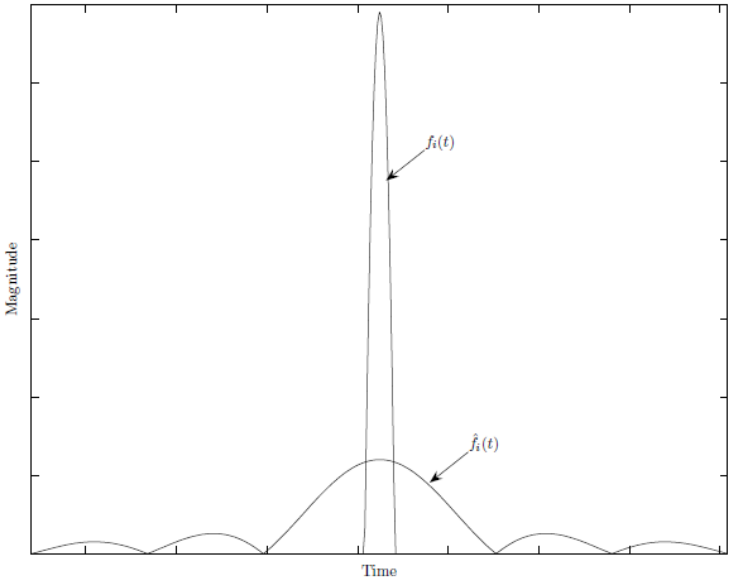

Figure 5.2. *The clipping pulse* $f_i(t)$ *and its filtered version* $\hat{f}_i(t)$

Mathematically kaiser window function can be represented as

$$H(m)=\begin{cases} 1 & 0 \le m \le N-1 \\ \dfrac{i_0\left(\beta\sqrt{1-\left(2\frac{m}{JN-1}\right)^2}\right)}{i_{0(\beta)}} R_{JN}(m) & N \le m \le JN-1 \end{cases} \quad (102)$$

where $R_{JN}(m)$ is

$$R_{JN}(m)=\begin{cases} 1 & 0 \le m \le JN-1 \\ 0 & otherwise \end{cases} \quad (103)$$

Where i_0 is the zero order modified Bessel function of first kind and β is the ripple control parameter $i_0(x)$ is calculated by power series expansion

$$i_0(x) = 1 + \sum_{k=1}^{L}[\frac{\left(\frac{x}{2}\right)^k}{k!}]^2 \quad (104)$$

Where L < 25. So, signal after clipping and filter operation is

$$\hat{x}_n(n) = IDFT(\overline{X_n}(n) \odot H(n)) \quad (105)$$

$\odot$ denotes element wise multiplication. The resultant filter is a time dependent filter, which passes in-band and attenuates OOB components. This means that it causes no distortion to the in-band of clipped signal $\bar{x}_n$. Since the filter operates on a symbol by symbol basis, it causes no ISI. This filtering technique also causes peak re-growth, but less and compared to rectangular window filtering and FIR filters. To reduce the peak re-growth iterative clipping and filtering can be performed [44]. ICF technique greatly reduces peak re-growth, attenuates OOB power but adds more clipping noise in in-band with subsequent iterations. Large number of iterations increases computational complexity also, convergence of PAPR reduction reduces with number of iterations. So, large number of iterations can be avoided to reduce computational complexity.

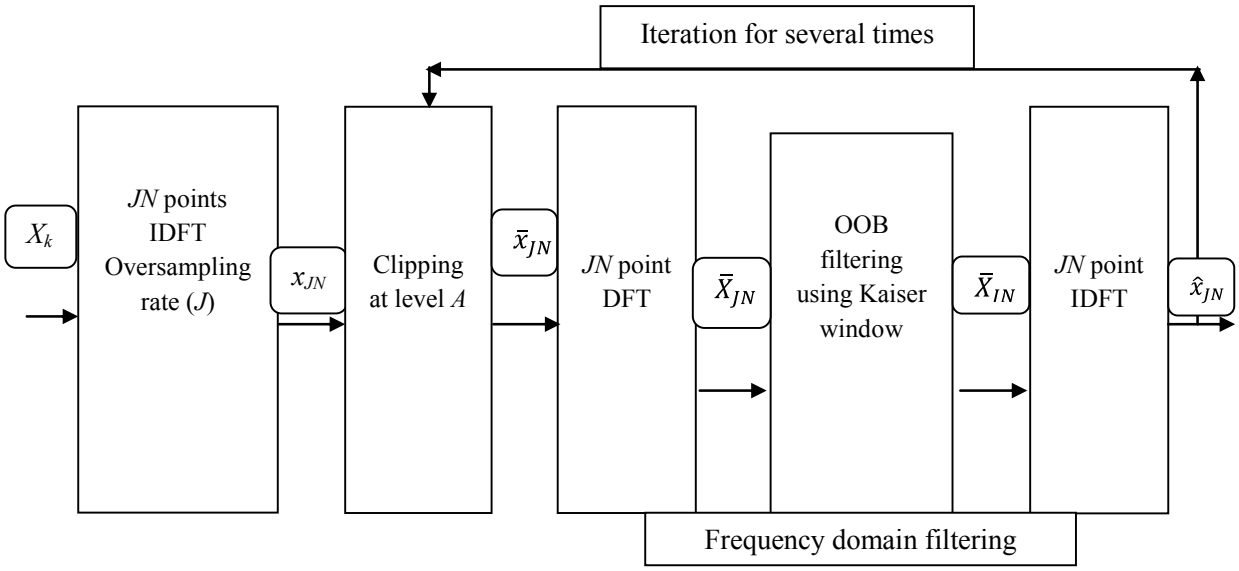

Figure 5.3. *Block diagram for Iterative Clipping and Filtering with Kaiser window*

Algorithm for this method is as follows

1. { X_k, k=0,1,…., N-1} be the complex quadrature phase shift keying (QPSK) modulated symbols, where N is the number of subcarriers. Then we can get {X_k=[X_0 ,…., X_{N-1} ,0,…..,0,0,0]$_{JN}$]} through the operation of oversampling (where J is the oversampling factor). So the oversampled discrete time domain OFDM signal x_{JN}=IDFT(X_k) [46, 66].

2. Convert the OFDM symbol to time domain as x_{JN} = IDFT(X_k).

3. Clip x_{JN} to the threshold A , let it be $\bar{x}_{JN}$.

4. Take DFT($\bar{x}_{JN}$) = $\bar{X}_{JN}$.

5. Treat the out of band components by kaiser window (105). We can also let only a part of OOB band or whole OOB treated by window function, let it be $\bar{X}_{JN}$.

6. Repeat steps 3, 4, 5 for making iterations.

7. After number of iterations take $\hat{x}_n$ = IDFT($\bar{X}_{JN}$) and transmit it.

5.5 Details of Problem Statement

To mitigate the problem of peak re-growth, the above explained ICF method at the transmitter side is of good practicality. But the convergence of PAPR reduction decreases after the few iterations. Each iteration requires two DFT or IDFT operations and after the last iteration, one extra IDFT is required to convert the clipped and filtered OFDM symbol to time domain. As a z iteration process requires 2z+1 DFT/IDFT, the increased number of iterations implies increased computational complexity, especially when the number of sub-carriers are very large. Other PAPR reduction methods given by [25-27] also require several iterations to suppress the high PAPR. Also in clipping noise cancellation technique explained in [16, 28] requires same number of iterations as of transmitter side at receiver side to cancel the clipping noise. Thus, the computational complexity increases with number of iterations both at transmitter and receiver side.

So, we need a one iteration process which would provide equivalent and/or better performance than ICF. The in-band noise obtained after first iteration is statistically scaled with factor B to

measure the in-band clipping noise for z iterations. This approximated in-band clipping noise may be further used for refining the OFDM signal and called as statistical clipping (SC).

Recalling, the clipping noise is $f(t) = x(t) - \bar{x}(t)$. The clipping noise $f(t)$ consists of segments of $x(t)$ where $|x(t)|$ exceeds A,

$$f(t) = \sum_{i=1}^{N_p} f_i(t) \tag{106}$$

Where $f_i(t)$ is the i^{th} clipping pulse with pulse duration τ_i, with its amplitude maximum at t_i and N_p is the number of clipping pulses. The filtered clipping noise $\hat{f}(t)$ is obtained by passing $f(t)$ through a filter whose passbands are on the reserved tones. The peak cancelling signal is a scaled version of the filtered clipping noise:

$$c(t) = -B\hat{f}(t) \tag{107}$$

Where B is the scaling factor which is optimized to minimize PAPR.

But still after scaling of clipping noise OOB power is very high and requires to be attenuated improve spectral efficiency. OOB of SC OFDM signal is then treated with kaiser window (102) to filter the OOB components and called as statistical clipping with window based filtering approach (SC-W).

CHAPTER 6

PROPOSED METHOD: STATISTICAL CLIPPING WITH WINDOW BASED NOISE FILTERING (SC-W)

SC-W method is an one iteration method which obtains the same PAPR reduction as of ICF with several iterations. Each clipping pulse is approximated as a parabolic function. The in-band noise obtained after first iteration is statistically scaled to measure the in-band clipping noise for *z* iterations. This approximated in-band clipping noise may be further used for refining the OFDM signal and called as statistical clipping (SC).

But still after scaling of clipping noise OOB power is very high and requires to be attenuated improve spectral efficiency. OOB of SC OFDM signal is then treated with kaiser window (102) to filter the OOB components and called as statistical clipping and window based filtering approach (SC-W).

Let the scaling factor be *B*, which is optimized to achieve minimum PAPR.

Let us temporally assume that the clipping noise at the first iteration $f^{(1)}(t)$ of ICF consist of only one dominant clipping pulse $f_i^{(1)}(t)$, with pulse duration $\tau_i^{(1)}$ that is much larger than other clipping pulses; i.e.

$$f^{(1)}(t) = \sum_k f_k^{(1)}(t) \ ,$$

$$\left|f_i^{(1)}(t)\right| \gg \left|f_k^{(1)}(t)\right|, \qquad \text{for all } k \neq i \tag{108}$$

In this case, the clipped and filtered OFDM signal after first iteration $\hat{x}^{(1)}(t) \approx x(t) - \hat{f}_i^{(1)}(t)$, where $\hat{f}_i^{(1)}(t)$ is the filtered version of $f_i^{(1)}(t)$, can be divided into three parts:

1. $|t| \leq \tau_i^{(1)}/2$

Within the range, $\hat{f}_i^{(1)}(t)$, $f_i^{(1)}(t)$ and *x(t)* have the same phase and $\left|\hat{f}_i^{(1)}(t)\right| < \left|f_i^{(1)}(t)\right|$. Therefore,

$$\left|\hat{x}^{(1)}(t)\right| \approx \left|x(t) - \hat{f}_i^{(1)}(t)\right| > \left|x(t) - f_i^{(1)}(t)\right| = A \tag{109}$$

In other words, after passing $\hat{x}^{(1)}(t)$ through SL, a clipping pulse, denoted as $f_i^{(2)}(t)$, occurs in the second clipping iteration at the same position as $f_i^{(1)}(t)$. By applying taylor's series expansion to (97) and because $\frac{\omega_c \tau_i^{(1)}}{2} \ll 1$, we can approximate the filtered clipping pulse $\hat{f}_i^{(1)}(t)$ as a constant

$$\hat{f}_i^{(1)}(t) \approx \frac{b_i(\tau_i^{(1)})^3 f_c}{6} = \hat{f}_i^{(1)}(t)_{max} \ , \ |t| \leq \frac{\tau_i^{(1)}}{2} \tag{110}$$

Then the clipping pulse at the second iteration $f_i^{(2)}(t)$ can be written as

$$f_i^{(2)}(t) = f_i^{(1)}(t) - \hat{f}_i^{(1)}(t) \approx -\frac{1}{2} b_i t^2 + \frac{1}{8} b_i (\tau_i^{(1)})^2 - \frac{b_i(\tau_i^{(1)})^3 f_c}{6} \tag{111}$$

Which is also parabolic arc with reduced magnitude. By solving $f_i^{(2)}(t) = 0$, the time duration of $f_i^{(2)}(t)$ can be found as

$$\tau_i^{(2)} = \tau_i^{(1)} \sqrt{1 - \frac{4}{3} \tau_i^{(1)} f_c} = \tau_i^{(1)} \sqrt{1 - \alpha^{(1)} \tau_i^{(1)}} \tag{112}$$

Where $\alpha^{(1)}$ is the α defined in chapter 5.

2. $\frac{\tau_i^{(1)}}{2} < |t| < T_2$, where T_2 is given in T_k in chapter 5. In this range $|x(t)| < A$ because only one clipping pulse exists. However, depending on the phase of $\hat{f}_i^{(1)}(t)$, $|\hat{x}^{(1)}(t)|$ may be greater than *A*. In other words, new clipping pulses may be generated in the second clipping iteration.

However, because $|\hat{f}_i^{(1)}(t)|_{max} \ll |f_i^{(1)}(t)|_{max}$, these new clipping pulses are very small as compared to clipping pulse $f_i^{(2)}(t)$, and their effect can be ignored.

3. $|t| > T_2$. Because the peaks of $\hat{f}_i^{(1)}(t)$ decay with the rate of 1/*t*, we can see that, in this range $\hat{x}^{(1)}(t) \approx x(t)$. Therefore no clipping pulses exist at $|t| > T_2$ in the second clipping iteration.
For *z* successive clipping and filtering same procedure is repeated. Therefore, we conclude:

For the case of only one dominant clipping pulse, in the z^{th} (z = 2, 3 ,…) clipping and filtering iteration, $f_i^{z-1}(t)$ shrinks to $f_i^z(t)$, and some new pulses possibly appears. Here, $f_i^{z-1}(t)$ and $f_i^z(t)$ are the dominant clipping pulses at the $(z-1)^{\text{th}}$ and z^{th} iterations, respectively. Until $f_i^z(t)$ is comparable to the new pulses, the latter can be omitted and the former can be written as

$$f_i^z(t) = -\frac{1}{2} b_i t^2 + \frac{1}{8} b_i (\tau_i^{(z)})^2 , \qquad i = 1, 2, 3, \ldots\ldots, \tag{113}$$

where

$$f_i^{(1)}(t) = f_i(t) \text{ and } \tau_i^{(1)} = \tau_i \tag{114}$$

$$\tau_i^{(z)} = \tau_i^{(z-1)} \sqrt{1 - \alpha \tau_i^{(z-1)}} , \quad i = 2, 3, 4, \ldots\ldots, \tag{115}$$

Moreover filtered clipping noise in the z^{th} iteration is

$$\hat{f}_i^{(z)}(t) = \frac{b_i (\tau_i^{(1)})^3 f_c}{6} sinc\ 2\pi f_c t \tag{116}$$

Thus, the filtered clipping noise generated in the z^{th} iteration is proportional to that generated in the first iteration. Define *B* as

$$B \triangleq \frac{\text{total clipping noise after } Z \text{ iterations}}{\text{clipping noise generated in first iteration}} \tag{117}$$

If only one dominant clipping pulse exists,

$$B = \frac{\sum_{l=1}^{z} \hat{f}_i^l(t)}{\hat{f}_i^1(t)} = \frac{\sum_{l=1}^{z-1} (\tau_i^{(l)})^3}{(\tau_i^{(l)})^3} \tag{118}$$

Finding $\bar{B}$, the mean of B, is difficult. However, an estimation of $\bar{B}$ can be obtained when z is not large. When A is large, $\alpha\tau_i^z \ll 1$. Then $\sqrt{1-\alpha\tau_i^z}$ can be treated as constant. $\bar{B}$ can then be estimated by replacing τ_i^z with its mean $\bar{\tau}$. Thus,

$$\bar{B} \approx \frac{1-(1-\alpha)^{\frac{3z}{2}}}{1-(1-\alpha)^{\frac{3}{2}}} \tag{119}$$

Where

$$\alpha = \frac{2\sqrt{2}\sigma}{\sqrt{3\pi}A} \tag{120}$$

We will use $\bar{B}$ in the SC-W algorithm.

After the scaling the in-band noise, the OOB power is very high, which have to be attenuated. This is done by treating the scaled version of OFDM signal with kaiser window (105) described in (102-104). Algorithm for SC-W method is as follows

1. { X_k, k=0,1,…., K-1} be the complex quadrature phase shift keying (QPSK) modulated symbols, where K is the number of subcarriers. Then we can get {X_k=[X_0 ,…., X_{k-1} ,0,…..,0,0,0]$_{JN}$} through the operation of oversampling (where J is the oversampling factor). So the oversampled discrete time domain OFDM signal x_{JN} = IDFT(X_k).

2. Convert the OFDM symbol to time domain as x_{JN} = IDFT(X_k).

3. Clip x_n to the threshold A and calculate the clipping noise $\hat{f}_n = x_{JN} - \bar{x}_{JN}$.

4. Convert $\hat{f}_n$ to frequency domain to obtain $\hat{F}_k$ by taking DFT($\hat{f}_n$).

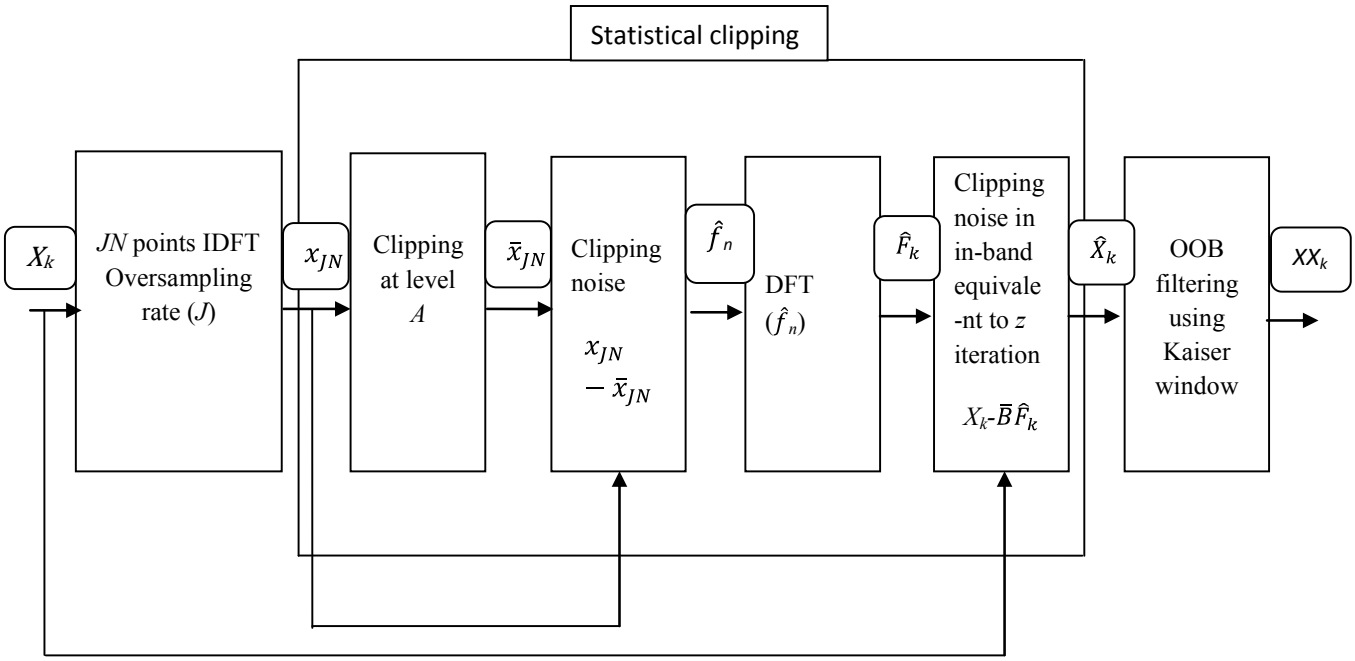

Figure 6.1. *Block diagram for Statistical Clipping with Window filtering (Kaiser window)*

5. The clipped OFDM signal then becomes $\hat{X}_k \approx X_k - \bar{B}\hat{F}_k$.

6. Treat the OOB by kaiser window. We can also let only a part of OOB or whole OOB treated by window function $XX_k = \hat{X}_k \odot H(k)$ (105).

7. Convert the treated signal XX_k to time domain and transmit it.

CHAPTER 7

SIMULATION RESULTS

The proposed PAPR reduction technique SC-W is investigated by considering two cases of clipping level (A) for 3dB and 6dB case, assuming maximum limit for linear range of solid state power amplifier (SSPA) as described in [28] be 7 dB above RMS level of transmitted OFDM symbol. The input-output relationship of SSPA can be written as

$$y_n = \frac{|x_n|}{\left(1+\left(\frac{|x_n|}{A}\right)^{2p}\right)^{\frac{1}{2p}}} e^{j\emptyset_n} \tag{121}$$

Where $|x_n|$ is the input, and y_n is the output of SSPA. The SSPA becomes linear when p is infinity. Usually p = 2 or 3 (here p = 3) is taken for practical SSPA. Cyclic prefix is not used with an assumption that it doesn't effect the results. Parameters for simulation taken,

Number of subcarriers (N) = 256

Oversampling factor (J) = 4

Total sub-channels (JN) = 1024

Ripple control parameter (β) = 6

Digital modulation technique = QPSK (Quaternary Phase Shift Keying)

Maximum OFDM symbols for CCDF curve = 10,000

Approximation to number of iterations (z) for SC-W = 3

Channel taken for measuring BER v/s Eb/No performance = AWGN

7.1 Complementary Cumulative Distribution Function (CCDF)

The complementary cumulative distribution function (CCDF) is one of the most frequently used performance measures for PAPR reduction techniques, which denotes the probability that the

PAPR of a data block exceeds a given threshold A. The CCDF of the PAPR of a data block of N symbols with nyquist rate sampling is derived as [28].

$$P(PAPR > A)=1-P(PAPR \leq A)=1-(1-e^{-A})^{N} \quad (122)$$

CASE 1: 3dB (A=1.4 σ)

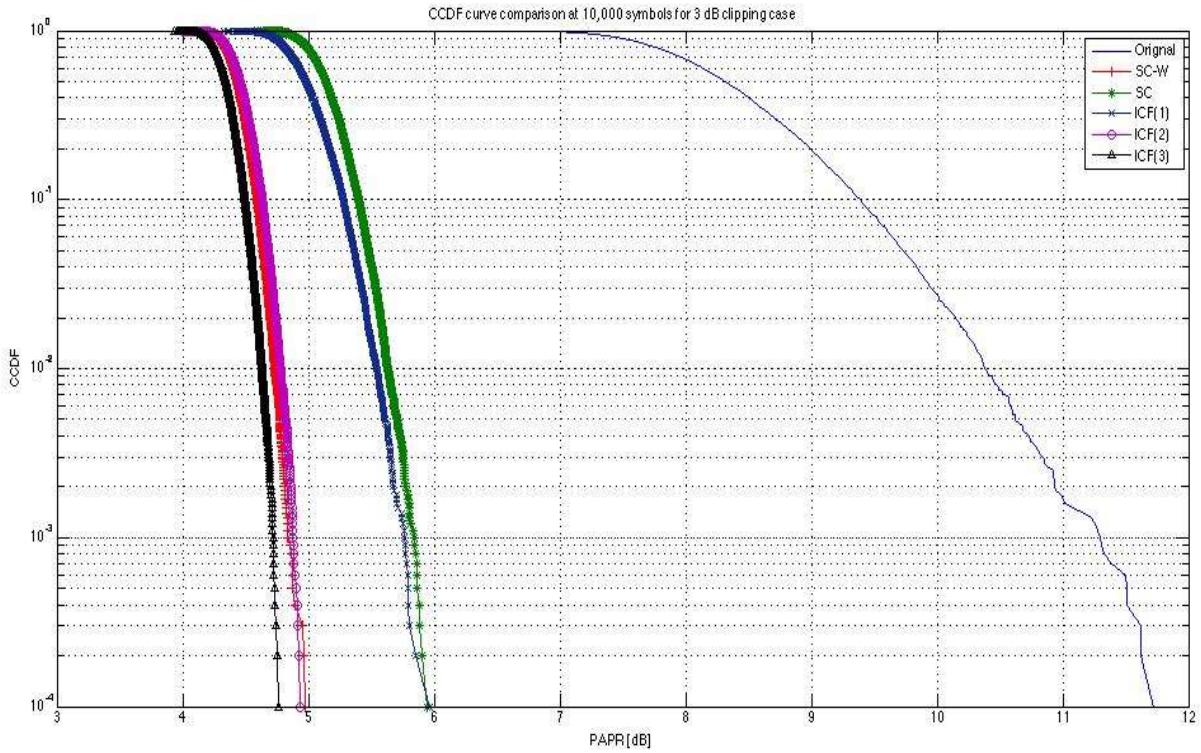

Figure 7.1. *CCDF curve comparison at 10,000 symbols(3dB)*

CASE 2: 6dB (A=1.9953 σ)

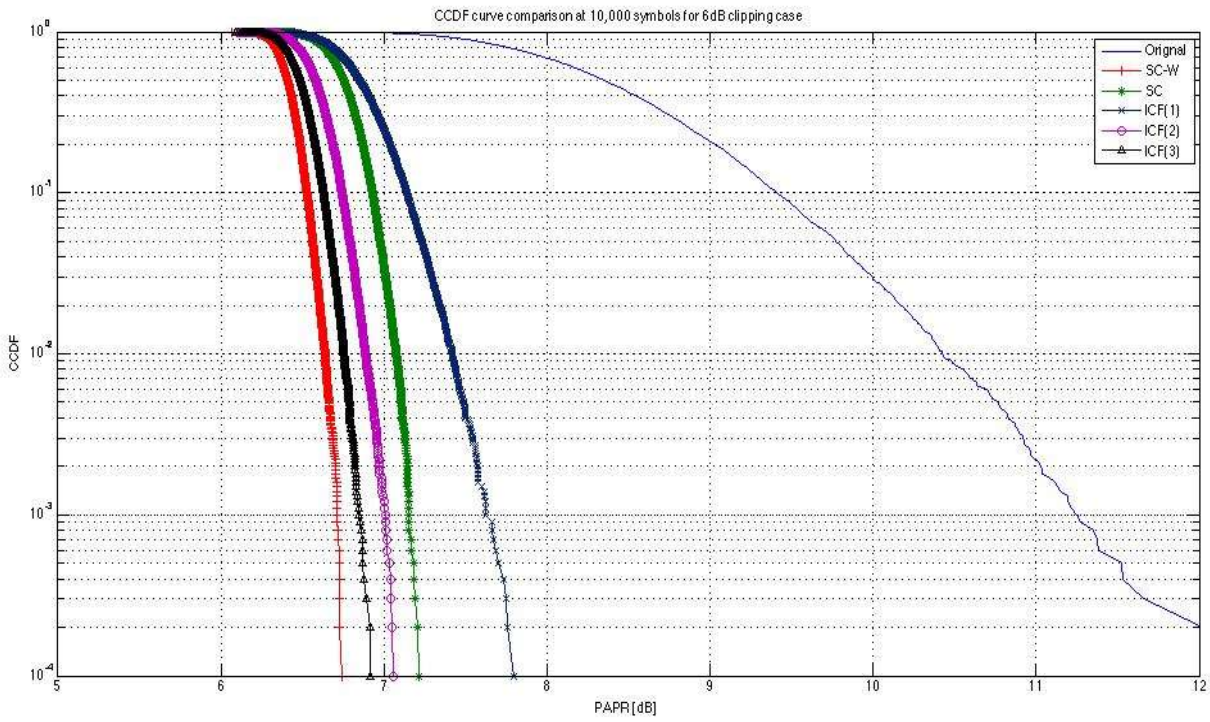

Figure 7.2. *CCDF curve comparison at 10,000 symbols(6dB)*

7.2 Power Spectral Density (PSD)

CASE 1: 3dB (A=1.4 σ)

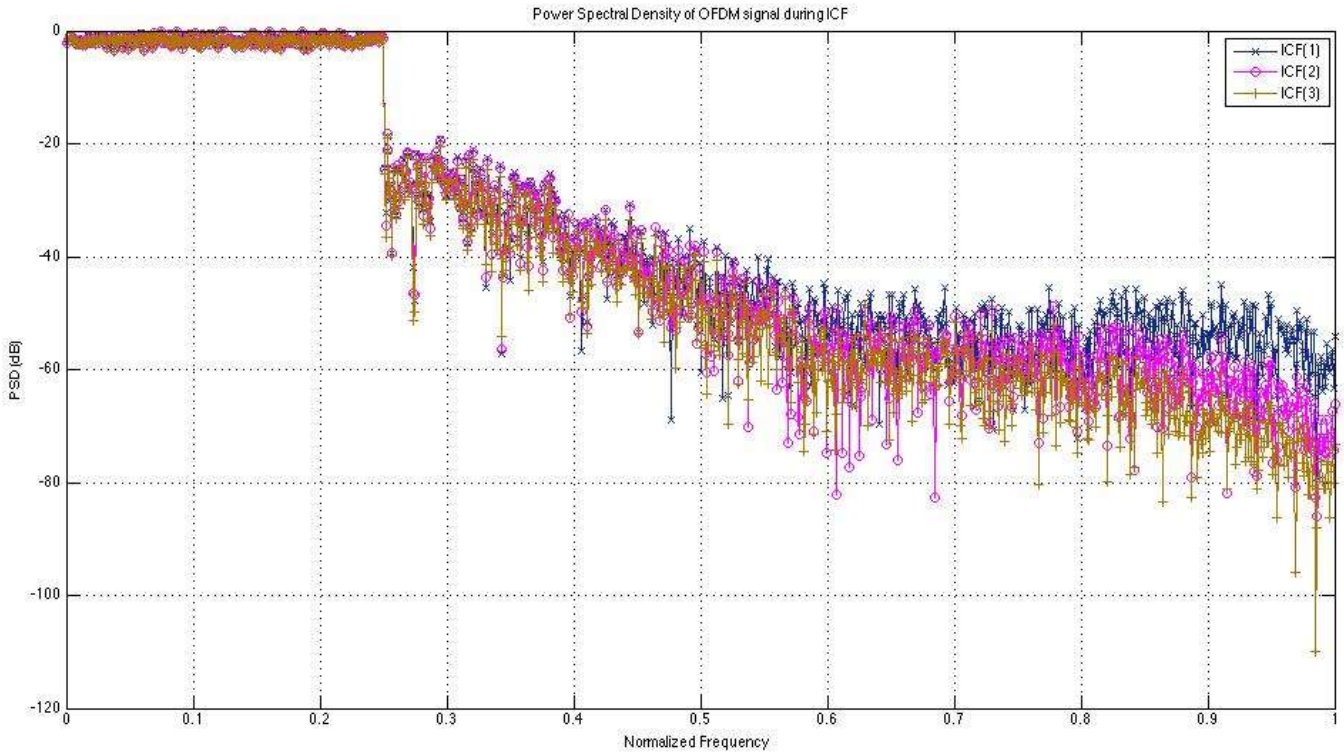

Figure 7.3. *PSD comparison for different number of iterations ICF(1), ICF(2), ICF(3)(3dB)*

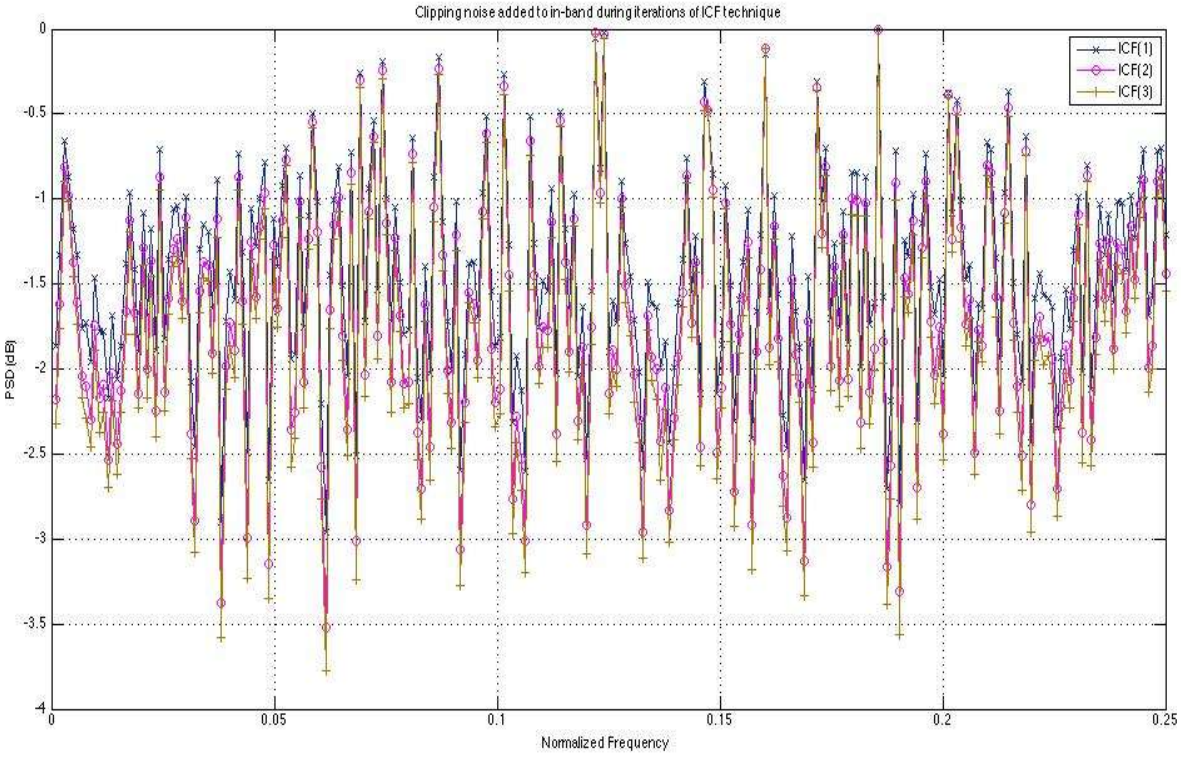

Figure 7.4. *In-band attenuation comparison for different number of iterations in ICF (3dB)*

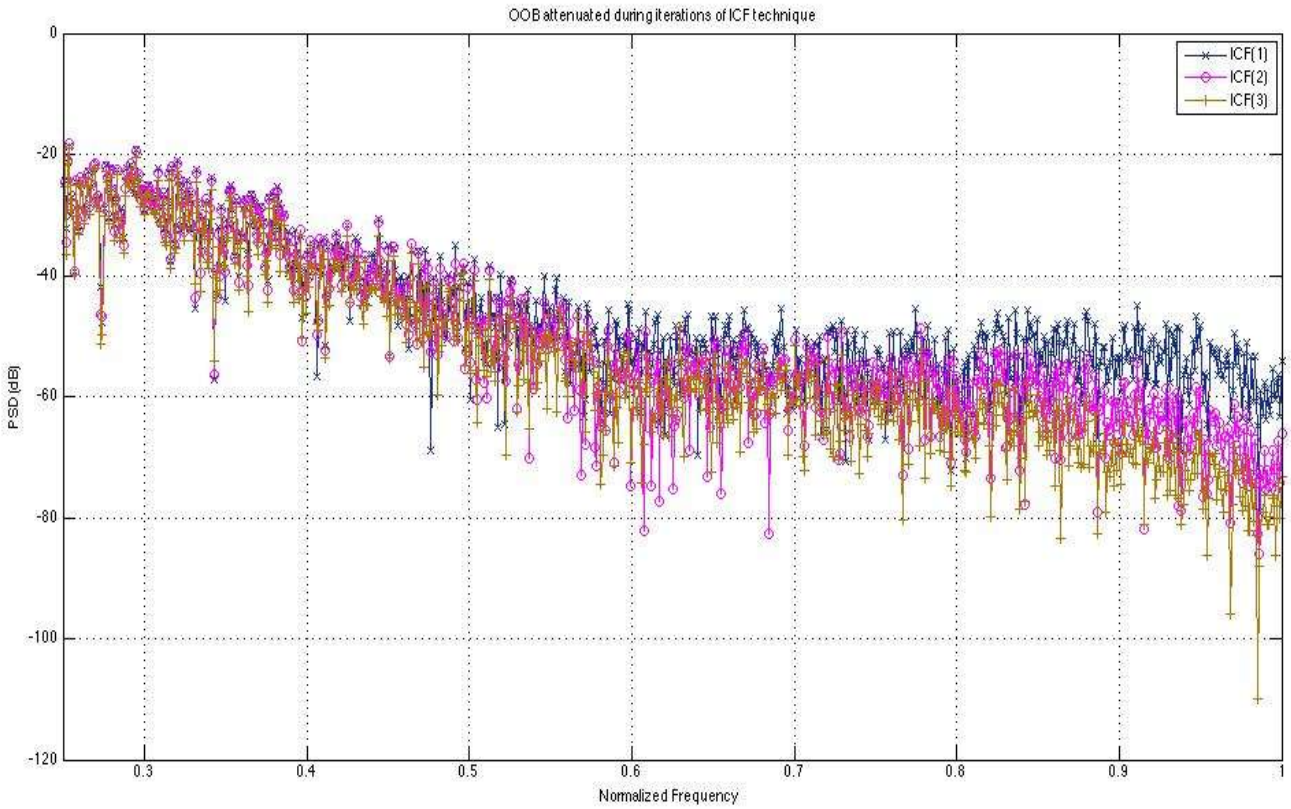

Figure 7.5. *OOB attenuation comparison for different number of iterations in ICF (3dB)*

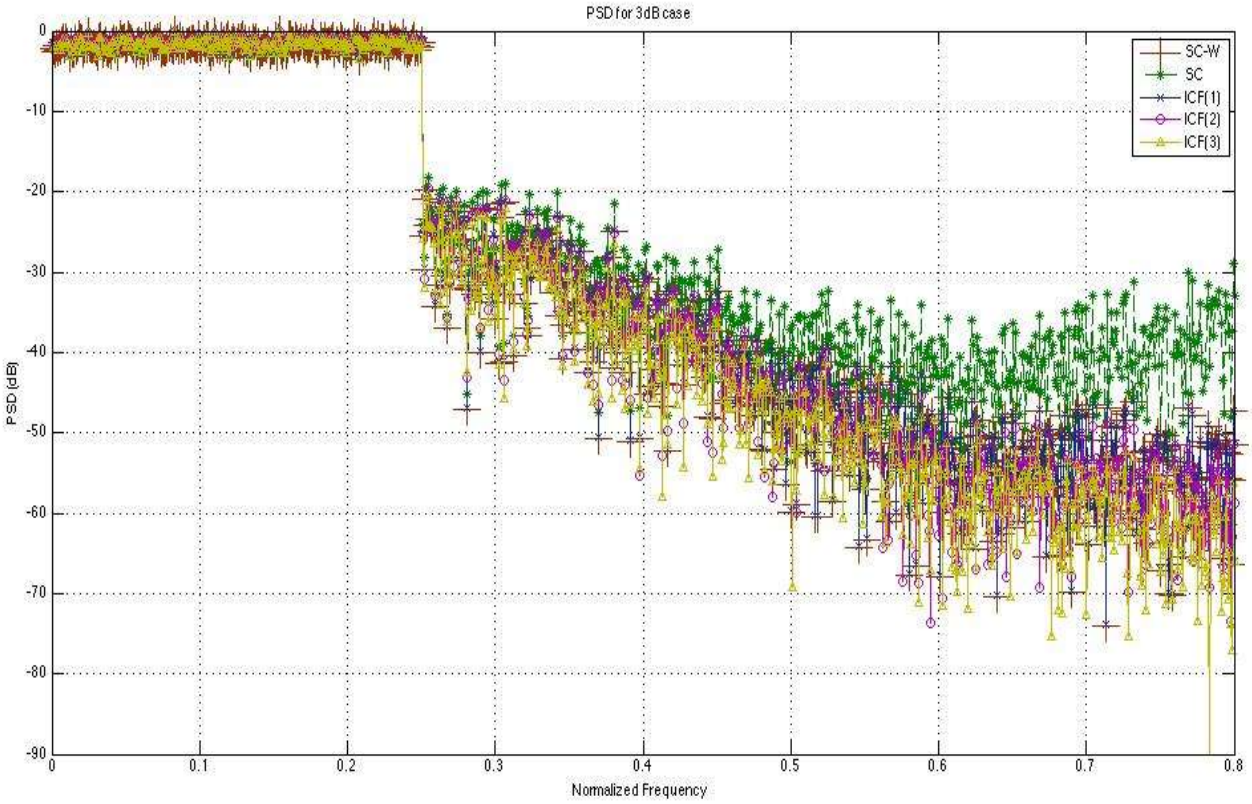

Figure 7.6. *PSD comparison for SC-W, SC, ICF(1), ICF(2), ICF(3)(3dB)*

CASE 2: 6dB (A=1.9953 σ)

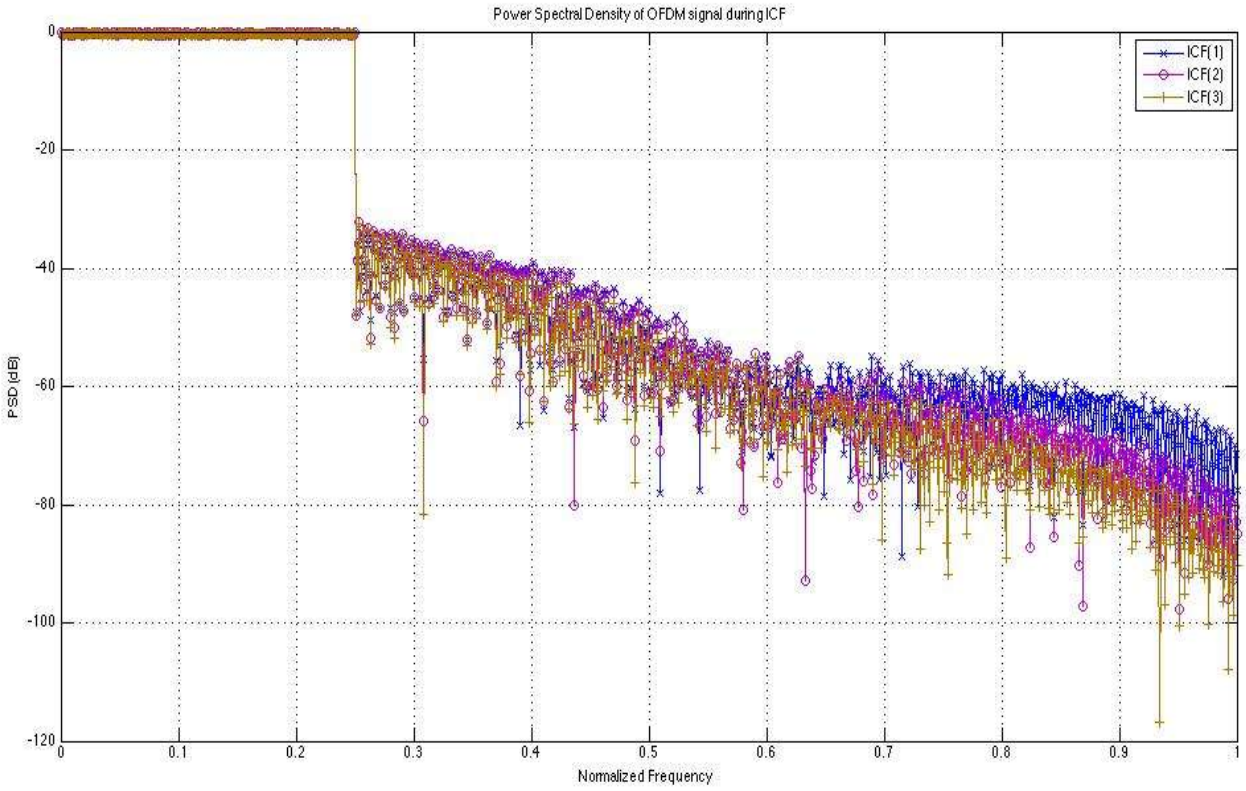

Figure 7.7. *PSD comparison for different number of iterations ICF(1), ICF(2), ICF(3)(6dB)*

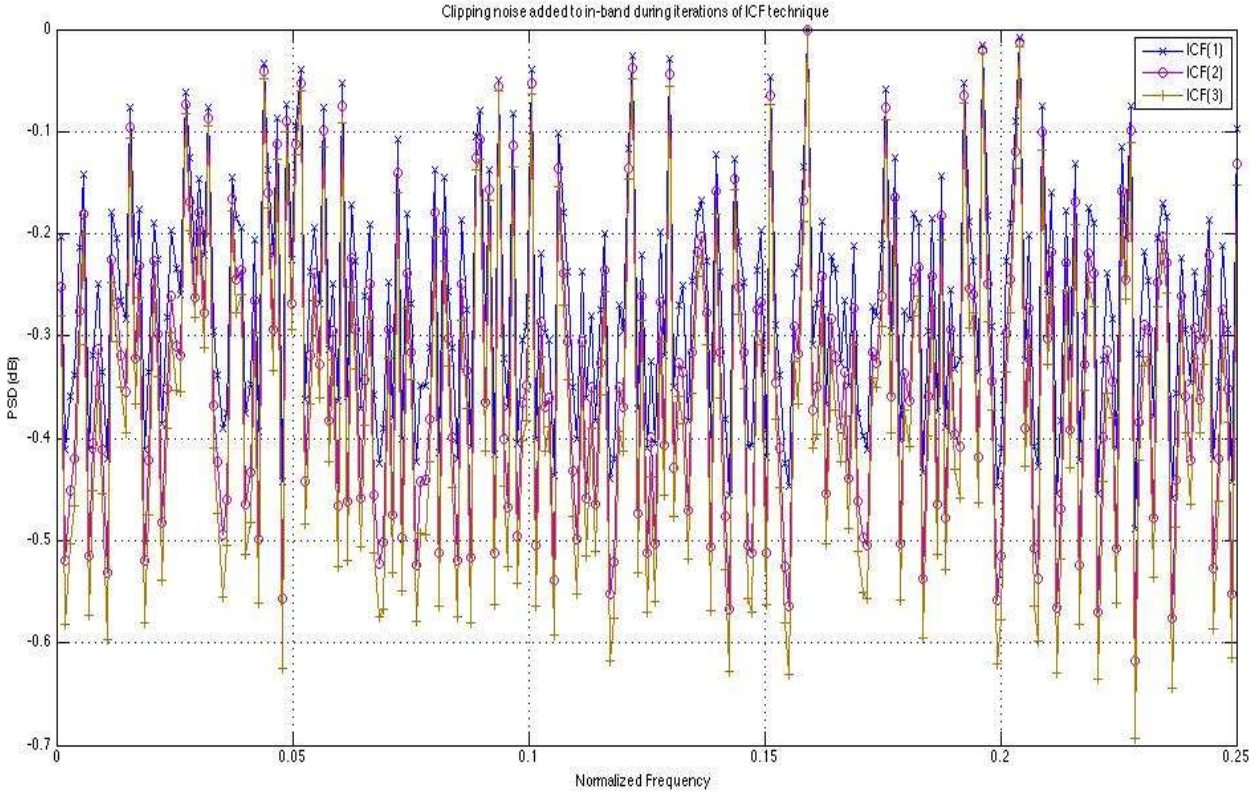

Figure 7.8. *In-band attenuation comparison for different number of iterations (6dB)*

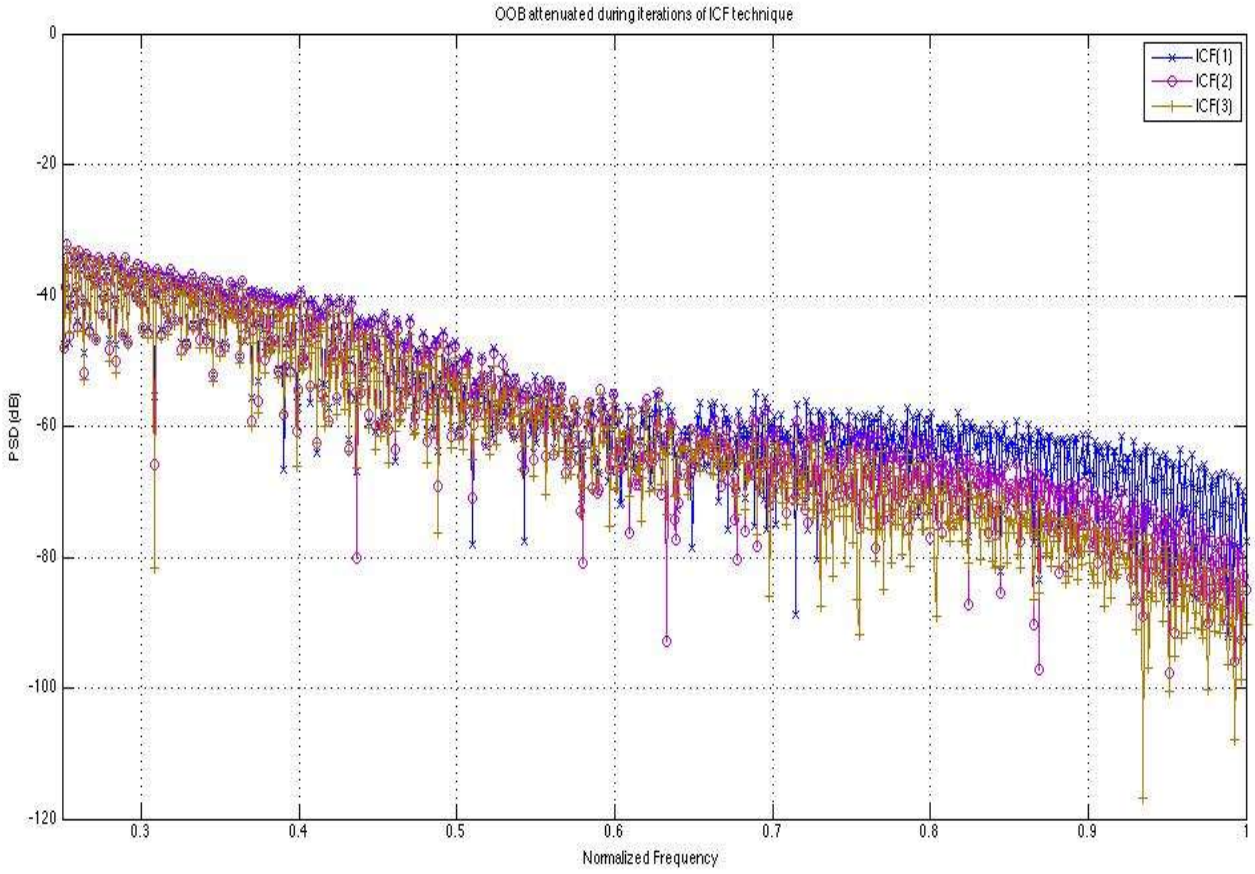

Figure 7.9. *Out of band attenuation comparison for different number of iterations*

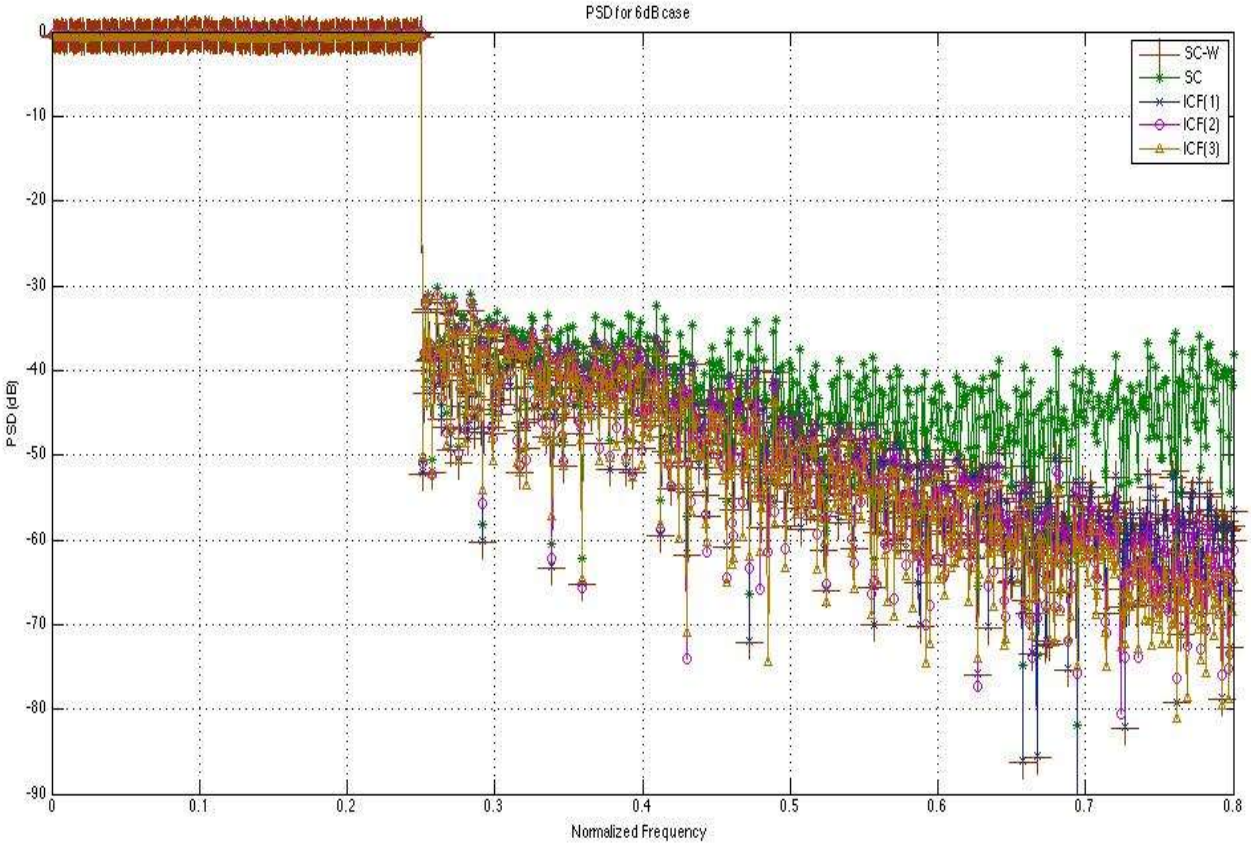

Figure 7.10. *PSD comparison for SC-W, SC, ICF(1), ICF(2), ICF(3)(6dB)*

7.3 Bit Error Rate (BER)

CASE 1: 3dB (A=1.4 σ)

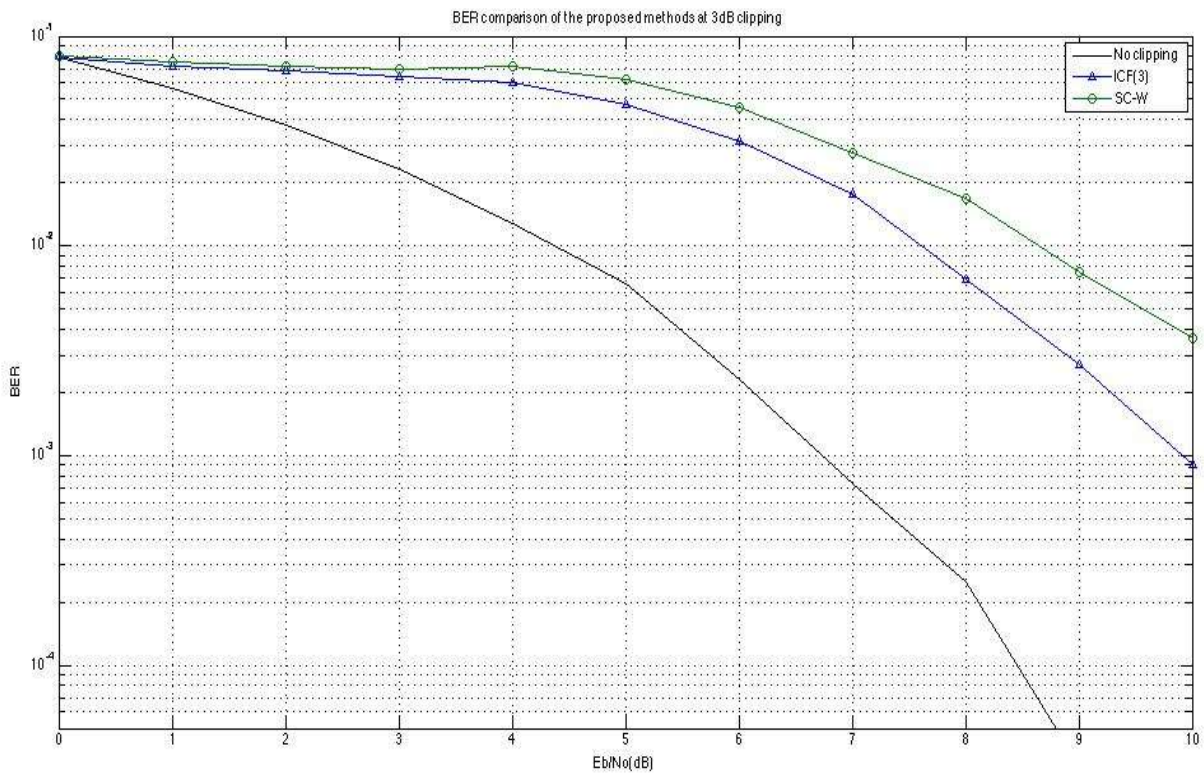

Figure 7.11. *BER comparison for SC-W and ICF(3)(3dB)*

CASE 2: 6dB (A=1.9953 σ)

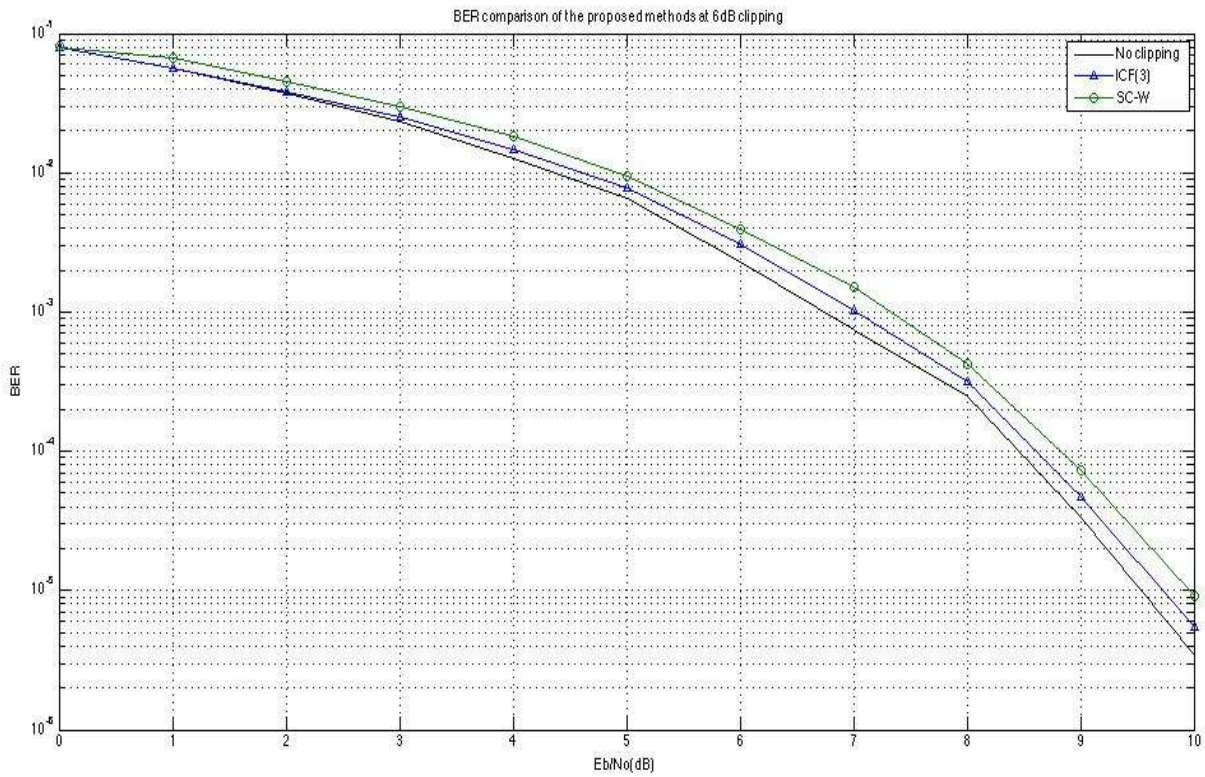

Figure 7.12. *BER comparison for SC-W and ICF(3)(6dB)*

7.4 Transmit spectrum of OFDM signal based on IEEE 802.11a

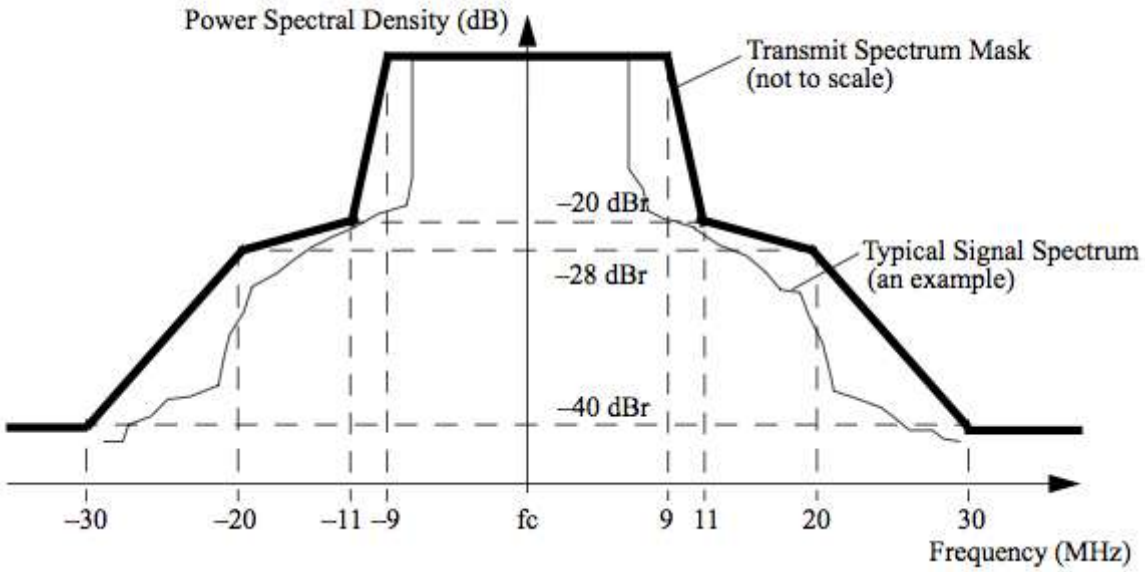

Figure 7.13 *Transmit spectrum of OFDM signal based on IEEE 802.11a* [93]

7.5 Response of Solid State Power Amplifier (SSPA) model

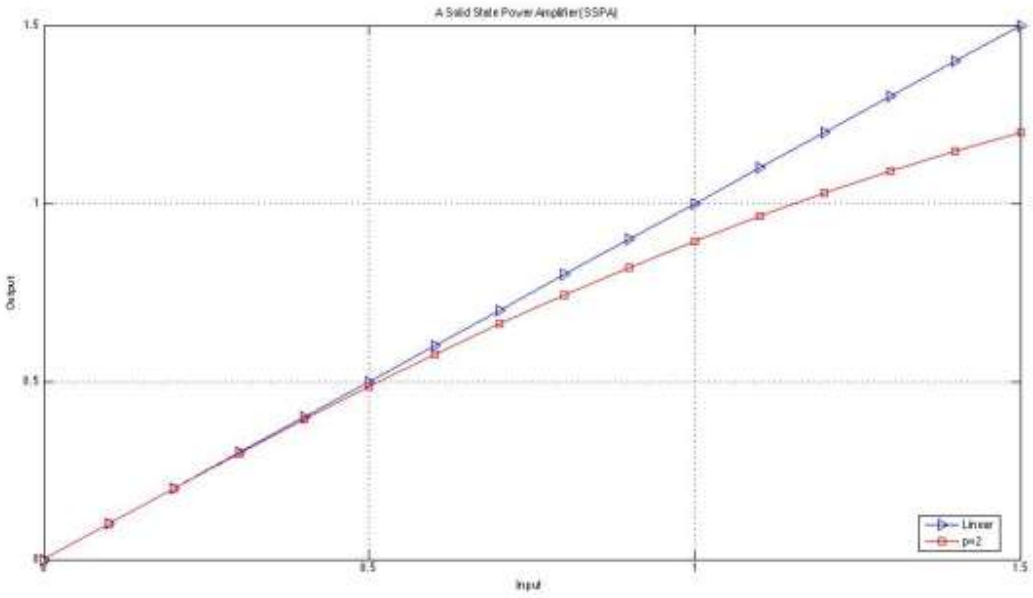

Figure 7.14 *Comparison of response of SSPA at p=∞ and p=2*

7.6 Peak Re-growth, its Reduction and Effect of Filter Action on Clipping Noise in ICF

CASE 1: 3dB (A=1.4 σ)

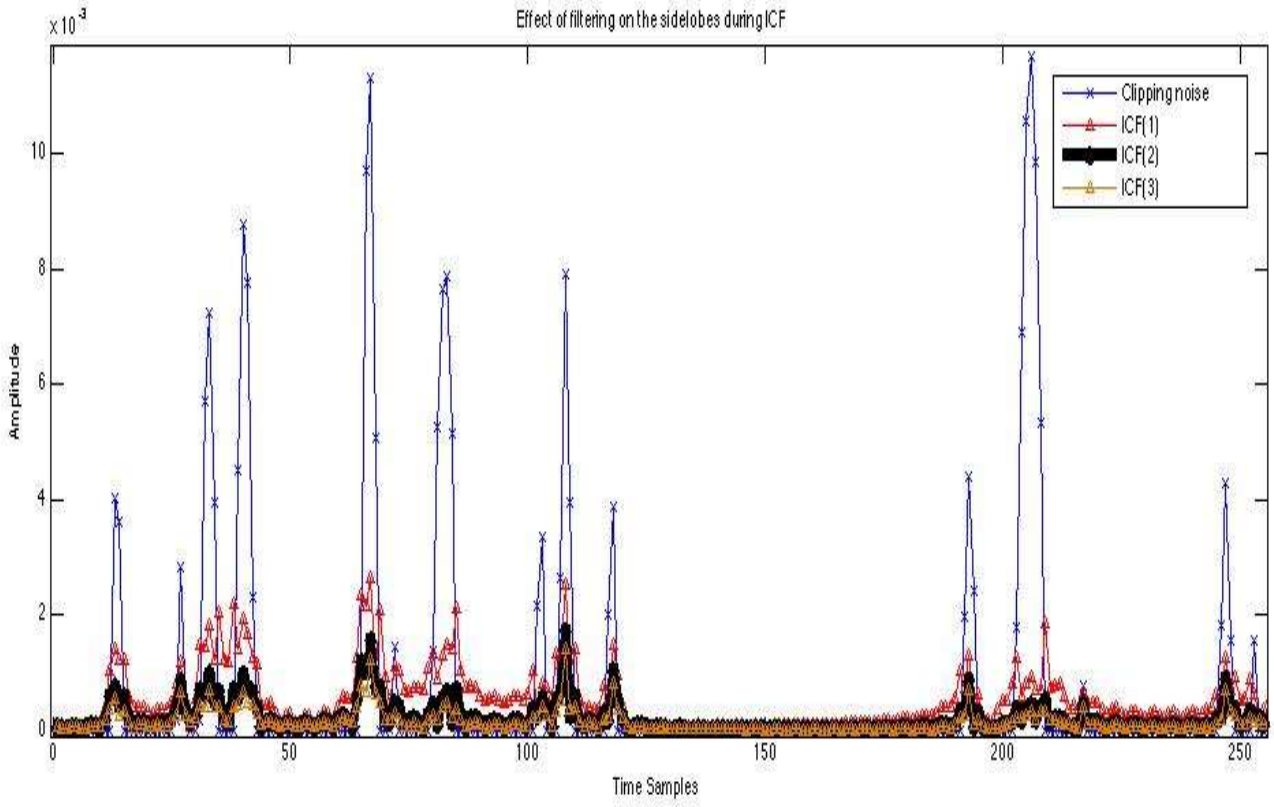

Figure 7.15. *Peak re-growth, its reduction and effect of filter on clipping noise in ICF(3dB)*

CASE 2: 6dB (A=1.9953 σ)

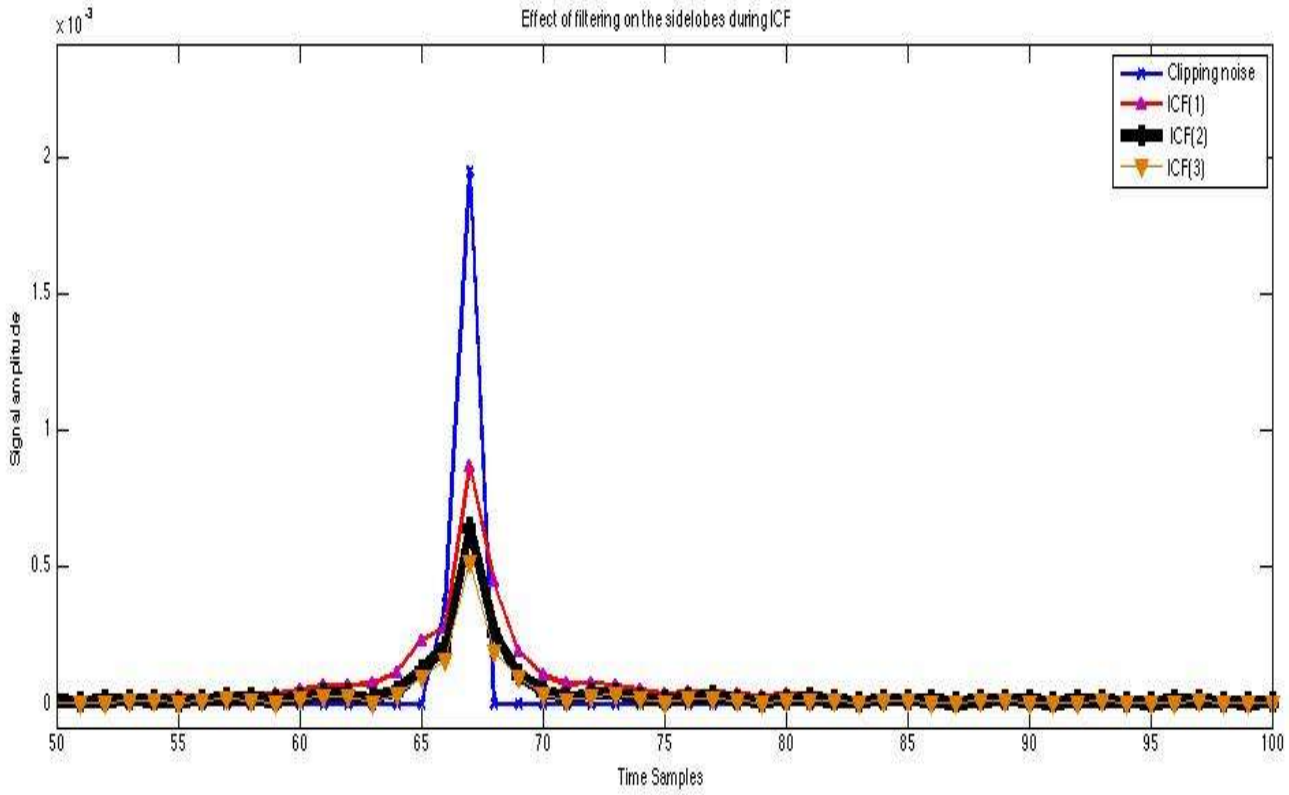

Figure 7.16. *Peak re-growth, its reduction and effect of filter on clipping noise in ICF(6dB)*

7.7 Comparison of SC-W, SC, ICF(1), ICF(2), ICF(3) in Time Domain

CASE 1: 3dB (A=1.4 σ)

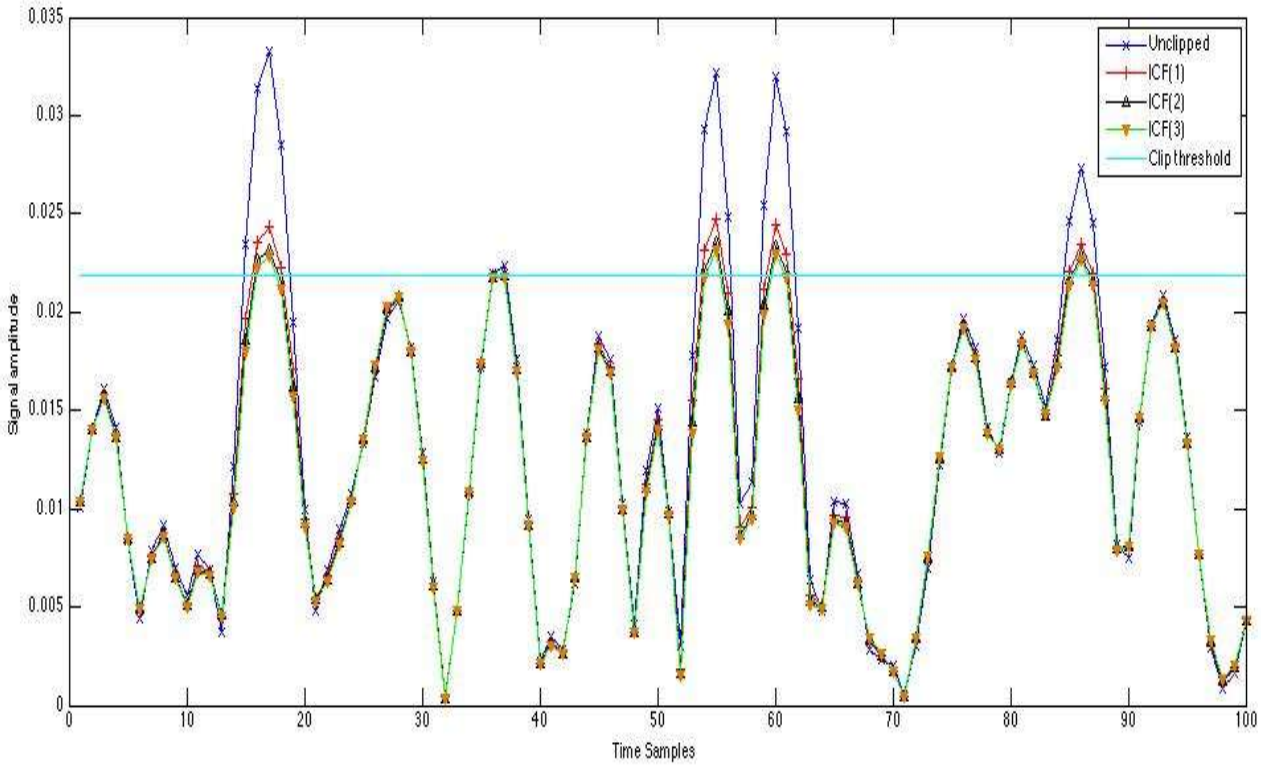

Figure 7.17. *Effect of ICF in time domain(3dB)*

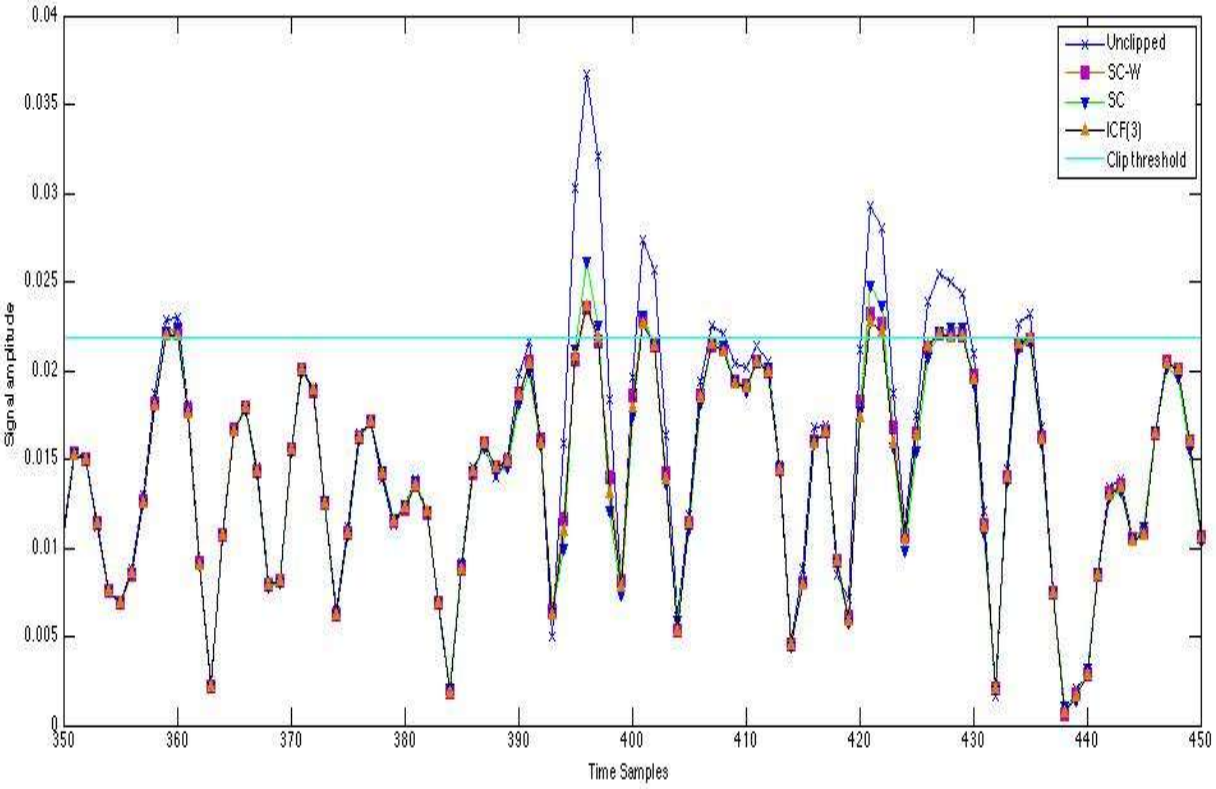

Figure 7.18. *Comparison of Effect of SC-W, SC and ICF(3) in time domain(3dB)*

CASE 2: 6dB (A=1.9953 σ)

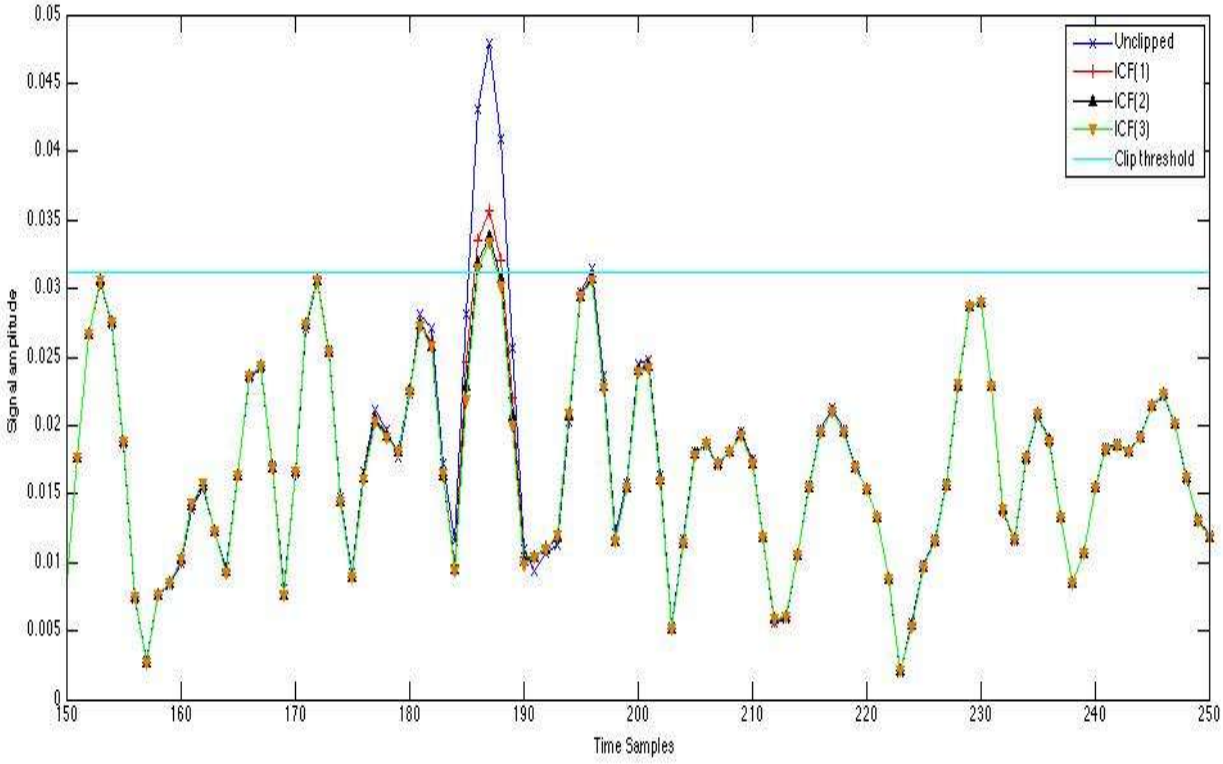

Figure 7.19. *Effect of ICF in time domain(6dB)*

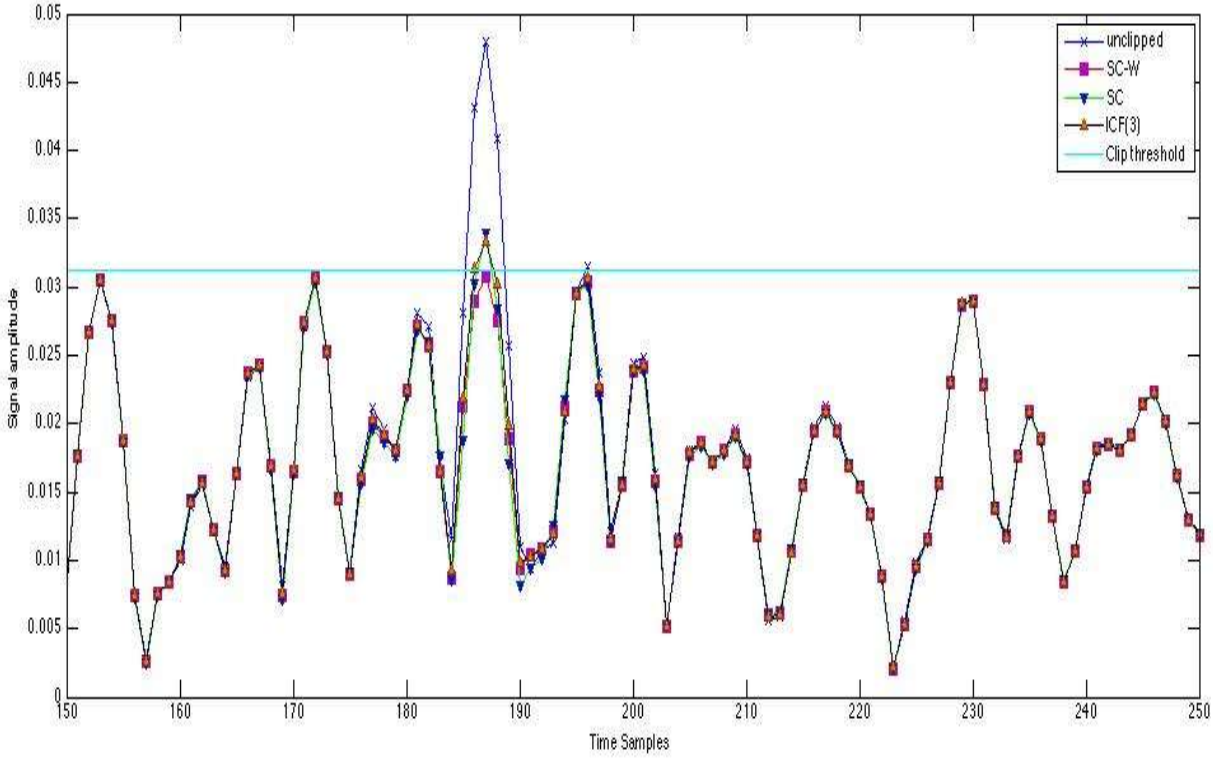

Figure 7.20. *Comparison of Effect of SC-W, SC and ICF(3) in time domain(6dB)*

7.8 Statistical Data Obtained from Simulations

CASE 1: 3dB (A=1.4 σ)

Table I. PAPR reduction comparison

	Original	ICF(1)	ICF(2)	ICF(3)	SC	SC-W
PAPR(dB)	11.81	5.878	4.956	4.814	5.99	4.92

Table II. Average attenuation comparison

Average attenuation(*dB*)	ICF(1)	ICF(2)	ICF(3)	SC	SC-W
In-band	1.4371	1.6805	1.7962	2.4286	2.4286
Out-band	47.3264	51.5524	54.4816	34.6375	47.4616

CASE 2: 6dB (A=1.9953 σ)

Table III. PAPR reduction comparison

	Original	ICF(1)	ICF(2)	ICF(3)	SC	SC-W
PAPR(dB)	11.72	7.728	7.033	6.902	7.248	6.766

Table IV. Average attenuation comparison

Average attenuation(*dB*)	ICF(1)	ICF(2)	ICF(3)	SC	SC-W
In-band	0.2646	.3304	0.3679	0.4091	0.4091
Out-band	57.3619	60.5887	62.9992	44.658	57.482

From the CCDF curves shown in figure 7.1, 7.2 and data provided in table I, III PAPR decreases with number of iterations, but its convergence decreases in both 3dB and 6dB case. In 3dB case ICF(1) is quite superior than SC method, whereas SC-W method is almost equal to ICF(2), .1 dB degraded from ICF(3) and provides 1 dB improvement over SC method. In 6 dB case SC method is far superior than ICF(1), whereas SC-W method provides .2 dB and .48 dB improved performance from ICF(3) and SC method respectively.

From the PSD graphs shown in figures 7.3 to 7.10 and data provided in table II, IV as number of iterations increases in ICF method, the in-band distortion and out of band attenuation increases. Due to the frequency domain filtering using kaiser window, in-band distortion is very less. In case of 3dB case in-band distortion is more and OOB attenuation is less as compared to 6dB case. In 3 dB case SC-W method provides .7 dB more in-band distortion and 7dB less OOB attenuation whereas in 6 dB case SC-W provides equal in-band distortion and 5dB less OOB attenuation than ICF(3). In both cases ICF and SC-W methods meets the requirement of IEEE 802.11a transmit spectrum mask specified in figure 7.13.

From the figures 7.15 to 7.20, we can see that for small clipping thresholds esp. 3 dB case clipping noise pulses are very close to each other. After filtering action, the side-lobes of pulses start to interfere with the adjacent pulses, but the interference is very small. This brings the error floor but in tolerable limits.

From BER graphs shown in figures 7.11, 7.12 the increase in error floor, due to increase in iterations in ICF is justified. Performance of SC-W method and ICF(3) is almost same with a difference of .32 dB in 6 dB case whereas in 3 dB case SC-W is slight inferior with a difference of 1.3 dB at 10^{-3} BER level.

7.9 Computational Complexity Analysis of Proposed Algorithm SC-W

We will now do computational complexity analysis of our proposed algorithm SC-W by considering number of real multiplications. Here, we count a complex multiplication as three real multiplications [94]. Only the runtime computational cost is considered, and the cost of the initializing stage can be omitted because it occurs only once. In the runtime stage, steps 1 and 2 explained in Figure 6.1 of chapter 6 are not counted, because all OFDM systems must execute atleast one iteration of these two steps.

In step 3, f_n can be calculated as $f_n = x_n - \bar{x}_n$ i.e. $f_n = x_n(1 - \frac{A}{|x_n|})$,

where $n \in \mathcal{F} = \{n: |x_n| > A\}$, and N_f is the size of $\mathcal{F}$. The execution time of this step is determined by that of calculating f_n.

By applying condition $|x_n| > A$ i.e.

$$\left(|x_{n,R}| \geq \frac{A}{\sqrt{2}} OR |x_{n,I}| \geq \frac{A}{\sqrt{2}}\right) AND \left(|x_{n,R}| + |x_{n,I}| \geq A\right) \quad (123)$$

Where $|x_{n,R}|$ and $|x_{n,I}|$ are the real and imaginary parts of x_n, respectively. Excluding small samples, the number of sample satisfying (123) is

$$\overline{N}_c = JN\left(1 - \left(erfc\left(\frac{A}{2\sigma}\right)\right)^2 - P1\right) \quad (124)$$

Where $P1 = \int_{A/\sqrt{2}}^{A} \frac{2\sqrt{2}}{\sigma\sqrt{\pi}} \text{erf}\left(\frac{A-x}{\sigma\sqrt{2}}\right) e^{-x^2/2\sigma^2} dx$.

Therefore, for A = 6dB case $\overline{N}_c \approx .057JN$ and for A = 3dB case $\overline{N}_c \approx .32JN$. Calculating $|x_n|$ then requires $2\overline{N}_c$ real multiplications.

Calculating f_n for $n \in \mathcal{F}$ requires $2N_f$ real multiplications and N_f real divisions. However N_f is a function of N, which can be seen by calculating its mean as

$$\overline{N}_f = \overline{N}_p \tau f_s \quad (125)$$

Where $f_s = \frac{JN}{T}$ is the sampling frequency, and $\overline{N}_p$ is the average number of pulses in an OFDM symbol duration, calculated in (71), we have

$$\overline{N}_f = JNe^{-A^2/2\sigma^2} \quad (126)$$

$\overline{N}_f$ may change after the first iteration. However, because the OFDM signal after the first iteration is $\hat{x}_n = x_n + c_n$, the N_f for $\hat{x}_n$, denoted as $\widehat{N}_f = N_f - N_1 + N_2$. Where N_1 is the number of samples that are higher than A in the first iteration but are lower than A after first iteration, and N_2 is the number of samples of the newly generated peaks. c_n is very small only those peaks of x_n that are slightly smaller or higher than A will contribute to N_1 and N_2.

By using (126), N_1 and N_2 can be easily shown to be small numbers, and their difference can be omitted. Thus N_f is roughly constant in all iterations. We may estimate the execution time of calculating f_n as $2\overline{N}_f$ real multiplications and $\overline{N}_f$ real divisions. Therefore, for A = 6dB case $\overline{N}_f \approx .019JN$ and for A = 3dB case $\overline{N}_f \approx .091JN$.

Step 4 and 5 would take $2JN+\log_2 JN$ operations for scaling and step 6 would have complexity of order $2JN\log_2 JN$.

So, the approximated computational complexity of SC-W method is given by

$$CC = 2(\overline{N}_f + \overline{N}_c + JN) + \log_2 JN(2JN + 1) \tag{127}$$

For comparison, complexity of C-PTS (Conventional Partial Transmit Sequence) method is compared, which is also a promising technique for PAPR reduction. Complexity of C-PTS increases as the number of sub-blocks increases [10]. To reduce it many techniques have been suggested. In [95] DSI-PTS method is presented which offers low computational complexity. For 512 sub-carriers, 4 sub-blocks C-PTS has a computational complexity of 60416 and with D=1 DSI-PTS has a computational complexity of 30208. For 512 sub-carriers (N) and oversampling factor (J)=2 complexity of SC-W is 22694 (127) and for ICF(3) computational complexity is in order of $3(2JN\log_2 JN)$ [55], which is 61440 for ICF(3) method. Thus, SC-W offers low computational complexity as compared to C-PTS, DSI-PTS and ICF. To further reduce the PAPR, the proposed methods can be merged with the clipping ratio estimation techniques at receiver side explained in [96].

CHAPTER 8

CONCLUDING REMARKS AND FUTURE WORK

8.1 Conclusions

OFDM has long been studied and implemented to combat transmission channel impairments. Its application have been extended from high frequency radio communications to telephone networks, digital audio broadcasting and terrestrial broadcasting of digital television. The advantages of OFDM, especially in the multipath propagation, interference and fading environment, make it promising technology in mobile communication.

In this thesis work, we have proposed a new SC-W PAPR reduction method based on kaiser windowing of out of band of OFDM symbol in the frequency domain to reduce PAPR of OFDM signal. Simulation results shows that, compared with the conventional ICF method, this method can dramatically reduce the peak re-growth and computational complexity by avoiding ICF operations. SC-W method provides better PAPR reduction over SC method and out of band power attenuation very close to ICF for both small and large clipping cases with the expense of tolerable BER degradation especially in small clipping case.

SC-W PAPR reduction method meets the requirement of transmit mask specified in IEEE 802.11a and is completely compatible with other transmitter designs. It can be implemented by replacing transmitter IDFT with an oversize IDFT followed by clipping, scaling and filtering circuit. No changes are required at receiver side and can be adopted without any change to telecommunication standards.

Major achievements:-

1.) PAPR reduction performance of proposed method SC-W is almost equal and better in 3dB (deep clipping) case and 6 dB (large clipping) case, respectively.

2.) PSD of OFDM signal formed by SC-W method is similar to that of formed by ICF method with three iterations.

3.) BER performance of SC-W method is almost same as that of ICF method in 6 dB case and 1.3 dB degraded in 3dB case at 10^{-3} level, which is tolerable.

4.) SC-W method greatly reduces the OOB power, and the computational complexity by 63% in 6dB case and by 62% in 3dB case.

8.2 Future Work

In SC-W method frequency domain filtering of whole out of band components is not required. But the number of components to filter varies from symbol to symbol for optimum PAPR reduction. An adaptive method can be realized to filter minimum number of OOB components with minimum BER degradation for a symbol. The future work also includes the implementation aspects of the proposed scheme using FPGA systems [97].

REFERENCES

[1] L. Wang and C. Tellambura, "A simplified clipping and filtering technique for PAR reduction in OFDM systems," *IEEE Signal Processing Letters*, vol. 12, no. 6, June 2005, pp. 453-456.

[2] T. Jiang and Y. Wu, "An Overview: Peak to average power ratio reduction techniques for OFDM signals," *IEEE Transactions on Broadcasting*, vol. 54, no. 2, June 2008, pp. 257–268.

[3] J. Armstrong, "Peak to average power reduction for OFDM by repeated clipping and frequency domain filtering," *IEEE Electronics Letters*, vol. 38, no. 5, Feb. 2002, pp. 246–247.

[4] X. B. Wang, T. T. Tjhung and C. S. Ng, "Reduction of peak to average power ratio of OFDM system using a companding technique," *IEEE Transactions on Broadcasting*, 1999, vol. 45, no. 3, Sept. 1999, pp. 303–307.

[5] T. Jiang, Y. Yang and Y. Song, "Exponential companding transform for PAPR reduction in OFDM systems", *IEEE Transactions on Broadcasting*, vol. 51, no. 2, June 2005, pp. 244–248.

[6] J. L. Huang, J. Zheng, K. B. Letaief and J. Gu, "Companding transform for reduction in peak to average power ratio of OFDM signals," *IEEE Transactions on Wireless Communications*, vol. 3, no. 6, Nov. 2004, pp. 2030-2039.

[7] A. A. Sulaiman, F. B. Ehab and D. A. E. Mohamed, "Linear companding transform for the reduction of peak to average power ratio of OFDM signals," *IEEE Transactions on Broadcasting*, vol. 55, no, 1, March 2009, pp. 155-160.

[8] J. Hou, J. H. Ge and J. Li, "Trapezoidal companding scheme for peak to average power ratio reduction of OFDM signals," *IEEE Electronics Letters*, vol. 45 , no. 25 , 2009, pp.1349 – 1351.

[9] S. S. Jeng and J. M. Chen, "Efficient PAPR reduction in OFDM system based on a companding techniques with trapezium distribution," *IEEE Transactions on Broadcasting*, vol. 57, no. 2, June 2011, pp. 291-298.

[10] S. H. Muller and J. B. Huber, "OFDM with reduced peak to average power ratio by optimum combination of partial transmit sequences," *IEEE Electronics Letters*, vol. 33, no. 5, Feb. 1997, pp. 368–369.

[11] R. W. Bäuml, R. F. H. Fischer and J. B. Huber, "Reducing the peak to average power ratio of multicarrier modulation by selected mapping," *IEEE Electronics Letters*, vol. 32, no. 22, Oct. 1996, pp. 2056–2057.

[12] A. D. S. Jayalath and C. Tellambura, "SLM and PTS peak power reduction of OFDM signals without side information," *IEEE Transactions on Wireless Communications*, vol. 4, no. 5, Sept. 2005, pp. 2006–2013.

[13] L. J. Cimini and N. R. Sollenberger, "Peak to average power ratio reduction of an OFDM signal using partial transmit sequences with embedded side information," in *Proceeding of IEEE GlobeComm'00*, vol. 2, Nov. 2000, pp. 746-750.

[14] M. Breiling, S. H. Muller-Weinfurtner and J. B. Huber, "SLM peak power reduction without explicit side information," *IEEE Communications Letters*, vol. 5, no. 6, June 2001, pp. 239–241.

[15] S. Y. Le Goff, S. S. Al-Samahi, K. K. Boon, C. C. Tsimenidis and B. S. Sharif, "Selected mapping without side information for PAPR reduction in OFDM," *IEEE Transactions on Wireless Communications*, vol. 8, no. 7, July 2009, pp. 3320–3325.

[16] N. V. Irukulapati, V. K. Chakka and A. Jain, "SLM based PAPR reduction of OFDM signal using new phase sequence", *IEEE Electronics Letters*, vol. 45, no. 24, Nov. 2009, pp. 1231–1232.

[17] Y. Zhou and T. Jiang, "A novel multi point square mapping combined with PTS to reduce PAPR of OFDM signals without side information," *IEEE Transactions on Broadcasting*, vol. 55, no. 4, Dec. 2009, pp. 831–835.

[18] Y. Zhao and S. G. Häggman, "Intercarrier interference self-cancellation scheme for OFDM mobile communication systems," *IEEE Transactions on Communications*, vol. 49, no. 7, July 2001, pp. 1185-1191.

[19] K. Sathananthan and R. M. A. P. Rajatheva, "Analysis of OFDM in the presence of frequency offset and a method to reduce performance degradation," in *Proceeding of Global Telecommunications Conference'00, San Francisco, USA*, vol. 1, Nov. 2000, pp. 72-76.

[20] A. Seyedi and G. J. Saulnier, "General ICI self-cancellation scheme for OFDM systems", *IEEE Transactions on Vehicular Technology*, vol. 54, no. 1, Jan. 2005, pp. 198-210.

[21] H. G. Yeh, Y. K. Chang and B. Hassibi, "A scheme for canceling intercarrier interference using conjugate transmission in multicarrier communication systems", *IEEE Transactions on Wireless Communications*, vol. 6, no. 1, Jan. 2007, pp. 3-7.

[22] C. L. Wang, Y. C. Huang, "Intercarrier interference cancellation using general phase rotated conjugate transmission for OFDM systems," *IEEE Transactions on Communications*, vol. 58, no. 3, Mar. 2010, pp. 812-819.

[23] A. Jayalath, *OFDM for wireless broadband communications (peak power reduction, spectrum and coding)*. Melbourne: Ph.D. dissertation, School of Computer Science and Software Engineering, Monash University, 2002.

[24] J. G. Proakis, *Digital Communications*. New York: 4th edition McGraw Hill Companies, Inc., 2001.

[25] C. Tellambura, "Use of m-sequence for OFDM peak to average power ratio reduction," *IEEE Electronics Letter*, vol. 33, no. 15, July 1997, pp. 1300–1301.

[26] L. Wang, "Phase optimisation criterion for reducing peak to average power ratio in OFDM," *IEEE Electronics Letters*, vol. 34, no. 2, Jan. 1998, pp. 169–170.

[27] H. Rowe, "Memoryless nonlinearities with gaussian inputs: elementary results," *Bell System Technology*, vol. 61, no. 7, Sept. 1982, pp. 1520–1523.

[28] R. van Nee, R. Prasad, *OFDM for Wireless Multimedia Communications*. Norwell: Artech House Publishers, 2000, ch. MA.

[29] C. Tellambura, "Upper bound on peak factor of N multiple carriers," *IEEE Electronics Letters*, vol. 33, no. 19, Sept. 1997, pp. 1608–1609.

[30] R. van Nee, A. de Wild, "Reducing the peak to average power ratio of OFDM," in *48th IEEE Vehicular Technology Conference (VTC 98), Ottawa,* vol. 3, May 1998, pp. 2072–2076.

[31] P. Banelli and S. Cacopardi, "Theoretical analysis and performance of OFDM signals in nonlinear AWGN channels," *IEEE Transactions on Communications*, vol. 48, no. 3, March 2000, pp. 430–441.

[32] P. Banelli, G. Baruffa and S. Cacopardi, “Effects of HPA nonlinearity on frequency multiplexed OFDM signals,” *IEEE Transactions on Broadcasting*, vol. 47, no. 2, June 2001, pp. 123–136.

[33] D. Dardari, V. Tralli and A. Vaccari, “A theoretical characterization of nonlinear distortion effects in OFDM systems,” *IEEE Transactions on Communications*, vol. 48, no. 10, Oct. 2000, pp. 1755–1764.

[34] N. Dinur and D. Wulich, “Peak to average power ratio in amplitude clipped high order OFDM,” In *Proceeding of IEEE Military Communications Conference (MILCOM), Boston, MA*, vol. 2, Oct. 1998, pp. 684–687.

[35] N. Dinur and D. Wulich, “Peak to average power ratio in high order OFDM,” *IEEE Transactions on Communications*, vol. 49, no. 6, June 2001, pp. 1063–1072.

[36] S. Litsyn and A. Yudin, “Discrete and continuous maxima in multicarrier communication,” *IEEE Transactions on Information Theory*, vol. 51, no. 3, March 2005, pp. 919–928.

[37] S. Litsyn and G. Wunder, “Generalized bounds on the crest factor distribution of OFDM signals with applications to code design,” *IEEE Transactions on Information Theory*, vol. 52, no. 3, March 2006, pp. 992–1006.

[38] H. Ochiai and H. Imai, “Channel capacity of clipped OFDM systems,” In *Proceedings of IEEE International Symposium on Information Theory (ISIT), Sorrento*, June 2000, pp. 219.

[39] L. Wang, “Performance of the deliberate clipping with adaptive symbol selection for strictly band-limited OFDM systems,” *IEEE Journal of Selection of Areas of Communications*, vol. 18, no. 11, Nov. 2000, pp. 2270–2277.

[40] H. Ochiai and H. Imai, “On the distribution of the peak to average power ratio in OFDM signals,” *IEEE Transactions on Communications*, vol. 49, no. 2, Feb. 2001, pp. 282–289.

[41] H. Ochiai, “Power efficiency comparison of OFDM and single-carrier signals,” in *56th IEEE Vehicular Technoogy Conference (VTC 2002-Fall)*, vol. 2, Sept. 2002, pp. 899–903.

[42] H. Ochiai and H. Imai, “Performance analysis of deliberately clipped OFDM signals,” *IEEE Transactions on Communications*, vol. 50, no. 1, Jan. 2002, pp. 89–101.

[43] H. Ochiai, “Performance analysis of peak power and band limited OFDM system with linear scaling,” *IEEE Transactions on Wireless Communications*, vol. 2, no. 5, Sept. 2003, pp. 1055–1065.

[44] K. Panta and J. Armstrong, “Effects of clipping on the error performance of OFDM in frequency selective fading channels,” *IEEE Transactions on Wireless Communications*, vol. 3, no. 2, Mar. 2004, pp. 668–671.

[45] H. G. Ryu and J. S. Park, “Threshold IBO of HPA in the predistorted OFDM communication system,” *IEEE Transactions on Broadcasting*, vol. 50, no.4, Dec. 2004, pp. 425–428

[46] M. Sharif, M. Gharavi-Alkhansari and B. Khalaj, “On the peak to average power of OFDM signals based on oversampling,” *IEEE Transactions on Communications*, vol. 51, no. 1, Jan. 2003, pp. 72–78.

[47] D. Wulich, N. Dinur and A. Glinowiecki, “Level clipped high order OFDM,” *IEEE Transactions on Communications*, vol. 48, no. 6, June 2000, pp. 928–930.

[48] G. Wunder and H. Boche, “Upper bounds on the statistical distribution of the crest factor in OFDM transmission,” *IEEE Transactions on Information Theory*, vol. 49, no. 2, Feb. 2003, pp. 488–494.

[49] G. Wunder and H.Boche, "Peak value estimation of bandlimited signals from their samples, noise enhancement and a local characterization in the neighborhood of an extremum," *IEEE Transactions on Signal Processing*, vol. 51, no. 3, March 2003, pp. 771–780.

[50] H. Wang and B. Chen, "Asymptotic distributions and peak power analysis for uplink OFDMA signals," in *Proceedings of IEEE International Conference on Acoustics, Speech, and Signal Processing (ICASSP)*, vol. 4, May 2004, pp. 1085–1088.

[51] N. M. Blachman, "Gaussian noise – part I: the shape of large excursions," *IEEE Transactions on Information Theory*, vol. 34, no. 6, Nov. 1988, pp. 1396–1400.

[52] A. Bahai, M. Singh, A. Goldsmith and B. Saltzberg, "A new approach for evaluating clipping distortion in multicarrier systems," *IEEE Journal of Selected Areas of Communications*, vol. 20, no. 5, June 2002, pp. 1037–1046.

[53] M. Aronowich and R. J. Adler, "Extrema and level crossings of χ^2 processes," *Advances in Applied Probability*, vol. 18, no. 4, Dec. 1986, pp. 901–920.

[54] X. Li and L. J. Cimini, "Effects of clipping and filtering on the performance of OFDM," *IEEE Communications Letters*, vol. 2, no. 5, May 1998, pp. 131–133.

[55] S. Leung, S. Ju and G. Bi, "Algorithm for repeated clipping and filtering in peak to average power reduction for OFDM," *IEEE Electronics Letters*, vol. 38, no. 25, Dec. 2002, pp. 1726–1727.

[56] N. Ermolova, "New companding transform for reduction of peak to average power ratio," in *56th IEEE Vehicular Technology Conference (VTC 2002-Fall)*, vol. 3, Sept. 2002, pp. 1404–1407.

[57] A. D. S. Jayalath and C. Tellambura, "Peak to average power ratio of IEEE 802.11a PHY layer signals," in *6th International Symposium on DSP for Communications Systems (DSPCS'2002), Manly-Sydney, Australia*, Jan. 2002, pp. 31–36.

[58] A. Aggarwal and T. Meng, "Minimizing the peak to average power ratio of OFDM signals via convex optimization," *IEEE Global Telecommunication Conference (GLOBECOM)*, vol. 4, Dec. 2003, pp. 2385–2389.

[59] S. K. Deng and M. C. Lin, "OFDM PAPR reduction using clipping with distortion control," In *Proceeding of IEEE International Conference on Communications (ICC)*, vol. 4, May 2005, pp. 2563–2567.

[60] A. Saul, "Peak reduction for OFDM by shaping the clipping noise," IEEE *60th Vehicular Technology Conference*, vol. 1, Sept. 2004, pp. 443–447.

[61] H. Chen and A. Haimovich, "Iterative estimation and cancellation of clipping noise for OFDM signals," *IEEE Communications Letters*, vol. 7, no. 7, July 2003, pp. 305–307.

[62] H. Chen and A. Haimovich, "An iterative method to restore the performance of clipped and filtered OFDM signals," In *Proceeding of IEEE International Conference on Communication (ICC)*, vol. 5, May 2003, pp. 3438–3442.

[63] J. Tellado, L. M. C. Hoo and J. M. Cioffi, "Maximum likelihood detection of nonlinearly distorted multicarrier symbols by iterative decoding," In *IEEE Global Telecommunication Conference (GLOBECOM)*, vol. 5, May 1999, pp. 2493–2498.

[64] J. Tellado, L. M. C. Hoo and J. M. Cioffi, "Maximum likelihood detection of nonlinearly distorted multicarrier symbols by iterative decoding," *IEEE Transactions on Communications*, vol. 51, no. 2, Feb. 2003, pp. 218–228.

[65] A. Gatherer and M. Polley, “Controlling clipping probability in DMT transmission,” In *31st Asilomar Conference on Signals, Systems and Computers, Pacific Grove, CA*, vol. 1, Nov. 1997, pp. 578–584.

[66] H. Saeedi, M. Sharif and F. Marvasti, “Clipping noise cancellation in OFDM systems using oversampled signal reconstruction,” *IEEE Communications Letters*, vol. 6, no. 2, Feb. 2002, pp. 73–75.

[67] D. Kim and G. L. Stuber, “Clipping noise mitigation for OFDM by decision aided reconstruction,” *IEEE Communications Letters*, vol. 3, no. 1, Jan. 1999, pp. 4–6.

[68] A. Gusmao and R. Dinis, “Iterative receiver techniques for cancellation of deliberate nonlinear distortion in OFDM type transmission,” In *International OFDM Workshop 04, Dresden*, Sept. 2004.

[69] A. Gusmao, R. Dinis and P. Torres, “Low PMEPR OFDM transmission with an iterative receiver technique for cancellation of nonlinear distortion,” In *62nd IEEE Vehicular Technology Conference (VTC 2005-Fall)*, vol. 4, Sept. 2005, pp. 2367–2371.

[70] L. Xia, Z. Ying, T. Youxi and L. Shaoqian, “Iterative estimation and cancellation of clipping distortion for turbo receiver in MIMO-OFDM system,” *IEEE International Conference on Communications, Circuits and Systems*, vol. 1, May 2005, pp. 185–188.

[71] J. Tellado, *Peak to average power reduction for multicarrier modulation*. California: Ph.D. dissertation, Stanford University, 1999.

[72] B. Krongold and D. Jones, “An active-set approach for OFDM PAR reduction via tone reservation,” *IEEE Transactions on Signal Processing*, vol. 52, no. 2, Feb. 2004, pp. 495– 509.

[73] Y. Xin and I. J. Fair, "Low complexity PTS approaches for PAPR reduction of OFDM signals," In *Proceeding of IEEE International Conference on Communication (ICC) 2005*, vol. 3, May 2005, pp. 1991–1995.

[74] T. T. Nguyen and L. Lampe, "On partial transmit sequences to reduce PAR in OFDM systems," In *IEEE Global Telecommunication Conference (GLOBECOM), San Francisco, CA, USA*, Nov. 2006, pp. 1–6.

[75] L. Wang and C. Tellambura, "Analysis of clipping noise and tone-reservation algorithms for peak reduction in OFDM systems," *IEEE Transactions on Vehicular Technology*, vol. 57, no. 3, May 2008, pp. 1675-1694.

[76] D. W. Lim, S. J. Heo, J. S. No and H. Chung, "On the phase sequence set of SLM OFDM scheme for a crest factor reduction," *IEEE Transactions on Signal Processing*, vol. 54, no. 5, May 2006, pp. 1931–1935.

[77] R. Bauml, R. Fischer and J. Huber, "Reducing the peak to average power ratio of multicarrier modulation by selected mapping," *IEEE Electronic Letters*, vol. 32, no. 22, Oct. 1996, pp. 2056–2057.

[78] S. H. Muller and J. B. Huber, "A novel peak power reduction scheme for OFDM," In *8th IEEE International Symposium on Personal, Indoor and Mobile Radio Communications (PIMRC)*, vol. 3, Sept. 1997, pp. 1090–1094.

[79] L. J. Cimini and N. R. Sollenberger, "Peak to average power ratio reduction of an OFDM signal using partial transmit sequences," *IEEE Communications Letters*, vol. 4, no. 3, March 2000, pp. 86–88.

[80] W. S. Ho, A. Madhukumar and F. Chin, "Peak to average power reduction using partial transmit sequences: a suboptimal approach based on dual layered phase sequencing," *IEEE Transactions on Broadcasting*, vol. 49, no. 2, June 2003, pp. 225–231.

[81] D. W. Lim, J. S. No, C. W. Lim and H. Chung, "A new SLM OFDM scheme with low complexity for PAPR reduction," *IEEE Signal Processing Letters*, vol. 12, no. 2, Feb. 2005, pp. 93–96.

[82] D. W. Lim, S. J. Heo, J. S. No and H. Chung, "A new PTS OFDM scheme with low complexity for PAPR reduction," *IEEE Transactions on Broadcasting*, vol. 52, no. 1, March 2006, pp. 77–82

[83] H. Qian, C. Xiao, N. Chen and G. Zhou, "Dynamic selected mapping for OFDM," In *Proceeding of IEEE International Conference on Acoustics, Speech, and Signal Processing (ICASSP)*, vol. 4, March 2005, pp. 325-328.

[84] G. D. Forney, "Trellis shaping," *IEEE Transactions on Information Theory*, vol. 38, no. 2, March 1992, pp. 281–300.

[85] J. Davis and J. Jedwab, "Peak to mean power control in OFDM, golay complementary sequences and reed-muller codes," *IEEE Transaction on Information Theory*, vol. 45, no. 7, Nov. 1999, pp. 2397–2417.

[86] K. G. Paterson, "Generalized reed-muller codes and power control in OFDM modulation," *IEEE Transactions on Information Theory*, vol. 46, no. 1, Jan. 2000, pp. 104–120.

[87] Y. Xin and I. J. Fair, "Multiple shift complementary sequences and their peak to average power ratio values," In *Proceeding of IEEE International Symposium on Information Theory (ISIT)*, June-July 2004, pp. 121-137.

[88] R. Rubinstein, *Simulation and the Monte Carlo Methods*. New York: John Wiley and Sons, 1981.

[89] M. Friese, "On the degradation of OFDM signal due to peak clipping in optimally predistorted power amplifiers" *IEEE Communication Society ICC, GLOBECOM, Sydney, Australia*, vol. 2, Sept. 1998, pp. 939-944.

[90] M. Patzold, *Mobile Fading Channels*. New York: John Wiley & Sons, Ltd., 2002.

[91] J. Mazo, "Asymptotic distortion spectrum of clipped, DC-biased, Gaussian noise [optical communication]," *IEEE Transactions on Communications*, vol. 40, no. 8, Aug. 1992, pp. 1339–1344.

[92] K. Sharpe, "Some properties of the crossings process generated by a stationary χ^2 process," *Advances in Applied Probability*, vol. 10, no. 2, June 1978, pp. 373–391.

[93] IEEE Standard, *802.11a: Part 11 Wireless LAN medium access control (MAC) and physical layer (PHY) specifications*. IEEE, 1999.

[94] W. H. Press, B. P. Flannery, S. A. Teukolsky, and W. T. Vetterling, *Numerical Recipes in C: The Art of Scientific Computing*. 2nd edition Cambridge, Cambridge University Press, 1992.

[95] P. Varahram and B. Mohd-Ali, "PTS scheme with new phase sequence for PAPR reduction" *IEEE Transactions on Consumer Electronics*, vol. 57, no. 2, May 2011, pp. 366-371.

[96] C. Lin and W. Wu, "Clipping ratio estimation for OFDM networks" *IEEE Vehicular Technology Conference*, vol. 2, May-June 2005, pp. 797-800.

[97] W. Saad, N. El-Fishawy, S. El-Rabaie and M. Shokair, "Efficient designed prototype technique for OFDM PAPR reduction using FPGA," *International Journal of Communication Systems*, doi:10.1002/dac.2413, 2012.

WILEY

JOURNAL

International Journal of Communication Systems

Vol 26 (12 Issues in 2013)
Edited by: Professor Mohammad S. Obaidat

Print ISSN: 1074-5351
Online ISSN: 1099-1131

Impact Factor: 0.712

READ NOW ONLINE

Subscription Information

Description

The *International Journal of Communication Systems* provides a forum for R&D, open to researchers from all types of institutions and organisations worldwide, aimed at the increasingly important area of communication technology. The Journal's emphasis is particularly on the issues impacting behaviour at the system, service and management levels. Published twelve times a year, it provides coverage of advances that have a significant potential to impact the immense technical and commercial opportunities in the communications sector. The *International Journal of Communication Systems* strives to select a balance of contributions that promotes technical innovation allied to practical relevance across the range of system types and issues.

The Journal addresses both public communication systems (Telecommunication, mobile, Internet, and Cable TV) and private systems (Intranets, enterprise networks, LANs, MANs, WANs). The following key areas and issues are regularly covered:

- Transmission/Switching/Distribution technologies (ATM, SDH, TCP/IP, routers, DSL, cable modems, VoD, VoIP, WDM, etc.)
- System control, network/service management

International Journal of Communication Systems

OFDM-PAPR reduction using statistical clipping and window based noise filtering

Journal:	*International Journal of Communication Systems*
Manuscript ID:	IJCS-13-0562
Wiley - Manuscript type:	Research Article
Date Submitted by the Author:	18-Jun-2013
Complete List of Authors:	Sehgal, Aman; Thapar University, Electronics and Communication KOHLI, AMIT KUMAR; Thapar University, Electronics and Communication Engineering
Keywords:	orthogonal Frequency division multiplexing, peak to average power reduction, statistical clipping, clipping and filtering, window method